NASA Technical Memorandum 83446

(NASA-TM-83446) DIGITAL COMPUTER PROGRAM FOR GENERATING DYNAMIC TURBOFAN ENGINE MODELS (DIGTEM) (NASA) 109 p HC A06/MF A01 CSCL 21E

N84-16185

Unclas
G3/07 18159

Digital Computer Program for Generating Dynamic Turbofan Engine Models (DIGTEM)

Carl J. Daniele, Susan M. Krosel, John R. Szuch, and Edward J. Westerkamp
Lewis Research Center
Cleveland, Ohio

September 1983

CONTENTS

SUMMARY 1

INTRODUCTION 1

MODEL DESCRIPTION 3

USERS MANUAL 4
  Simulation Flow Diagram 4
  Program Setup 7

OUTPUT - TEST CASE 12

INTEGRATION TIME STEP STUDY 13

SIMULATION OF OTHER CONFIGURATIONS 14

CONCLUDING REMARKS 15

APPENDIXES:
  A - SYMBOLS 16
  B - ANALYTICAL MODEL 21
  C - INTEGRATION AND ITERATION SCHEMES 37
  D - FLOW CHARTS 44
  E - DIGTEM STEADY-STATE OPERATING POINTS 70
  F - TURBOSHAFT ENGINE MODEL 71

REFERENCES 73

PRECEDING PAGE BLANK NOT FILMED

I, II

DIGITAL COMPUTER PROGRAM FOR GENERATING DYNAMIC TURBOFAN ENGINE MODELS (DIGTEM)

Carl J. Daniele, Susan M. Krosel, John R. Szuch, and Edward J. Westerkamp

National Aeronautics and Space Administration
Lewis Research Center
Cleveland, Ohio 44135

E-1748

SUMMARY

This report describes DIGTEM, a digital computer program that simulates two-spool, two-stream turbofan engines. The turbofan engine model in DIGTEM contains steady-state performance maps for all of the components and has control volumes where continuity and energy balances are maintained. Rotor dynamics and duct momentum dynamics are also included. Altogether there are 16 state variables and state equations. DIGTEM features a backward-difference integration scheme for integrating stiff systems. It "trims" the model equations to match a prescribed design point by calculating correction coefficients that balance out the dynamic equations. It uses the same coefficients at off-design points and iterates to a balanced engine condition.

Transients can also be run. They are generated by defining controls as a function of time (open-loop control) in a user-written subroutine (TMRSP). DIGTEM has run on the IBM 370/3033 computer using implicit integration with time steps ranging from 1.0 msec to 1.0 sec.

DIGTEM is generalized in the aerothermodynamic treatment of components. This feature along with DIGTEM's "trimming" calculations at a design point makes it a very useful tool for developing models of specific engines having the same two-spool, two-stream configuration. Also subsets of the turbofan engine configuration such as a turbojet or a turboshaft can be simulated with minor modifications to the Fortran coding. With extensive modifications to the coding, arbitrary configurations can be modeled.

Included in this report is complete documentation of DIGTEM. Input requirements, flow charts, modeling equations, and a test case are given along with a listing of the user-written subroutine TMRSP. Finally the use of DIGTEM to generate models for engines whose configurations are subsets of the generalized turbofan engine configuration is described.

INTRODUCTION

The development of aircraft propulsion systems depends, to a great extent, on being able to predict the performance of the propulsion system and its associated controls. Computer simulations provide the means for analyzing the behavior and interactions of these complex systems prior to the building and testing of expensive hardware. Simulations can also serve as aids in understanding and solving problems that arise after the propulsion system is developed.

Computer simulations can be either generalized or specific to a particular propulsion system. Generalized simulations are desirable in that they allow for paper studies of many different engine configurations. Many generalized digital engine simulations exist today. Most of them are limited to steady-state performance calculations for a fixed number of engine configurations (refs. 1 to 4). But, since they are generalized, the user need only specify which of the configurations is to be analyzed and supply the correct input data. One generalized code, NNEP (ref. 5), lets the user build up arbitrary configurations through input definitions. Another generalized code, DYNGEN (ref. 6), has transient capability but is limited to the fixed engine configurations of references 3 and 4 (GENENG and GENENG II). All of the generalized codes described have various limitations: they are limited to steady-state calculations, or they have many but fixed engine configurations. Some (DYNGEN and GENENG) are difficult to change, and none can scale its model equations to reflect real engine data. Thus there is a need for a computer code that can do both steady-state and dynamic calculations, is flexible for modeling various engine configurations, and can also be easily adapted to model real engine data.

Such a generalized dynamic engine program has been developed for the hybrid computer. That program is called HYDES (ref. 7) and can handle the same fixed engine configurations as DYNGEN. However, by utilizing the capabilities of both the analog and digital computers, HYDES is able to provide improved engine model fidelity and an interactive user environment.

Even when using the HYDES program, the development of hybrid simulations is time consuming and requires experience in dynamic system modeling, hybrid computer programming, and hybrid computer operations. To simplify this development process, a systematic, computer-aided approach for generating hybrid computer simulations of a particular class of engine (i.e., two-spool, two-stream turbofan) has been developed (refs. 8 and 9). This approach features more generalized aerothermodynamic models of engine components and automated calculation of scale factors and simulation coefficients. Also a specified operating point, designated as the design point, is used to scale the component maps and to determine correction coefficients that will balance the dynamic equations at the design point. This assures good steady-state accuracy at the design point.

Despite the advantages of hybrid simulations they are generally not portable or easily modified. Thus a digital computer model possessing the capabilities of the hybrid model presented in references 8 and 9 is desirable. Such a model has been developed and is the subject of this report. The digital portion of the hybrid model was retained and the dynamic equations that were on the analog were added to the digital code. The model was also unscaled to make it easier to modify or to integrate with controls. A numerical integration scheme was added to provide dynamic capability to the digital program. The integration technique is implicit and is well suited for integrating "stiff" systems such as the turbofan engine model. The resultant digital computer code is called DIGTEM for DIGital Turbofan Engine Model.

DIGTEM is generalized in a different sense than DYNGEN. DIGTEM, although having only one engine configuration in the code, is written in modular form to permit variations of the engine configuration (i.e., turbojets and turboshafts) to be simulated. This provides more flexibility (at the cost of recoding the Fortran) than DYNGEN, which is limited to a fixed set of configurations and which is difficult to change. Both DYNGEN and DIGTEM do component map scaling to match input data at a design point. However, DIGTEM also calculates correction coefficients to balance the dynamic equations so that a steady-state balance at the design point is generated. The same values of the correction coefficients are used at off-design points. If the coefficients do not balance the dynamic equations at the operating points, DIGTEM iterates to a new balanced engine condition. DIGTEM's flexibility should allow it to be a useful tool for engine dynamics studies and controls analysis.

DIGTEM has been run on the IBM 370/3033 mainframe computer with time steps ranging from 0.1 msec to 1.0 sec. Since DIGTEM utilizes an implicit integration scheme, the larger time steps can be used to generate fast, stable, transient solutions. However, if the time step is too large relative to the smallest engine time constant, there will be a loss in dynamic accuracy.

This report provides documentation of the DIGTEM program. Input requirements, flow charts, and modeling equations are provided. A test case is included that makes use of a user-written, open-loop control subroutine, TMRSP. Also, a complete users manual is provided as a section of this report. Check with COSMIC, University of Georgia, Athens, Ga. 30602, for the availability of this program. Finally the use of DIGTEM to model turbojet and turboshaft engines is described.

MODEL DESCRIPTION

The engine model supplied with DIGTEM represents a two-spool, two-stream augmented turbofan engine. Figure 1 shows a schematic representation of that engine. A single inlet is used to supply airflow to the fan. Air leaving the fan is separated into two streams - one passing through the engine core and another passing through an annular bypass duct. The fan is driven by a low-pressure turbine. The core airflow passes through a compressor that is driven by a high-pressure turbine. Both the fan and compressor are assumed to have variable geometry for better stability at low speeds. Engine airflow bleeds are extracted at the compressor exit (station 3) and used for turbine cooling (flow returns to the cycle). Fuel flow is injected in the main combustor and burned to produce hot gas for driving the turbines. The engine core and bypass streams combine in an augmentor duct, where the flows are assumed to be thoroughly mixed. Additional fuel is added to further increase the gas temperature (and thus thrust). The augmentor flow is discharged through a variable convergent-divergent nozzle. The nozzle throat area (station 8) and exhaust nozzle area (station E) are varied to maintain engine airflow and to minimize drag during augmentor operation.

Figure 2 contains a computational flow diagram of the engine model. All symbols are defined in appendix A. The analytical model includes multivariate maps to model the steady-state performance of the engine's rotating components. Fluid momentum in the bypass duct and the augmentor, mass and energy storage within control volumes, and rotor inertias are included in the model to provide transient capability. The complete engine model is presented in appendix B.

The integration technique used in DIGTEM is a backward-difference (implicit) integration scheme that is well suited for integrating "stiff systems." A typical engine model will have time constants that differ by three or four orders of magnitude. This requires the use of very small time steps when using forward-difference (explicit) integration schemes to insure stability. The backward-difference scheme uses a multivariable Newton-Raphson iteration method for convergence at each time point. A complete description of the integration technique is given in appendix C. In DIGTEM the iteration variables correspond to the state variables. The 16 state variables are the two rotor speeds N_L and N_H; the six stored masses W_3, W_4, $W_{4.1}$, W_6, W_7, and W_{13}; the six gas temperatures T_3, T_4, $T_{4.1}$, T_6, T_7, and T_{13}; and the two mass flow rates $\dot{w}_{13}$ and $\dot{w}_6$. The ordering of the state variables in the state vector $\overline{VS}$ is important. The elements of $\overline{VS}$ and the corresponding state derivative vector $\overline{VDOT}$ are defined in terms of computer variables as follows:

VS(1) = XNL	VDOT(1) = DXNL
VS(2) = XNH	VDOT(2) = DXNH
VS(3) = W3	VDOT(3) = DW3
VS(4) = T3	VDOT(4) = DT3
VS(5) = W4	VDOT(5) = DW4
VS(6) = T4	VDOT(6) = DT4
VS(7) = W41	VDOT(7) = DW41
VS(8) = T41	VDOT(8) = DT41
VS(9) = W6	VDOT(9) = DW6
VS(10) = T6	VDOT(10) = DT6
VS(11) = W7	VDOT(11) = DW7
VS(12) = T7	VDOT(12) = DT7
VS(13) = WA13	VDOT(13) = DWA13
VS(14) = WG6	VDOT(14) = DWG6
VS(15) = W13	VDOT(15) = DW13
VS(16) = T13	VDOT(16) = DT13

The order of the state variables is set up such that the duct variables and the core nozzle variables are at the end. This facilitates the use of DIGTEM for simulating engines other than two-spool, two-stream turbofan engines. This will be discussed later. DIGTEM subroutines associated with the integration scheme (ENGBD, TMRSP, ERROR, GUESS, DMINV, and BDPRNT) are written in terms of the state variable vector $\overline{VS}$ and the state derivative vector $\overline{VDOT}$. The state variables and their corresponding derivatives do not appear explicitly in these subroutines. The user must be careful if he or she wishes to redefine the state variable order in DIGTEM. Subroutines ENGBD, TMRSP, and BDPRNT are order dependent (the others mentioned above are not). All three subroutines must be changed accordingly. This will be discussed later.

Although the integration scheme featured in DIGTEM is a backward-difference integration scheme, a forward-difference integration scheme (Euler) is also provided (a user option). How to invoke the different options in DIGTEM is described in the section USERS MANUAL.

USERS MANUAL

Simulation Flow Diagram

The overall simulation structure is shown in figure 3 in the form of a flow chart for the main program DIGTEM. First, DIGTEM writes out a heading identifying the type of engine being simulated. User data are then read in to define the integration time step, printout interval, operating point, and transient duration. Next, INDATA is called to read in component maps and steady-state operating-point data. Both nonaugmented (dry) and augmented (wet) operating points may be input. By definition, the first dry point and the first wet point are design points. Once the desired design point or points is specified, DSGNPT is called to calculate the scaling coefficients for the specified dry and wet design points. Next the engine parameters are calculated in ENGINE and vectors are set up for the integration routines. Then BDINTG or FDINTG is called to generate transient results depending on which integration method is desired. Once the transient is completed, the simulation is stopped.

Flow charts for the subroutines are shown in appendix D. The following list defines the functions of the various subroutines:

DIGTEM The main program for the simulation is used to control the simulation.

BDINTG The BDINTG subroutine performs implicit integration of the dynamic equations in DIGTEM. This subroutine is discussed in detail in appendix C.

BDPRNT The BDPRNT subroutine prints out either a short or a detailed output when backward difference is used.

DCTINT The DCTINT subroutine calculates the derivative of the duct flow and performs a forward-difference integration if desired.

DMINV The DMINV subroutine performs a double-precision matrix inversion of the Jacobian error matrix.

DSGNPT The DSGNPT subroutine is used to calculate correction coefficients from design-point data. At the dry and wet design points the scaling coefficients are calculated from input values of pressure, temperature, flow, etc. The correction coefficients are used to compensate for small modeling errors (e.g., map interpolation errors or mismatched component models) and to give zero derivatives at the design points. Additional coefficients are calculated at the wet design points so that a balanced condition exists in the augmentor at the wet design (maximum thrust) point. This subroutine is discussed in more detail in appendix B.

DUCT The DUCT subroutine calculates the duct integration constants and losses.

ENGINE The ENGINE subroutine solves the turbofan engine model by using the correction coefficients from DSGNPT and by calling the 14 engine subroutines in order. This routine is called by DIGTEM to calculate initial conditions when forward-difference integration is specified.

ENGBD The ENGBD subroutine performs the same function as ENGINE but is used when backward-difference integration is specified.

ENG1 The ENG1 subroutine calculates fan performance.

ENG2 The ENG2 subroutine calculates compressor performance.

ENG3 The ENG3 subroutine calculates continuity and energy balances in the fan mixing volume and performs integration if not in steady state.

ENG4 The ENG4 subroutine calculates bleed flows.

ENG5 The ENG5 subroutine calculates continuity and energy balances in the compressor mixing volume and performs integration if not in steady state.

ENG6 The ENG6 subroutine calculates the high-pressure-turbine performance.

ENG7 The ENG7 subroutine calculates the continuity and energy balances in the combustor and performs integration if not in steady state.

ENG8 The ENG8 subroutine calculates the low-pressure-turbine performance.

ENG9 The ENG9 subroutine calculates the continuity and energy balances in the high-pressure-turbine mixing volume and performs integration if not in steady state.

ENG10 The ENG10 subroutine performs continuity and energy balances in the low-pressure-turbine mixing volume and performs integration if not in steady state.

ENG11 The ENG11 subroutine calculates nozzle performance.

ENG12 The ENG12 subroutine calculates continuity and energy balances in the augmentor mixing volume and performs integration if not in steady state.

ENG13 The ENG13 subroutine calculates the low- and high-spool derivatives and performs integration if not in steady state.

ENG14 The ENG14 subroutine calculates duct parameters and performs integration if not in steady state.

ERROR The ERROR subroutine calculates the error vector for implicit integration.

FDINTG The FDINTG subroutine performs forward-difference integration of the dynamic equations.

FLCOND The FLCOND subroutine calculates ambient pressure and fan inlet total pressure and temperature from specified values of altitude, Mach number, and sea-level ambient temperature.

FOOR The FOOR subroutine indicates when data input to a function is out of range of the function data. It also indicates if the implicit integration routine is generating a Jacobian matrix. If MATRIX = 0, the routine is not generating a new matrix and the data should be checked.

FUN1 The FUN1 subroutine does a single-value interpolation.

FUN1L The FUN1L subroutine is called following the call to FUN1 when the same pair of breakpoints can be used to compute a second function value.

GUESS The GUESS subroutine updates the guess vector for the implicit integration scheme.

INDATA The INDATA subroutine initializes and reads in map data.

MAP The MAP subroutine does a double-value interpolation.

MAPL The MAPL subroutine is called following a call to MAP when the same four breakpoints can be used to compute a second function value.

MOOR The MOOR subroutine indicates when data input to a map are out of range of the map data. It also indicates if the implicit integration routine is generating a Jacobian matrix. If MATRIX = 0, the routine is not generating a new matrix and the data should be checked.

NOZZL The NOZZL subroutine calculates nozzle performance for both subsonic and supersonic flow conditions.

PROCOM The PROCOM subroutine calculates the values of JP-4/air thermodynamic properties based on supplied values of temperature and fuel-air ratio. The thermodynamic properties are the specific heats, the specific heat ratio, and the specific enthalpy.

SPLINT The SPLINT subroutine calculates the spool speed derivative and performs forward-difference integration if specified.

SPOOL The SPOOL subroutine calculates the spool integration constant from the moment of inertia.

TPRINT The TPRINT subroutine prints out short or detailed output when forward-difference integration is used.

TRAT The TRAT subroutine calculates the isentropic temperature rise parameter based on specified values of pressure ratio and specific heat ratio.

VOLINT The VOLINT subroutine performs continuity and energy integrations for forward-difference integration and forms derivatives for the backward-difference integration.

VOLUME The VOLUME subroutine calculates control volume stored mass by using the ideal-gas law.

A final subroutine TMRSP is user written. It defines open-loop controls as a function of time for transient operation.

Program Setup

Data are input to DIGTEM via three methods. First, all component map data and operating-point data are specified in an input data set; second, integration routine selection, integration time step, printout options, and transient data are specified in the main routine DIGTEM; and third, open-loop controls are specified in a user-written subroutine TMRSP.

Input data set. - The input data set supplied with DIGTEM is shown in figure 4. These data are read in by the main program DIGTEM and by subroutine INDATA. The first line contains constants for the fraction of turbine cooling bleeds that perform work for the high- and low-pressure turbines, respectively. For the test case the constants are K_{BLWHT} and K_{BLWLT} and the input format is (5F12.5). The next six sets of data are component maps that are normalized to dry design operating-point values.

Before the contents of each of the component map data sets are described, a general discussion of the data input procedure is presented. Figure 5 shows an example of map data where there are three common functions of the independent variables. The first line of the data contains five numbers in (5I3) format. They are

MAPNO NCV NPT NFCT NCOM

where MAPNO is a map number to be used in the $Z_1 = f_1 (X,Y)$ function call; NCV is the number of curves Y on the map; NPT is the number of points (X,Z) on each curve; NFCT is the number of common functions Z_1 of the same independent variables; and NCOM is the switch to indicate that the X breakpoint values can be used for all of the NCV curves. (A zero indicates that the X values are different for each curve.)

The next line indicates the formats to be used in reading the remaining map statements. A (8X,7(4A2)) format is used to specify the formats of (1) the X values, (2) the Y values, and (3) the Z_1 values. The remaining lines in the data set contain (in order) the Y values, the X values for the first curve, the Z_1 values for the first curve of each function, the X values for the second curve, the Z_1 values for the second curve of each function, and so forth. For those functions where each curve can be defined by exactly the same X values (NCOM = 1) those X values need be only input once immediately following the Y values.

Now, returning to figure 4, the first input data set is for the fan variable-geometry effect. This map gives the adjustment to the value of corrected fan airflow due to off-schedule geometry. The effects are modeled as a bivariate map with fan variable-geometry position and fan corrected speed as the inputs. That is,

$$\Delta\dot{W}_2 = f_8\left(FVGP,\ N_L/\theta_2^{1/2}\right) \tag{1}$$

The first line of data is

1 14 11 1 0 (understood)

Thus the map number is 1; there are 14 curves; 11 points per curve; 1 function of Z for each X value; and 0 is understood to be the NCOM switch value. The next line indicates the formats for reading the data. Lines 3 and 4 are the Y values (normalized speeds), lines 5 and 6 are the X values for curve 1 (the FVGP values - not normalized), and lines 7 and 8 are the Z values for curve 1 (the flow shifts). Lines 9 and 10 are the X values (FVGP positions) for curve 2, and lines 11 and 12 are the corresponding flow shifts. Data for 12 more curves of flow shift as a function of FVGP and speed follow. Note that the twelfth value of corrected speed is 1.000. Therefore the corresponding curves (lines 49 to 52) pass through the design point ($X = 1.0$, $Z = 1.0$).

The next set of data defines the compressor variable-geometry effects map. This map gives the shift in corrected airflow due to off-schedule compressor geometry. As is the case of the fan, the shift is assumed to correlate with actual variable-geometry position and corrected speed:

$$\Delta\dot{W}_{2.2} = f_{12}\left(CVGP,\ N_H/\theta_{2.2}^{1/2}\right) \tag{2}$$

The first line of data is

2 14 11 1 0 (understood)

which is similar to the fan variable-geometry data. The 2 corresponds to the map number. The next line is again the formats for reading the data. Lines 3 and 4 are the normalized speeds; lines 5 and 6 are the CVGP values and lines 7 and 8 are the flow shifts corresponding to the first corrected speed (0.70). Thirteen more curves are defined for the compressor.

The next data set is the baseline (scheduled FVGP) fan performance. Here NFCT = 4; thus there are four maps with the same input values. Lines 3 and 4 are the normalized fan speeds $N_L/\theta_2^{1/2}$. Lines 5 and 6 are the fan duct pressure ratios P_{13}/P_{12}. Both input values are normalized to the design-point value. Lines 7 and 8 define the corrected fan flow curve for the first corrected speed (0.3000):

$$(\dot{W}_c)_{fan,M} = f_6\left(\frac{P_{13}}{P_2},\ \frac{N_L}{\theta_2^{1/2}}\right) \tag{3}$$

In addition to the corrected flow map there are three other maps associated with fan performance. They are fan tip region efficiency

$$\eta_{fan,OD} = f_9\left(\frac{P_{13}}{P_2},\ \frac{N_L}{\theta_2^{1/2}}\right) \tag{4}$$

the fan tip region pressure ratio.

ORIGINAL PAGE IS OF POOR QUALITY

$$\frac{P_{2.1}}{P_2} = f_7\left(\frac{P_{13}}{P_2}, \frac{N_L}{\theta_2^{1/2}}\right) \tag{5}$$

and finally the fan hub region efficiency

$$\eta_{fan,ID} = f_{10}\left(\frac{P_{13}}{P_2}, \frac{N_L}{\theta_2^{1/2}}\right) \tag{6}$$

The next set of data is for the baseline (scheduled CVGP) compressor performance. Here NFCT = 2. Thus there are two maps with the same input variables, namely pressure ratio and speed. Lines 3 and 4 are the normalized corrected speeds $N_H / \theta_{2.2}^{1/2}$. Lines 5 and 6 are the normalized compressor pressure ratios $P_3/P_{2.2}$ for the first speed (0.700). Lines 7 and 8 contain the corresponding compressor corrected flows for the first speed:

$$(\dot{w}_c)_{C,M} = f_{11}\left(\frac{P_3}{P_{2.2}}, \frac{N_H}{\theta_{2.2}^{1/2}}\right) \tag{7}$$

The second map for the compressor is the compressor efficiency:

$$\eta_C = f_{13}\left(\frac{P_3}{P_{2.2}}, \frac{N_H}{\theta_{2.2}^{1/2}}\right) \tag{8}$$

The next set of data is for the high-pressure-turbine performance. Here NFCT = 2. Thus there are two maps. In this case, NCOM = 1. Hence all curves for both maps are defined by the same pressure ratio breakpoints. Each map has eight curves with nine points per curve. Line 3 contains the eight normalized speed values $N_H / \theta_{2.2}^{1/2}$. Line 4 contains nine normalized pressure ratio values $P_3/P_{2.2}$. Line 5 defines the normalized flow parameter curve for the first speed (0.7129):

$$(\dot{w}_p)_{HT} = f_{14}\left(\frac{P_{4.1}}{P_4}, \frac{N_H}{T_4^{1/2}}\right) \tag{9}$$

Line 6 defines the first curve of the map (i.e., the turbine enthalpy drop parameter):

$$(h_p)_{HT} = f_{15}\left(\frac{P_{4.1}}{P_4}, \frac{N_H}{T_4^{1/2}}\right) \tag{10}$$

Lines 7 and 8 define the same two maps at the second speed (0.7548). Note that the same pressure ratio breakpoints are assumed for all speeds.

The final set of component map data is for the low-pressure-turbine performance. The data are organized in exactly the same way as those for the high-pressure turbine. Line 5 is the normalized flow parameter for the first speed (0.4076):

$$(\dot{w}_p)_{LT} = f_{16}\left(\frac{P_5}{P_{4.1}}, \frac{N_L}{T_{4.1}^{1/2}}\right) \tag{11}$$

and line 6 is the normalized turbine enthalpy drop parameter:

$$(h_p)_{LT} = f_{17}\left(\frac{P_5}{P_{4.1}}, \frac{N_L}{T_{4.1}^{1/2}}\right)$$

After the component map data are read in, a blank line must be inserted. The next set of input data are the bias values for the fan and compressor variable geometry. These values are subtracted from the actual variable-geometry position values in the simulation so that inputs to the flow shift maps are always positive (a requirement of the interpolation routine). The biases are 0.000 and 4.000 for BSFVGP and BSCVGP, respectively, and the format is (2F10.0). The next two numbers are the number of dry and wet operating points (NDRY and NAUG, respectively) to be input by the user. The format is (1X,2(I2,2X)).

The following number is a label for designating the operating point (POINT). The format is (9X,I3). The first operating point is assumed to be the dry design point. The operating-point data are organized as follows:

P0	P2	P13	P22	P3
P4	P41	P5	P6	P7
TAM	T2	T13	T22	T3
T4	T41	T6	T7	WA2
WA13	WA22	WA3	WG4	WG41
WG6	WG7	DH4	DH41	ETAB
ETAAB	FN	XNL	XNH	WF4
WF7	A8	AE	ALT	XMN
CDN	CVN	FVGP	CVGP	FG

The format is (5F12.5). The next set of variables read in are the physical volumes, reactances, and rotor moments of inertia:

V13	V3	V4	V41	V6	V7
AQL13	AQL6	XIH	XIL		

The format is (6F12.5). The final values read in for the operating point are the fan tip region, fan hub region, and compressor efficiencies:

ETAOF ETAIF ETAHC

The format is (3F12.5).

The following sets of data contain additional dry-operating-point data. Once all the dry operating points are read in, the augmented operating points are read in. Again, the first wet operating point is assumed to be the wet design point.

Transient specifications in DIGTEM. - Setup data for DIGTEM transients (except for open-loop controls) are specified in the main routine DIGTEM. The data are listed in table I. NOPER denotes the desired initial-condition operating point; H is the integration time step; and TMAX is the duration of the transient in seconds. If TMAX = 0.0, a steady-state (converged) point will be generated. Steady-state solutions for the five operating points listed in figure 4 are given in appendix E. TOUT is the printout interval. Note that TOUT and H need not be the same. The integration method to be used is set by IBDINT. If IBDINT = 0, a forward-difference Euler integration is used; if IBDINT = 1, backward-difference (implicit) integration is used. The implicit integration scheme is discussed in appendix C. IHPCNV provides for matrix generation and convergence at every time point, if desired. If IHPCNV = 0, internal logic is to be used to determine when new matrices are computed. Finally N is the system order (16 for the turbofan engine model in DIGTEM).

User-written open-loop control subroutine TMRSP. - Transients are run in DIGTEM by specifying open-loop controls as a function of time in a user-written subroutine TMRSP. Control inputs for the two-spool, two-stream turbofan engine in DIGTEM are

$\dot{w}_{F,4}$ main combustor fuel flow

$\dot{w}_{F,7}$ augmentor fuel flow

A_8 nozzle throat area

FVGP fan variable-geometry parameter

CVGP compressor variable-geometry parameter

Figure 6 shows time histories of the control inputs for a typical engine acceleration from operating point 3 (low dry power) to operating point 4 (high wet power). Main combustor fuel flow $\dot{w}_{F,4}$ is ramped in 2 sec from 0.37 to 1.7 lbm/sec. FVGP and CVGP are varied in a manner designed to stay within the ranges of the fan and compressor flow shift maps. After 10 sec afterburning is initiated. Augmentor fuel flow $\dot{w}_{F,7}$ is ramped in 3 sec from 0 to 5.0 lbm/sec. Also, at 10 sec the nozzle throat area A_8 and the exhaust nozzle area A_E are ramped to their new operating-point values (also in 3 sec).

Figure 7 shows the corresponding Fortran coding to produce these open-loop controls (subroutine TMRSP). All the inputs have been described except for JSS, which is set internally in DIGTEM. JSS is set equal to 0 when a steady-state run is requested. Thus specifying TMAX = 0.0 in DIGTEM causes JSS to be set equal to 0. Note that in figure 7 the FVGP and CVGP values are both biased and inverted before leaving TMRSP. This is done to accommodate the map interpolation routines.

OUTPUT - TEST CASE

The previously defined transient is used as a test case. The lowest power operating point, operating point 3, is used as the initial condition for the transient. The engine is to be accelerated from low power to full afterburning in 20 sec. The main routine DIGTEM to run this transient is shown in figure 8. Note that backward-difference integration is desired (ICDINT = 1); the integration time step is to be 0.01 sec (H = 0.01); the printout interval is to be 0.1 sec (TOUT = 0.1); the transient duration is to be 20 sec (TMAX = 20.0); the initial condition is operating point 3 (NOPER = 3); internal logic is to be used to determine when a new Jacobian matrix is needed (IHPCNV = 0); and there are 16 state variables (N = 16).

The output listing from DIGTEM is shown in figure 9. At the initial condition (in this case, OPERATING POINT NUMBER 3) a detailed printout of the engine parameters is generated at TIME = 0.0 SECONDS. This printout corresponds to the user-supplied INPUT DATA. However, the input values may be slightly different from the input data because of the effects of the correction coefficient scaling described earlier. Pressures, temperatures, temperature derivatives, mass flows, mass flow derivatives, stored mass, stored mass derivatives, energy derivatives, and enthalpies are listed for the various engine stations. Below the table, low and high spool speeds and their corresponding derivatives are listed along with main combustor and augmentor fuel flows, bleed flows, and variable geometries. The variables FSHIFT and CSHIFT are near zero since the specified values for the variable geometry positions result in small flow shifts out of the fan and compressor flow shift maps.

A second printout is generated if implicit integration is selected. This second printout is generated after DIGTEM converges to a balanced steady-state condition. If explicit integration is used, a startup transient will occur (if all the control inputs are held constant) because of any nonzero derivatives that exist at the initial operating point. When explicit integration is used, DIGTEM prints out the input data table as described for the implicit integration and then prints out a message

FORWARD DIFFERENCE INTEGRATION IS BEING USED. IF ALL THE DERIVATIVES ARE NOT CLOSE TO ZERO, A TRANSIENT SHOULD BE RUN TO BALANCE OUT THE ENGINE BEFORE CHANGING ANY OF THE CONTROLS IN TMRSP.

Since implicit integration is being used here, DIGTEM iterates to a converged condition and then prints out CONVERGED STEADY STATE POINT and again gives a detailed printout of the engine parameters at TIME = 0.0 SECONDS. Note that all of the derivatives have been driven to near zero and also that the converged data are very close to the input data. This indicates that the input data along with the correction coefficients calculated at the dry design point led to a nearly balanced engine at the operating point. Steady-state results are given in appendix E for all five DIGTEM operating points. Note that if explicit integration is used, this second printout of converged data does not occur.

Next DIGTEM prints out transient results at each specified printout point. This is done for both integration schemes. Shown are TIME and the pressures at all engine stations in row 1; temperatures at all stations in row 2; and speeds and control inputs in row 3. MATTOT is shown in row 3 when implicit integration is used. This is the total number of Jacobian matrices calculated to that point in the transient. In this case data are printed out every 0.1 sec for 20 sec. At the end of the desired transient run (TMAX = 20.0 in this case) DIGTEM again prints out a detailed list of the engine parameters at all stations. This occurs independent of the integration scheme selected. Figure 10 shows plots of some of the results. Shown are plots of high rotor speed N_H, low rotor speed N_L, combustor pressure P_3, turbine inlet temperature T_4, and augmentor temperature T_7 as functions of time. As shown in figure 6, main combustor fuel flow was ramped for 2 sec and then held constant. All five variables shown in figure 10 increased smoothly to their new values and then held constant until augmentor fuel flow was added at t = 10 sec. Note that all engine variables stayed constant during afterburning except the augmentor temperature, which increased smoothly to its final value.

INTEGRATION TIME STEP STUDY

The integration time step for the test case was 0.01 sec. The 20-sec transient took 13.1 sec of central processing unit (CPU) time on the IBM 370/3033 computer when the implicit integration scheme was used. Six Jacobian matrices were generated during the transient. To determine the effect of time step on the simulation response and on CPU times, the integration time step was varied from 0.001 sec to 1.0 sec for the same 20-sec transient. Figure 11(a) shows the effect of time step on CPU time. For the 0.001-sec integration time step, 98.34 sec of CPU time was needed for the 20-sec transient. This is primarily due to the large number of steps (i.e., passes through the model). Increasing the time step to 0.01 sec caused an 87-percent reduction in CPU time to 13.1 sec. A further increase to 0.1 sec caused another reduction of 69 percent in CPU time to 4.01 sec. Finally an increase to 1.0 sec caused another reduction of 9.8 percent to 3.69 sec.

Figure 11(b) shows the corresponding number of Jacobian matrices needed for the 20-sec transient with the various integration time steps. As the time step increased, the number of Jacobian matrices needed for convergence also increased from two matrices at the 0.001-sec time step to 31 at 1.0 sec. For time steps less than 0.01 sec the CPU time was primarily a function of the number of passes through the model. For larger time steps, however, the generation of Jacobian matrices (and subsequent inverses) contributed a great deal to the CPU time and offset much of the expected speedup.

In all cases, stable and converged solutions were obtained. However, with the 1.0-sec time step, some problems occurred early in the transient with inputs to maps and functions going out of range. Also some damped oscillations were observed. For time steps between 0.001 and 0.1 there was little difference between the transient responses. Figure 12 shows a comparison obtained with the 0.01 and 1.0 time steps. Low rotor speed is shown in figure 12(a). Note that at 1.0 sec there was a large speed difference between the two responses. This occurred because the inputs to the map and function input routines went out of range. By 2.0 sec the H = 1.0-sec response recovered but then overshot at 3.0 sec and finally showed some oscillations about the final value of speed. The combustor pressure responses are shown in figure 12(b) for the first 2 sec of the transient. Note the loss in accuracy for the larger time-step solutions. Although not shown in figure 12, the high rotor speeds and turbine inlet temperatures exhibited the same characteristics.

Finally a transient was run using the explicit Euler integration scheme supplied in DIGTEM. To obtain a stable solution, the integration time step had to be less than or equal to 0.1 msec. For the same 20-sec transient, 417 sec of CPU time was needed. . .

SIMULATION OF OTHER CONFIGURATIONS

DIGTEM contains normalized component maps and a generalized aerothermodynamic treatment of its components. It also can scale the analytical model to match a user-specified design point. These features make it useful for simulating turbofan engines other than the one described in DIGTEM. Also, with minimal Fortran reprogramming, variations from a turbofan engine such as a turbojet or turboshaft engine can be simulated. With major modifications to the coding it is possible to model arbitrary engine configurations.

To simulate an engine such as a turboshaft, the user need only mask (comment) out those areas of code that are not needed and equate variables where needed. The order of the state variables has been set to facilitate the required modifications to the implicit integration routine. Simulation of a turboshaft engine is described in appendix F.

For particular engine configurations some change to the state variable order may be necessary. The user is cautioned that the state variable derivatives must also be ordered as described in the section MODEL DESCRIPTION. For example, one may wish to simulate a single-spool turbojet such as the one shown in figure 13. In comparing this configuration with the turbofan configuration of figure 2, it is clear that the fan duct, fan, and low-pressure turbine must be eliminated. A suitable state variable and state variable derivative order is

VS(1) = XNH	VDOT(1) = DXNH
VS(2) = W3	VDOT(2) = DW3
VS(3) = T3	VDOT(3) = DT3
VS(4) = W4	VDOT(4) = DW4
VS(5) = T4	VDOT(5) = DT4
VS(6) = W6	VDOT(6) = DW6
VS(7) = T6	VDOT(7) = DT6
VS(8) = W7	VDOT(8) = DW7
VS(9) = T7	VDOT(9) = DT7
VS(10) = WG6	VDOT(10) = DWG6

Variables must be eliminated or equated as follows:

$$\dot{w}_{BLLT} = 0 \tag{13}$$

$$FVGP = CVGP = 0 \tag{14}$$

$$\dot{w}_{13} = 0 \tag{15}$$

$$\dot{w}_{2.2} = \dot{w}_2 \tag{16}$$

$$P_{2.2} = P_2 \tag{17}$$

$$T_{2.2} = T_2 \tag{18}$$

$$P_6 = P_{4.1} \tag{19}$$

$$T_6 = T_{4.1} \tag{20}$$

$$\dot{w}_6 = \dot{w}_{4.1} \tag{21}$$

In the main routine DIGTEM the number of state variables must be reduced to n = 10. The Fortran recoding to accomplish the variable changes is done in the DSGNPT and the appropriate ENGi subroutines. The state variable reordering is done in the ENGBD, TMRSP, and BDPRNT subroutines.

CONCLUDING REMARKS

The design and development of aircraft propulsion systems depends to a large extent on computer simulations. The generalized computer codes for developing these simulations must be flexible in being able to model many different engine configurations and also must predict engine performance in both steady-state and transient operation. Once an engine configuration is picked, the simulation must then model the specifics of that engine. Generalized codes, however, do not lend themselves well to modeling specific engines because of their generality. Also, the simulations must perform the engine calculations in a reasonable amount of computer time.

Until now, the generalized computer codes available performed some but not all of the above functions. DIGTEM, the digital turbofan engine model computer code presented in this report, has been shown to provide all of these functions. Besides being able to model many different configurations, DIGTEM provides both steady-state and transient capability, and scales itself to match engine operating-point data and thus tailors itself to model specific engines.

DIGTEM provides all of this capability at the expense of requiring much more user interaction than the other generalized codes. However, it is written in such a manner that even someone unfamiliar with gas turbine engine simulations can modify and use the simulation. To do so does require the user to have knowledge of Fortran. DIGTEM contains both implicit and explicit numerical integration schemes. It is segmented on a component basis (each component and mixing volume is in its own subroutine). Thus it can be used to do numerical integration studies using integration methods other than those supplied with the computer code. Also, because of the segmentation, parallel processing methods can be studied. Open-loop control implementation is described in DIGTEM. Closed-loop controls can be implemented by adding control equations and integrating the controls and state variables simultaneously or by using the subroutines in appendix C of Sellers, which were derived to be compatible with the modified Euler solution method. In addition to being a useful tool for simulation research and development, DIGTEM provides the flexibility to study a variety of engine dynamics and controls problems.

APPENDIX A

SYMBOLS

A	cross-sectional area, cm^2 (in^2)
a	altitude, m (ft)
C_d	nozzle flow coefficient
C_v	nozzle velocity coefficient
CC	correction coefficient
CVGP	compressor variable-geometry parameter, deg
c_p	specific heat at constant pressure, kg/J K (Btu/lbm °R)
c_v	specific heat at constant volume, kg/J K (Btu/lbm °R)
dt	differential time, sec
F	thrust, N (lbf)
FVGP	fan variable-geometry parameter, deg
$f_i()$	functional relationship, $i = 1,30$
f/a	fuel-to-air ratio
g_c	gravitational constant, 100 cm kg/N sec^2 (386.3 lbm in/lbf sec^2)
H	heat, J (Btu)
HVF	heating value of fuel, J/kg (Btu/lbm)
h	specific enthalpy, J/kg (Btu/lbm)
Δh	enthalpy change, J/kg (Btu/lbm)
h_p	turbine enthalpy drop, J/kg $K^{1/2}$ rpm (Btu/lbm $°R^{1/2}$ rpm)
I	polar moment of inertia, N cm sec^2 (lbf in sec^2)
J	mechanical equivalent of heat, 100 N cm/J (9339.6 lbf in/Btu)
K_{AB}	augmentor pressure loss coefficient, N^2 sec^2/kg^2 cm^4 K (lbf^2 sec^2/lbm^2 in^4 °R)
K_B	main combustor pressure loss coefficient, N^2 sec^2/kg^2 cm^4 K (lbf^2 sec^2/lbm^2 in^4 °R)
K_{BLWHT}	fraction of high-pressure-turbine bleed doing work
K_{BLWLT}	fraction of low-pressure-turbine bleed doing work
K_D	duct pressure loss coefficient, N^2 sec^2/kg^2 cm^4 K (lbf^2 sec^2/lbm^2 in^4 °R)
K_{PR5}	low-pressure-turbine discharge pressure loss coefficient
ℓ	length, cm (in.)
M	Mach number
N	rotational speed, rpm
P	total pressure, N/cm^2 (psia)
P/P	pressure ratio
p	static pressure, N/cm^2 (psia)
Q	torque, N cm (in. lbf)
R	gas constant, N cm/kg K (in lbf/lbm °R)
T	total temperature, K (°R)
T/T	temperature ratio
$\Delta T/T$	temperature rise parameter
t	time, sec
u	internal energy, J/kg (Btu/lbm)
V	volume, cm^3 (in^3)
v	velocity, cm/sec (in/sec)
W	stored mass, kg (lbm)
$\dot{w}$	mass flow rate, kg/sec (lbm/sec)
$\dot{w}_c$	corrected mass flow rate, kg/sec (lbm/sec)

$\dot{w}_p$	turbine flow parameter, kg K cm^2/N rpm sec (lbm °R in /lbf rpm sec)
X,Y	map inputs
x	variable
Z	map output
β	interpolation constant
δ	ratio of total pressure to sea-level pressure
γ	ratio of specific heats
η	efficiency
θ	ratio of total temperature to standard-day temperature

Subscripts (note that subscripts may be combined, e.g., $\dot{w}_{F,4}$):

A	air
AB	augmentor
a	actual value
am	ambient
B	main combustor
BL	bleed
BLHT	high-pressure-turbine cooling bleed
BLLT	low-pressure-turbine cooling bleed
BLOV	overboard bleed
C	compressor
cr	critical flow
D	design input
E	exit nozzle plane
es	expelled nozzle shock
F	fuel
fan	fan
H	high-pressure spool
HT	high-pressure turbine
I	inlet
i	initial condition
ID	fan hub region
id	ideal
in	into volume
j	station, j = 0, 2, 2.1, 2.2, 3.4, 4.15, 6, 7, 8, 9, 13, 16
j'	entrance to volume at station j, j = 3, 7, 13
L	low-pressure spool
LT	low-pressure turbine
load	load
M	map
n	net
new	new
OD	fan tip region
old	old
out	out of volume
x	upstream side of shock
y	downstream side of shock

Superscripts:

( )*	sonic flow condition
($\dot{}$)	derivative
-1	inverse matrix

Computer variables:

AE	nozzle exit area, cm^2 (in^2)
ALT	altitude, m (ft)
AQL6	augmentor reactance, kg cm^2/N sec^2 (lbm in^2/lbf sec^2)
AQL13	duct reactance, kg cm^2/N sec^2 (lbm in^2/lbf sec^2)
A8	nozzle throat area, cm^2 (in^2)
BSCVGP	bias on CVGP, deg
BSFVGP	bias on FVGP, deg
CDN	nozzle flow coefficient
CSHIFT	change in compressor flow due to variable geometry
CVGP	compressor variable-geometry parameter, deg
CVN	nozzle velocity coefficient
DELT	change in time, sec
DELTAV	vector change in guess variable
DH4	enthalpy change across high-pressure turbine, J/kg (Btu/lbm)
DH41	enthalpy change across low-pressure turbine, J/kg (Btu/lbm)
DT3	temperature derivative in compressor mixing volume, deg/sec
DT4	temperature derivative in combustor mixing volume, deg/sec
DT41	temperature derivative in high-pressure-turbine mixing volume, deg/sec
DT6	temperature derivative in low-pressure-turbine volume, deg/sec
DT7	temperature derivative in augmentor mixing volume, deg/sec
DT13	temperature derivative in fan mixing volume, deg/sec
DWA13	fluid momentum derivative in duct, kg/sec^2 (lbm/sec^2)
DW3	flow derivative in compressor mixing volume, kg/sec (lbm/sec)
DW4	flow derivative in combustor mixing volume, kg/sec (lbm/sec)
DW41	flow derivative in high-pressure-turbine mixing volume, kg/sec (lbm/sec)
DW6	flow derivative in low-pressure-turbine mixing volume, kg/sec (lbm/sec)
DW7	flow derivative in augmentor mixing volume, kg/sec (lbm/sec)
DW13	flow derivative in fan mixing volume, kg/sec (lbm/sec)
DWG6	fluid momentum derivative in augmentor, kg/sec^2 (lbm/sec^2)
DXNH	high-rotor-speed derivative, rpm/sec
DXNL	low-rotor-speed derivative, rpm/sec
E	error vector
EMAT	Jacobian matrix
ERRBSE	vector of past errors
ETAAB	augmentor efficiency
ETAB	combustor efficiency
ETAHC	compressor efficiency
ETAIF	fan hub efficiency
ETAOF	fan tip efficiency
FG	gross thrust, N (lbf)
FN	net thrust, N (lbf)
FRAC	external control for matrix convergence
FVGP	fan variable-geometry parameter, deg

FSHIFT	change in fan flow due to variable geometry
H	time step, sec
IBDINT	integration select switch
IHPCNV	matrix calculation select switch
IPRINT	print select switch
ISS	initial-condition switch
JSS	steady-state switch
MAPNO	indicator for component map
MATRIX	switch for generating a new Jacobian matrix
MPAS	maximum allowable iteration passes
N	system order
NCOM	map interpolation switch
NCV	number of curves on a map
NFCT	number of common functions
NOBUG	debug printout select switch
NOPER	operating-point select switch
NPT	number of points on a curve
P0	inlet pressure, N/cm^2 (psia)
P2	fan inlet pressure, N/cm^2 (psia)
P13	duct pressure, N/cm^2 (psia)
P22	compressor inlet pressure, N/cm^2 (psia)
P3	combustor pressure, N/cm^2 (psia)
P4	high-pressure-turbine inlet pressure, N/cm^2 (psia)
P41	low-pressure-turbine inlet pressure, N/cm^2 (psia)
P5	intermediate pressure, N/cm^2 (psia)
P6	augmentor inlet pressure, N/cm^2 (psia)
P7	nozzle inlet pressure, N/cm^2 (psia)
PCNCHG	iteration convergence rate
POINT	operating point
REF	desired value of summation of errors
TAM	ambient temperature, K (°R)
T2	fan inlet total temperature, K (°R)
T22	compressor inlet temperature, K (°R)
T3	combustor inlet temperature, K (°R)
T4	high-pressure-turbine inlet temperature, K (°R)
T41	low-pressure-turbine inlet temperature, K (°R)
T6	augmentor inlet temperature, K (°R)
T7	nozzle inlet temperature, K (°R)
T13	duct temperature, K (°R)
TMAX	transient duration, sec
TOL1	lower limit for partial derivative
TOL2	upper limit for partial derivative
TOLPCG	convergence rate at which a new Jacobian matrix is generated
TOLSS	error tolerance
TOUT	output time step, sec
V3	compressor volume, cm^3 (in^3)
V13	duct volume, cm^3 (in^3)
V4	combustor volume, cm^3 (in^3)
V41	high-pressure-turbine volume, cm^3 (in^3)
V6	low-pressure-turbine volume, cm^3 (in^3)
V7	augmentor volume, cm^3 (in^3)
$\underline{\text{VDELTA}}$	initial perturbation in state variables for matrix generation
$\underline{\text{VDOT}}$	vector of state variable derivatives at current time
$\underline{\text{VDOTSV}}$	vector of state variable derivatives at previous time
VDOTT	vector of average state variable derivatives

$\overline{VS}$	vector of state variables
WA13	duct fluid momentum, kg/sec^2 (lbm/sec^2)
WA2	mass flow rate at station 2, kg/sec (lbm/sec)
WA22	mass flow rate at compressor inlet, kg/sec (lbm/sec)
WA3	mass flow rate at combustor inlet, kg/sec (lbm/sec)
WG4	mass flow rate at high-pressure-turbine inlet, kg/sec (lbm/sec)
WG41	mass flow rate at low-pressure-turbine inlet, kg/sec (lbm/sec)
WG7	mass flow rate at nozzle, kg/sec (lbm/sec)
W13	duct volume stored mass, kg (lbm)
W3	compressor volume stored mass, kg (lbm)
W4	combustor volume stored mass, kg (lbm)
W41	high-pressure-turbine volume stored mass, kg (lbm)
W6	low-pressure-turbine volume stored mass, kg (lbm)
W7	augmentor volume stored mass, kg (lbm)
WBLHT	high-pressure-turbine cooling bleed flow, kg/sec (lbm/sec)
WBLLT	low-pressure-turbine cooling bleed flow, kg/sec (lbm/sec)
WBLOV	overboard bleed, kg/sec (lbm/sec)
WF4	main combustor fuel flow, kg/sec (lbm/sec)
WF7	augmentor fuel flow, kg/sec (lbm/sec)
WG6	augmentor fluid momentum, kg/sec^2 (lbm/sec^2)
XIH	high rotor moment of inertia, N cm/sec^2 (lbf in/sec^2)
XIL	low rotor moment of inertia, N cm/sec^2 (lbf in/sec^2)
XMN	Mach number
XNH	low rotor speed, rpm
XNL	high rotor speed, rpm
$\underline{XXX}$	summation of squares of changes in errors to maximum error
$\overline{YYY}$	state change vector

APPENDIX B

ANALYTICAL MODEL

The mathematical model describing the two-spool, two-stream turbofan engine in DIGTEM is described in detail in reference 8. Overall performance maps are used to provide the steady-state representations of the engine's rotating components. Fluid momentum in the bypass duct and the augmentor, mass and energy storage within control volumes, and rotor inertias are also included to provide transient capability. For completeness, the mathematical model is presented below.

Steady-State Model

Flight condition and inlet. - The following conditions define the flight conditions and inlet model:

$$P_0 = f_1(a) \tag{B1}$$

$$T_0 = f_2(a) + T_{am} \tag{B2}$$

$$\begin{aligned} \eta_I &= 1.0 \quad \text{if } M_0 \le 1.0 \\ &= 1.0 - 0.075\,(M_0 - 1.0)^{1.35} \quad \text{if } M_0 > 1.0 \end{aligned} \tag{B3}$$

$$T_2 = T_0\left[1.0 + \frac{(\gamma_I - 1)M_0^2}{2}\right] \tag{B4}$$

$$P_2 = P_0\eta_I\left(\frac{T_2}{T_0}\right)^{\gamma_I/(\gamma_I - 1)} \tag{B5}$$

$$\gamma_I = \gamma_0 = 1.4 \tag{B6}$$

where functions f_1 and f_2 are curve fits to atmospheric data from reference 10.

Gas properties. - Curve fits of data found in reference 11 are used to compute variable thermodynamic gas properties. JP-4 is assumed to be the fuel. For each control volume the following equations are used:

$$c_p = f_3(T, f/a) \tag{B7}$$

$$R = f_4(f/a) \approx R_A \tag{B8}$$

$$c_v = c_p - \frac{R}{J} \tag{B9}$$

$$\gamma = \frac{c_p}{c_v} \tag{B10}$$

$$h = f_5(T, f/a) \tag{B11}$$

Fan. - Fan performance is represented by a set of overall performance maps. Separate maps are used for the tip and hub sections. The maps are assumed to represent fan performance with variable geometry at nominal, scheduled positions. Map-generated, fan-corrected airflow is adjusted to account for off-schedule geometry effects. The following equations describe the fan model:

$$(\dot{w}_c)_{fan,M} = f_6\left(\frac{P_{13}}{P_2}, \frac{N_L}{\theta_2^{1/2}}\right) \tag{B12}$$

ORIGINAL PAGE IS OF POOR QUALITY

$$P_{2.1} = P_{2.2} = P_2 f_7\left(\frac{P_{13}}{P_2}, \frac{N_L}{\theta_2^{1/2}}\right) \tag{B13}$$

$$\dot{w}_2 = \frac{(\dot{w}_c)_{fan,M}\,\delta_2\left[1 + f_8\left(FVGP,\ N_L/\theta_2^{1/2}\right)\right]}{\theta_2^{1/2}} \tag{B14}$$

$$\eta_{fan,OD} = f_9\left(\frac{P_{13}}{P_2}, \frac{N_L}{\theta_2^{1/2}}\right) \tag{B15}$$

$$\left(\frac{\Delta T}{T}\right)_{fan,OD,id} = \left(\frac{P_{13}}{P_2}\right)^{(\gamma_{fan}-1)/\gamma_{fan}} - 1.0 \tag{B16}$$

$$T_{13}' = \left[\frac{(\Delta T/T)_{fan,OD,id}}{\eta_{fan,OD}} + 1\right] T_2 \tag{B17}$$

$$\eta_{fan,ID} = f_{10}\left(\frac{P_{13}}{P_2}, \frac{N_L}{\theta_2^{1/2}}\right) \tag{B18}$$

$$\left(\frac{\Delta T}{T}\right)_{fan,ID,id} = \left(\frac{P_{2.1}}{P_2}\right)^{(\gamma_{fan}-1)/\gamma_{fan}} - 1.0 \tag{B19}$$

$$T_{2.1} = T_{2.2} = \left[\frac{(\Delta T/T)_{fan,ID,id}}{\eta_{fan,ID}} + 1\right] T_2 \tag{B20}$$

$$\gamma_{fan} = \gamma_2 \tag{B21}$$

Compressor. - Overall performance maps are used for the compressor with a shift in the corrected airflow based on off-schedule values of variable-geometry position. The following equations describe the compressor model:

$$(\dot{w}_c)_{C,M} = f_{11}\left(\frac{P_3}{P_{2.2}}, \frac{N_H}{\theta_{2.2}^{1/2}}\right) \tag{B22}$$

$$\dot{w}_{2.2} = \frac{(\dot{w}_c)_{C,M}\delta_{2.2}\left[1 + f_{12}\left(CVGP, N_H/\theta_{2.2}^{1/2}\right)\right]}{\theta_{2.2}^{1/2}} \tag{B23}$$

$$\eta_C = f_{13}\left(\frac{P_3}{P_{2.2}}, \frac{N_H}{\theta_{2.2}^{1/2}}\right) \tag{B24}$$

$$\left(\frac{\Delta T}{T}\right)_{C,id} = \left(\frac{P_3}{P_{2.2}}\right)^{(\gamma_C-1)/\gamma_C} - 1.0 \tag{B25}$$

$$T_C = \beta_C T_{2.2} + (1 - \beta_C)T_3 \tag{B26}$$

$$T_3' = \left[\frac{(\Delta T/T)_{C,id}}{\eta_C} + 1\right] T_{2.2} \tag{B27}$$

Bleeds. - Flow through the bleed passages is assumed to be choked. Both turbine cooling and overboard bleeds are modeled. The equations are as follows:

$$\left(\frac{\dot{w}}{A}\right)_{BL} = P_3\left(\frac{g_c\gamma_3}{R_A T_3}\right)^{1/2}\left(\frac{2}{\gamma_3 + 1}\right)^{(\gamma_3+1)/2(\gamma_3-1)} \tag{B28}$$

$$\dot{w}_{BLHT} = A_{BLHT}\left(\frac{\dot{w}}{A}\right)_{BL} \tag{B29}$$

$$\dot{w}_{BLLT} = A_{BLLT}\left(\frac{\dot{w}}{A}\right)_{BL} \tag{B30}$$

$$\dot{w}_{BLOV} = A_{BLOV}\left(\frac{\dot{w}}{A}\right)_{BL} \tag{B31}$$

Turbines. - Overall performance of the highand low-pressure turbines is represented by bivariate maps. Cooling bleed for each turbine is assumed to reenter the cycle at the turbine discharge although a portion of each bleed is assumed to do work:

$$(\dot{w}_p)_{HT} = f_{14}\left(\frac{P_{4.1}}{P_4}, \frac{N_H}{T_4^{1/2}}\right) \tag{B32}$$

$$\dot{w}_4 = \frac{(\dot{w}_p)_{HT} P_4 N_H}{T_4} \tag{B33}$$

ORIGINAL PAGE IS
OF POOR QUALITY

$$(h_p)_{HT} = f_{15}\left(\frac{P_{4.1}}{P_4}, \frac{N_H}{T_4^{1/2}}\right) \tag{B34}$$

$$(\Delta h)_{HT} = (h_p)_{HT} N_H T_4^{1/2} \tag{B35}$$

$$(\dot{w}_p)_{LT} = f_{16}\left(\frac{P_5}{P_{4.1}}, \frac{N_L}{T_{4.1}^{1/2}}\right) \tag{B36}$$

$$\dot{w}_{4.1} = \frac{(\dot{w}_p)_{LT} P_{4.1} N_L}{T_{4.1}} \tag{B37}$$

$$(h_p)_{LT} = f_{17}\left(\frac{P_5}{P_{4.1}}, \frac{N_L}{T_{4.1}^{1/2}}\right) \tag{B38}$$

$$(\Delta h)_{LT} = (h_p)_{LT} N_L T_{4.1}^{1/2}. \tag{B39}$$

Combustors and ducts. - Total pressure losses are included in the models of the main combustor, bypass duct, mixer entrance, and augmentor. Heat addition associated with the burning of fuel in the main combustor and augmentor is assumed to take place in volumes V_4 and V_7, respectively. The following equations describe the combustor and duct models:

$$\dot{w}_3 = \left[\frac{P_3(P_3 - P_4)}{K_B T_3}\right]^{1/2} \tag{B40}$$

$$T_B = \beta_B T_3 + (1 - \beta_B) T_4 \tag{B41}$$

$$\Delta h_B = HVF \eta_B \tag{B42}$$

$$\eta_B = f_{18}[(f/a)_4] \tag{B43}$$

$$(f/a)_4 = \frac{\dot{w}_{F,4}}{\dot{w}_3} \tag{B44}$$

$$P_5 = K_{PR5} P_6 \tag{B45}$$

$$P_7' = \frac{P_6 - K_{AB}\dot{w}_6^2 T_6}{P_6} \tag{B46}$$

$$T_{AB} = \beta_{AB}T_6 + (1 - \beta_{AB})T_7 \tag{B47}$$

$$Ah_{AB} = HVF\eta_{AB} \tag{B48}$$

$$\eta_{AB} = f_{19}[(f/a)_7] \tag{B49}$$

$$(f/a)_7 = \frac{\dot{w}_{F,7} + \dot{w}_{F,4}}{\dot{w}_6 - \dot{w}_{F,4}} \tag{B50}$$

$$P_6 = \frac{P_{13} - K_D\dot{w}_{13}^2T_{13}}{P_{13}} \tag{B51}$$

$$T_6 = T_{13} \tag{B52}$$

Exhaust nozzle. - A convergent-divergent nozzle configuration is assumed. The following equations define the basic nozzle model and are based on material from reference 12. Simplifications to the basic model, intended to reduce computation time, are noted:

$$\dot{w}_7 = P_7A_E^*C_{d,N}\left(\frac{g_c\gamma_N}{R_AT_7}\right)^{1/2}\left(\frac{2}{\gamma_N + 1}\right)^{(\gamma_N+1)/2(\gamma_N-1)} \tag{B53}$$

$$F_N = \frac{\dot{w}_7V_E}{g_c} + A_E(P_E - P_0) \tag{B54}$$

$$C_{d,N} = f_{20}\left(\frac{P_0}{P_7}\right) \tag{B55}$$

$$\left(\frac{P_0}{P_7}\right)_{cr} = f_{21}\left(\frac{A_E}{A_8}\right) \tag{B56}$$

If $P_0/P_7 \geq (P_0/P_7)_{cr}$, the flow is subsonic in the nozzle and

$$P_E = P_0 \tag{B57}$$

$$\frac{A_E}{A_E^*} = f_{21}^{-1}\left(\frac{P_0}{P_7}\right) \tag{B58}$$

ORIGINAL PAGE IS
OF POOR QUALITY

$$A_E^* = \frac{A_E}{A_E/A_E^*} \tag{B59}$$

$$M_E^* = f_{22}\left(\frac{P_0}{P_7}\right) \tag{B60}$$

$$v_E = M_E^* C_{v,N}\left(\frac{2g_c\gamma_N R_A T_7}{\gamma_N + 1}\right)^{1/2} \tag{B61}$$

$$C_{v,N} = f_{23}\left(\frac{P_0}{P_7}\right) \tag{B62}$$

Otherwise a shock may exist in the divergent portion of the nozzle. To compute the required parameters under these conditions, shock tables such as those in reference 12 must be used.

$$M_x = f_{24}\ \frac{A_E}{A_8} \tag{B63}$$

$$\frac{P_y}{P_x} = f_{25}(M_x) \tag{B64}$$

$$\frac{P_y}{P_x} = f_{26}(M_x) \tag{B65}$$

$$\frac{P_y}{P_x} = f_{27}(M_x) \tag{B66}$$

$$\left(\frac{P_0}{P_7}\right)_{es} = \frac{(P_y/P_x)(p_y/p_x)}{P_y/p_x} \tag{B67}$$

If $P_0/P_7 = (P_0/P_7)_{es}$, the shock will be in the nozzle exit plane. Then

$$P_E = P_0 \tag{B68}$$

$$M_x^* = f_{28}\left(\frac{A_E}{A_8}\right) \tag{B69}$$

$$v_x = M_x^*\left(\frac{2\gamma_N R_A g_c T_7}{\gamma_N + 1}\right)^{1/2} \tag{B70}$$

$$\frac{V_x}{V_y} = f_{29}(M_x) \quad \text{(B71)}$$

$$V_E = \frac{C_{v,N} V_x}{V_x V_y} \quad \text{(B72)}$$

If $P_0/P_7 < (P_0/P_7)_{es}$, the shock is external to the nozzle. Then

$$M_E^* = f_{28}\left(\frac{A_E}{A_8}\right) \quad \text{(B73)}$$

$$\frac{P_E}{P_7} = f_{30}\left(\frac{A_E}{A_8}\right) \quad \text{(B74)}$$

$$P_E = P_7\left(\frac{P_E}{P_7}\right) \quad \text{(B75)}$$

$$V_E = M_E^* C_{v,N}\left(\frac{2\gamma_N R_A g_c T_7}{\gamma_N + 1}\right)^{1/2} \quad \text{(B76)}$$

If $(P_0/P_7)_{cr} > P_0/P_7 > (P_0/P_7)_{es}$, the shock is in the divergent section and

$$P_E = P_0 \quad \text{(B77)}$$

$$\frac{A_x^*}{A_y^*} = \frac{P_y}{P_x} = f_{25}(M_x) \quad \text{(B78)}$$

$$\frac{A_E}{A_y^*} = \left(\frac{A_E}{A_8}\right)\left(\frac{A_x^*}{A_y^*}\right) \quad \text{(B79)}$$

$$\frac{P_E}{P_y} = f_{21}\left(\frac{A_E}{A_y^*}\right) \quad \text{(B80)}$$

$$\frac{P_E}{P_x} = \left(\frac{P_E}{P_y}\right)\left(\frac{P_y}{P_x}\right) \quad \text{(B81)}$$

$$P_E = P_7\left(\frac{P_E}{P_x}\right) \quad \text{(B82)}$$

To solve these equations, M_x can be varied until equations (B82) and (B77) produce the same values for P_E. Then

$$M_E^* = f_{28}\left(\frac{A_E}{A_y^*}\right) \tag{B83}$$

Equations (B53) to (B83) are in subroutine NOZZL. The inputs to NOZZL are ambient pressure, nozzle inlet total pressure, nozzle inlet total temperature, nozzle throat area, nozzle exit area, nozzle pressure ratio, nozzle flow coefficient, and nozzle velocity coefficient. FUN1 is called by NOZZL to interpolate tabular data of functions $f_{21}(A_E/A_8)$, f_{21}^{-1} (P_0/P_7), $f_{22}(P_0/P_7)$, $f_{24}(A_E/A_8)$, and $f_{30}(A_E/A_8)$. Functions $f_{25}(M_x)$ and $f_{26}(M_x)$ are represented by quadratic functions. The iterative loop associated with shock in the divergent section is replaced by a quadratic function of pressure ratio and is biased by a cubic function of area ratio. The result M_E^* is used to compute nozzle exit velocity:

$$V_E = M_E^* C_{V,N}\left(\frac{2\gamma_N R_A g_c T_7}{\gamma_N + 1}\right)^{1/2} \tag{B84}$$

The net thrust is computed by subtracting inlet ram drag from gross thrust:

$$F_n = F_N - M_0 \dot{w}_2 \left(\frac{\gamma_0 R_A T_0}{g_c}\right)^{1/2} \tag{B85}$$

Engine Dynamics

Intercomponent volumes. - As shown in figure 2, intercomponent volumes are assumed at engine locations where (1) gas dynamics are considered important or (2) gas dynamics are required to avoid an iterative solution of the equations. In these volumes storage of energy and mass occurs. The following equations define the dynamic models of the intercomponent volumes (fig. 2):

$$W_{13} = \int_0^t (\dot{w}_2 - \dot{w}_{2.2} - \dot{w}_{13})dt + W_{13,i} \tag{B86}$$

$$T_{13} = \int_0^t \left\{\left[(\dot{w}_2 - \dot{w}_{2.2})(h_{13}' - h_{13})/c_{v,13} + T_{13}(\dot{w}_2 - \dot{w}_{2.2} - \dot{w}_{13})(\gamma_{13} - 1)\right] \Big/ W_{13}\right\} dt + T_{13,i} \tag{B87}$$

$$P_{13} = \frac{R_A W_{13} T_{13}}{V_{13}} \tag{B88}$$

$$W_3 = \int_0^t (\dot{w}_{2.2} - \dot{w}_{BLHT} - \dot{w}_{BLLT} - \dot{w}_{BLOV} - \dot{w}_3)\, dt + W_{3,i} \tag{B89}$$

$$T_3 = \int_0^t \left\{\left[\dot{w}_{2.2}(h_3' - h_3)/c_{v,3} + T_3(\dot{w}_{2.2} - \dot{w}_{BLHT} - \dot{w}_{BLLT} - \dot{w}_{BLOV} - \dot{w}_3) \times (\gamma_3 - 1)\right]\Big/ W_3\right\} dt + T_{3,i} \tag{B90}$$

ORIGINAL PAGE IS OF POOR QUALITY

$$P_3 = \frac{R_A W_3 T_3}{V_3} \tag{B91}$$

$$W_4 = \int_0^t (\dot{w}_3 + \dot{w}_{F.4} - \dot{w}_4)dt + W_{4,i} \tag{B92}$$

$$T_4 = \int_0^t \left(\left\{\left[\dot{w}_3 h_B + \dot{w}_{F,4}\,\Delta h_B - h_4(\dot{w}_3 + \dot{w}_{F,4})\right]\Big/ c_{v,4} + T_4(\dot{w}_3 + \dot{w}_{F,4} - \dot{w}_4)(\gamma_4 - 1)\right\}\Big/ W_4\right) dt + T_{4,i} \tag{B93}$$

$$P_4 = \frac{R_A W_4 T_4}{V_4} \tag{B94}$$

$$W_{4.1} = \int_0^t (\dot{w}_4 + \dot{w}_{BLHT} - \dot{w}_{4.1})dt + W_{4.1,i} \tag{B95}$$

$$T_{4.1} = \int_0^t \left(\left\{\left[\dot{w}_4\,(h_4 - \Delta h_{HT}) + \dot{w}_{BLHT}\,(h_3 - K_{BLWHT}\,\Delta h_{HT}) - h_{4.1}(\dot{w}_4 + \dot{w}_{BLHT})\right]\Big/ c_{v,4.1} + T_{4.1}(\dot{w}_4 + \dot{w}_{BLHT} - \dot{w}_{4.1})(\gamma_{4.1} - 1)\right\}\Big/ W_{4.1}\right) dt + T_{4.1,i} \tag{B96}$$

$$P_{4.1} = \frac{R_A W_{4.1} T_{4.1}}{V_{4.1}} \tag{B97}$$

$$W_6 = \int_0^t (\dot{w}_{4.1} + \dot{w}_{BLLT} + \dot{w}_{13} - \dot{w}_6)dt + W_{6,i} \tag{B98}$$

$$T_6 = \int_0^t \left(\left\{\left[\dot{w}_{4.1}(h_{4.1} - \Delta h_{LT}) + \dot{w}_{BLLT}(h_3 - K_{BLWLT}\,\Delta h_{LT}) + \dot{w}_{13}h_{16} - h_6(\dot{w}_{4.1} + \dot{w}_{BLLT} + \dot{w}_{13})\right]\Big/ c_{v,6} + T_6(\dot{w}_{4.1} + \dot{w}_{BLLT} + \dot{w}_{13} - \dot{w}_6)(\gamma_6 - 1)\right\}\Big/ W_6\right) dt + T_{6,i} \tag{B99}$$

$$P_6 = \frac{R_A W_6 T_6}{V_6} \tag{B100}$$

$$W_7 = \int_0^t (\dot{w}_6 + \dot{w}_{F,7} - \dot{w}_7)dt + W_{7,i} \tag{B101}$$

$$T_7 = \int_0^t \left(\left\{\left[\dot{w}_6 h_{AB} + \dot{w}_{F,7}\, \Delta h_{AB} - h_7(\dot{w}_6 + \dot{w}_{F,7})\right] \Big/ c_{v,7} + T_7(\dot{w}_6 + \dot{w}_{F,7} - \dot{w}_7)(\gamma_7 - 1)\right\} \Big/ W_7\right) dt + T_{7,i} \tag{B102}$$

$$P_7 = \frac{R_A W_7 T_7}{V_7} \tag{B103}$$

Fluid momentum. - The effects of fluid momentum are considered in the bypass duct and augmentor duct models:

$$\dot{w}_{13} = g_c \left(\frac{A}{\ell}\right)_D \int_0^t (P_{16} - P_6)dt + \dot{w}_{13,i} \tag{B104}$$

$$\dot{w}_6 = g_c \left(\frac{A}{\ell}\right)_{AB} \int_0^t (P_7' - P_7)dt + \dot{w}_{6,i} \tag{B105}$$

Rotor inertias. - Rotor speeds are computed from dynamic forms of the angular momentum equations:

$$N_L = \left(\frac{30}{\pi}\right)^2 \frac{J}{I_L} \int_0^t \left\{\left[\Delta h_{LT}(\dot{w}_{4.1} + K_{BLWLT}\dot{w}_{BLLT}) - (\dot{w}_2 - \dot{w}_{2.2})(h_{13}' - h_2) - \dot{w}_{2.2}(h_{2.2} - h_2)\right] \Big/ N_L\right\} dt + N_{L,i} \tag{B106}$$

$$N_H = \left(\frac{30}{\pi}\right)^2 \frac{J}{I_H} \int_0^t \left\{\left[\Delta h_{HT}(\dot{w}_4 + K_{BLWHT}\dot{w}_{BLHT}) - \dot{w}_{2.2}(h_3' - h_{2.2})\right] \Big/ N_H\right\} dt + N_{H,i} \tag{B107}$$

Correction Coefficients for "Trimming" Model

In DIGTEM, design-point data throughout the engine are specified as input. If the turbofan engine model in DIGTEM was exact, the specified input data would lead to a perfectly balanced engine condition. However, incompatibilities between the DIGTEM input data and the model will result in nonzero derivatives or mismatches between predicted and specified outputs of component maps. To compensate for these differences, a "self-trimming" feature has been built into DIGTEM. Correction coefficients are calculated in subroutine DSGNPT to balance the engine at the dry design point. For example, the input data include $P_{0,D}$, $P_{2,D}$, $T_{2,D}$, T_{am}, M_D, and a_D, where subscript D indicates design-point input data. In DSGNPT, subroutine FLCOND is called by using a_D, M_D, and T_{am} as inputs. The resulting output variables are $P_{2,a}$, $T_{2,a}$, $P_{0,a}$, and $T_{0,a}$, where subscript a stands for the actual calculated value. Ideally

$$P_{2,a} = P_{2,D} \tag{B108}$$

$$T_{2,a} = T_{2,D} \tag{B109}$$

$$P_{0,a} = P_{0,D} \tag{B110}$$

However, if they are not equal, the equations that use these values will be scaled by correction coefficients. DSGNPT is called only once (at the design point) to calculate these coefficients. The correction coefficients are then part of the model. They are used at both the design point and the off-design points. The scaling coefficients for the inlet conditions are

$$CC_1 = \frac{P_{2,D}}{P_{2,a}} \tag{B111}$$

$$CC_2 = \frac{T_{2,D}}{T_{2,a}} \tag{B112}$$

$$CC_3 = \frac{P_{0,D}}{P_{0,a}} \tag{B113}$$

These coefficients are used to scale the inlet model. Equation (B1) becomes

$$P_0 = f_1(a) \times CC_3 \tag{B114}$$

equation (B4) becomes

$$T_2 = T_0 \left[1.0 + \frac{(\gamma_I - 1) M_0^2}{2}\right] \times CC_2 \tag{B115}$$

and equation (B5) becomes

$$P_2 = P_0 \eta_I \left(\frac{T_2}{T_0}\right)^{\gamma_I/(\gamma_I - 1)} \times CC_1 \tag{B116}$$

The other correction coefficients and their corresponding "trimmed" equation are presented below. For the fan

ORIGINAL PAGE IS
OF POOR QUALITY

$$CC_4 = \frac{\dot{w}_{2,D}}{\dot{w}_{2,a}} \tag{B117}$$

and equation (B14) becomes

$$w_2 = \frac{(\dot{w}_c)_{fan,M}\,\delta_2\left[1 + f_8(FVGP,\ N_L/\theta_2^{1/2})\right]}{\theta_2^{1/2}} \times CC_4 \tag{B118}$$

Also

$$CC_5 = \frac{(\Delta T/T)_{fan,OD,id,D}}{\eta_{fan,OD,D}\ (T_{13,D}/T_{2,D} - 1.0)} \tag{B119}$$

and equation (B17) becomes

$$T_{13}' = \left[\frac{(\Delta T/T)_{fan,OD,id}}{\eta_{fan,OD} \times CC_5} + 1\right] \times T_2 \tag{B120}$$

Also

$$CC_6 = \frac{P_{2.2,D}}{P_{2.2,a}} \tag{B121}$$

and equation (B13) becomes

$$P_{2.1} = P_{2.2} = P_2 f_7\left(\frac{P_{13}}{P_2},\ \frac{N_L}{\theta_2^{1/2}}\right) \times CC_6 \tag{B122}$$

Also

$$CC_7 = \frac{(\Delta T/T)_{fan,ID,id,D}}{\eta_{fan,ID,D}\ (T_{2.2,D}/T_{2,D} - 1.0)} \tag{B123}$$

and equation (B20) becomes

$$T_{2.1} = T_{2.2} = \left[\frac{(\Delta T/T)_{fan,ID,id}}{\eta_{fan,ID} \times CC_7} + 1\right] \times T_2 \tag{B124}$$

For the compressor the same scaling procedure is used. That is

$$CC_8 = \frac{\dot{w}_{2.2,D}}{\dot{w}_{2.2,a}} \tag{B125}$$

and equation (B23) becomes

$$\dot{w}_{2.2} = \frac{(\dot{w}_C)_{C,M}\delta_{2.2}\left[1 + f_{12}(CVGP, N_H/\theta_{2.2}^{1/2})\right]}{\theta_{2.2}^{1/2}} \times CC_8 \qquad (B126)$$

Also

$$CC_9 = \frac{(\Delta T/T)_{C,id,D}}{\eta_{C,D}\,(T_{2.2,D}/T_{2,D} - 1.0)} \qquad (B127)$$

and equation (B27) becomes

$$T_3' = \left[\frac{(\Delta T/T)_{C,id}}{\eta_C \times CC_9} + 1\right] \times T_{2.2} \qquad (B128)$$

For the turbines

$$CC_{11} = \frac{\dot{w}_{4,D}}{\dot{w}_{4,a}} \qquad (B129)$$

and

$$CC_{13} = \frac{\dot{w}_{4.1,D}}{\dot{w}_{4.1,a}} \qquad (B130)$$

Equations (B33) and (B37) become, respectively

$$\dot{w}_4 = \frac{(\dot{w}_p)_{HT} P_4 N_H}{T_4} \times CC_{11} \qquad (B131)$$

and

$$\dot{w}_{4.1} = \frac{(\dot{w}_p)_{LT} P_{4.1} N_L}{T_{4.1}} \times CC_{13} \qquad (B132)$$

The next set of correction coefficients zeros out the state variable derivatives associated with energy balances in the intercomponent volumes:

$$CC_{10} = \frac{h_{4,D}\left(\dot{w}_{3,D} + \dot{w}_{F,4,D}\right) - \dot{w}_{3,D} h_{B,D}}{\dot{w}_{F,4,D}\,\Delta h_{B,D}} \qquad (B133)$$

ORIGINAL PAGE IS
OF POOR QUALITY

and equation (B93) becomes

$$T_4 = \int_0^t \left(\left\{ \left[\dot{w}_3 h_B + \dot{w}_{F,4} \Delta h_B \times CC_{10} - h_4 (\dot{w}_3 + \dot{w}_{F,4}) \right] \Big/ c_{v,4} + T_4 (\dot{w}_3 + \dot{w}_{F,4} - \dot{w}_4) (\gamma_4 - 1) \right\} \Big/ W_4 \right) dt + T_{4,i} \tag{B134}$$

Note that

$$\dot{w}_3 + \dot{w}_{F,4} - \dot{w}_4 = 0 \tag{B135}$$

in steady state. Also

$$CC_{12} = \frac{\dot{w}_{4,D} h_{4,D} + h_{3,D} \dot{w}_{BLHTD} - h_{4.1D} (\dot{w}_{4,D} + \dot{w}_{BLHTD})}{\Delta h_{HTD} (\dot{w}_{4,D} + \dot{w}_{BLHTD} K_{BLWHTD})} \tag{B136}$$

and equation (B96) becomes

$$T_{4.1} = \int_0^t \left(\left\{ \left[\dot{w}_4 h_4 + h_3 \dot{w}_{BLHT} - h_{4.1} (\dot{w}_4 + \dot{w}_{BLHT}) - CC_{12} \Delta h_{HT} (\dot{w}_4 + \dot{w}_{BLHT} K_{BLWHT}) \right] \Big/ c_{v,4.1} + T_{4.1} (\dot{w}_4 + \dot{w}_{BLHT} - \dot{w}_{4.1}) (\gamma_{4.1} - 1) \right\} \Big/ W_{4.1} \right) dt + T_{4.1,i} \tag{B137}$$

In steady state

$$\dot{w}_4 + \dot{w}_{BLHT} - \dot{w}_{4.1} = 0 \tag{B138}$$

Also

$$CC_{14} = \frac{\dot{w}_{4.1,D} h_{4.1,D} + h_{3,D} \dot{w}_{BLLTD} + \dot{w}_{13,D} h_{16,D} - h_{6,D} (\dot{w}_{4.1,D} + \dot{w}_{BLLTD} + \dot{w}_{13,D})}{\Delta h_{LTD} (\dot{w}_{4.1,D} + \dot{w}_{BLLTD} K_{BLWLTD})} \tag{B139}$$

and equation (B99) becomes

$$T_6 = \int_0^t \left(\left\{ \left[\dot{w}_{4.1} h_{4.1} + h_3 \dot{w}_{BLLT} + \dot{w}_{13} h_{16} - h_6 (\dot{w}_{4.1} + \dot{w}_{BLLT} + \dot{w}_{13}) \right. \right. \right.$$

$$- CC_{14}\,\Delta h_{LT}(\dot{w}_{4.1} + \dot{w}_{BLLT}K_{BLWLT})\Big]\Big/ c_{v,b}$$

$$+ T_6\,(\dot{w}_{4.1} + \dot{w}_{BLLT} + \dot{w}_{13} - \dot{w}_6)\,(\gamma_6 - 1)\Big\}\Big/W_6\Big)\,dt + T_{6,1} \tag{B140}$$

In steady state

$$\dot{w}_{4.1} + \dot{w}_{BLLT} + \dot{w}_{13} - \dot{w}_6 = 0 \tag{B141}$$

The next two correction coefficients are used to zero the speed derivatives at the design point. For the high rotor speed

$$CC_{15} = \frac{\dot{w}_{2.2,D}\,(h_{3,D} - h_{2.2,D})}{\Delta h_{HTD}\,(\dot{w}_{4,D} + K_{BLWHTD}\dot{w}_{BLHTD})} \tag{B142}$$

and equation (B107) becomes

$$N_H = \left(\frac{30}{\pi}\right)^2 \frac{J}{I_H} \int_0^t \Big\{\Big[\Delta h_{HT}\,(\dot{w}_4 + K_{BLWHT}\dot{w}_{BLHT}) \times CC_{15}$$

$$- \dot{w}_{2.2}\,(h_3' - h_{2.2})\Big]\Big/ N_H\Big\}\,dt + N_{H,1} \tag{B143}$$

For the low rotor speed

$$CC_{16} = \frac{(\dot{w}_{2,D} - \dot{w}_{2.2,D})(h_{13,D} - h_{2,D}) + \dot{w}_{2.2,D}\,(h_{2.2,D} - h_{2,D})}{\Delta h_{LTD}\,(\dot{w}_{4.1,D} + K_{BLWLTD}\dot{w}_{BLLTD})} \tag{B144}$$

and equation (B106) becomes

$$N_L = \left(\frac{30}{\pi}\right)^2 \frac{J}{I_L} \int_0^t \Big\{\Big[\Delta h_{LT}\,(\dot{w}_{4.1} + K_{BLWLT}\dot{w}_{BLLT}) \times CC_{16}$$

$$- (\dot{w}_2 - \dot{w}_{2.2})\,(h_{13}' - h_2) - \dot{w}_{2.2}\,(h_{2.2} - h_2)\Big]\Big/ N_L\Big\}\,dt + N_{L,1} \tag{B145}$$

The last three correction coefficients compensate for the imbalances in the augmentor and nozzle models

$$CC_{17} = \frac{\dot{w}_{7,D}}{\dot{w}_{7,a}} \tag{B146}$$

and equation (B53) becomes

$$\dot{w}_7 = P_7 A_E^* C_{d,N} \left(\frac{g_c \gamma_N}{R_A T_7}\right)^{1/2} \left(\frac{2}{\gamma_N + 1}\right)^{(\gamma_N+1)/2(\gamma_N-1)} \times CC_{17} \tag{B147}$$

In the augmentor

$$CC_{18} = \frac{h_{7,D} \left(\dot{w}_{6,D} + \dot{w}_{F,7,D}\right) - \dot{w}_{6,D}\, h_{AB,D}}{\dot{w}_{F,7,D}\, \Delta h_{AB,D}} \tag{B148}$$

and equation (B102) becomes

$$T_7 = \int_0^t \left(\left\{\left[\dot{w}_6 h_{AB} + \dot{w}_{F,7}\, \Delta h_{AB} \times CC_{18} - h_7 \left(\dot{w}_6 + \dot{w}_{F,7}\right)\right] \Big/ c_{v,7} + T_7 \left(\dot{w}_6 + \dot{w}_{F,7} - \dot{w}_7\right) \left(\gamma_7 - 1\right)\right\} \Big/ W_7\right) dt + T_{7,1} \tag{B149}$$

Note that in steady state

$$\dot{w}_6 + \dot{w}_{F,7} - \dot{w}_7 = 0 \tag{B150}$$

Finally for the thrust

$$CC_{19} = \frac{F_{N,D} - A_E \left(P_E - P_0\right)}{F_{N,a} - A_E \left(P_E - P_0\right)} \tag{B151}$$

and equation (B54) becomes

$$F_N = \frac{\dot{w}_7 V_E}{g_c} \times CC_{19} + A_E \left(P_E - P_0\right) \tag{B152}$$

APPENDIX C

INTEGRATION AND ITERATION SCHEMES

Steady-State Balancing Technique

The following discussion explains the iterative method that DIGTEM uses to calculate steady-state operating points. The calculation of a steady-state operating point requires the solution of a system of nonlinear equations, corresponding to various engine matching constraints such as rotational speeds, airflows, compressor and turbine work functions, and nozzle flow functions. To satisfy these constraints, there must be available an equal number of engine parameters that can be varied (such as compressor and turbine pressure ratios and flow functions). For the turbofan engine model in DIGTEM there are 16 engine parameters (independent variables) and 16 error variables (dependent variables). DIGTEM searches for the value of each engine parameter that results in the engine error variables being reduced to zero.

If the independent variables are denoted by VS and the dependent variables by E, the matching equations can be written as

$$E_i (VS_j) = 0 \qquad i = 1,2,\ldots, N;\ j = 1,2,\ldots, N \tag{C1}$$

The procedure used to satisfy the set of nonlinear equations is the multivariable Newton-Raphson method, where changes in E are assumed to be related to changes in VS by a first-order, finite-difference equation

$$\Delta E = EMAT \times \Delta VS \tag{C2}$$

where ΔVS and ΔE are N-vectors denoting changes in VS and E from some reference condition (operating point) and EMAT is an NXN Jacobian matrix of partial derivatives of E with respect to VS

$$EMAT_{ij} = \frac{\partial E_i}{\partial VS_j} \tag{C3}$$

EMAT is calculated by using finite differences about an operating point such that equation (C3) is approximated by

$$EMAT_{ij} = \frac{\Delta E_i}{\Delta VS_j} \qquad i = 1,2,\ldots,N;\ j = 1,2,\ldots,N \tag{C4}$$

Once the Jacobian matrix is obtained, the steady-state balance at the operating point is improved by

$$\overline{VS}_{new} = \overline{VS}_{old} - \overline{EMAT}^{-1} \times \bar{E}_{old} \tag{C5}$$

If the system of equations were linear, the process would lead to convergence in one iteration. In practice, nonlinearities in the system prevent immediate convergence. In this case the new VS and E are taken to be the reference values and a new matrix is generated. If the system is not too nonlinear and the initial guesses for VS are reasonably accurate, convergence is achieved in relatively few iterations.

Dynamic Equations

Once an initial steady-state solution has been obtained, a time-varying solution may be generated. This requires the solution of a set of differential equations that model the system. In this section the procedure used to solve the set of differential equations in DIGTEM is discussed.

Consider the differential equation

$$\dot{x} = f(x,t) \tag{C6}$$

To obtain the numerical solution on a digital computer, the differential equation must be approximated by a difference equation. One common method is to use Euler's method where equation (C6) is approximated by

$$X_{n+1} = X_n + f(X_n, t_n)\ \Delta T \tag{C7}$$

Equation (C7) allows for explicit calculation of X_{n+1} as a function of the previous values of X_n and t_n. This Euler integration method is the forward-difference integration scheme included in DIGTEM. When an explicit method is used for integrating a system of equations, the integration time step is restricted by the highest frequency in the system (as derived in ref. 6). However, dynamic engine simulations contain both high and low frequencies. The high frequencies result from the lumped-volume representation of component dynamics, which includes storage of mass and energy. Low frequencies result from rotor dynamics. In DIGTEM the range of frequencies for the test case is 0.4 to 330 Hz. Frequently the simulation user is interested in low-frequency effects such as rotor transients and is not concerned about high-frequency effects. These transients typically are 5 to 10 sec in duration. However, the user must still use a small integration time step to insure numerical stability. Although it gives very accurate results, this requirement can cause large amounts of computer time to be used. In DIGTEM the largest time step that can be used with the Euler integration method is approximately 0.1 msec for the test case. Thus the 20-sec transient used in the DIGTEM test case consumed 417 sec of CPU time on the IBM 370/3033 computer.

Another method for approximating equation (C6) is the improved Euler:

$$X_{n+1} = X_n + f(X_{n+1}, t_{n+1})\ \Delta T \tag{C8}$$

In general equation (C8) cannot be solved explicitly for X_{n+1} because of the dependence of f on X_{n+1}. Thus some form of iteration must be used at each time step. For this implicit formulation there is no restriction on step size (ref 6) to guarantee numerical stability. However, some loss in dynamic accuracy can occur if the step size is too large.

Experience has shown that a modification to equation (C8) can speed up convergence at each time step. This form of the improved Euler is

$$X_{n+1} = X_n + \frac{\Delta T}{2}\left[f(X_n, t_n) + f(X_{n+1}, t_{n+1})\right] \tag{C9}$$

where the first guess at X_{n+1} is given by

$$X_{n+1} = X_n + f(X_n, t_n)\,\Delta T \tag{C10}$$

Equation (C9) is iteratively used to correct X_{n+1} until convergence criteria are satisfied. This is the integration method used in DIGTEM.

Implementation in DIGTEM

In DIGTEM, data are read in for each operating point. If the operating point is a design point, correction coefficients are calculated to try to force a balanced engine condition. The derivatives are calculated by using the input data and the correction coefficients. For a steady-state condition the error vector is the derivative vector; thus

$$\overline{VDOT} = \overline{0.0} = \overline{E} \tag{C11}$$

where all errors are scaled by the corresponding state variables. If all of the errors are within tolerance (TOLSS - set by the user), the operating point is a balanced condition; if not, DIGTEM iterates to force a balanced condition. The iteration technique is the steady-state balancing technique described earlier.

To perform the iteration, a Jacobian matrix $\overline{EMAT}$ must be formed. $\overline{EMAT}$ is a matrix of partial derivatives of changes in error variables with respect to changes in guess variables. In DIGTEM the guess variables are the state variables (VS) and EMAT is formed by finite differences:

$$EMAT(I,J)=(E(J) - ERRBSE(J))/DELTAV(I) \tag{C12}$$

For each iteration, guess variables are updated by using the old guess vector VS_{old}, the current error vector $\overline{E}$, and the inverted Jacobian matrix:

$$\overline{VS}_{new} = -\overline{EMAT}^{-1} \times \overline{E} + \overline{VS}_{old} \tag{C13}$$

Updating takes place until all derivatives ($\overline{VDOT}$) are within tolerance.

If a transient is to be run, the procedure is as follows: one of the controls or input conditions is offset from the steady-state balanced condition. For transient operation the error vector is redefined by using the improved Euler approximation

$$\overline{VDOTT} \times DELT - (\overline{VS}_{new} - \overline{VS}_{old}) = \overline{E} \tag{C14}$$

where

$$\overline{VDOTT} = \frac{\overline{VDOT} + \overline{VDOTSV}}{2.0} \tag{C15}$$

and all errors are scaled by the last converged corresponding state variable.

Note that in steady state $\overline{VDOT}$ equals $\overline{VDOTSV}$ and $\overline{VS}_{new}$ equals $\overline{VS}_{old}$. However, once an input or control is changed, one or more of the errors are forced to be nonzero ($\overline{VDOT}$ changes). This forces a change in $\overline{VS}_{new}$ to satisfy the equations. Updating is accomplished by using the already generated $\overline{EMAT}$ and equation (C13).

As $\overline{VS}_{new}$ starts to move away from the initial operating point, the original Jacobian matrix is used until it no longer provides a good approximation of the change in errors with respect to the change in states. The decision to calculate a new matrix is defined by the user by setting TOLPCG. DIGTEM calculates a convergence rate, PCNCHG, during a transient. A new matrix is calculated if

$$PCNCHG < TOLPCG \tag{C16}$$

A new matrix is also calculated if the maximum number of allowable passes MPAS is exceeded during an iteration. Here again MPAS is set by the user. Both these conditions are used to try to minimize the number of Jacobian matrices and subsequent inverses since these calculations are time consuming. Table II lists the implicit integration parameter settings in BDINTG. These settings work well with the model and data supplied with DIGTEM but can be changed by the user if problems occur with different input data or a different engine configuration.

Matrix Calculation

There are several features in BDINTG that help the implicit integration scheme converge.

Perturbation calculation. - Since finite differences are used to generate the Jacobian matrix, the sizes of the perturbations of the states are important. If they are too large, errors will be introduced by the system nonlinearities. If they are too small, the partial derivatives will be in error because of numerical problems (without double-precision arithmetic).

Thus a tuning mechanism has been included in BDINTG to optimize the sizes of the perturbations. For the first point the first perturbation of each state variable is 0.1 percent (VDELTA = 0.001). For each perturbation the sum of squares of the errors is calculated. Once this is done, the "goodness" of the partial is checked by calculating

$$XXX = \frac{1}{N} \sqrt{\sum_{I=1}^{N} \left[E(I) - ERRBSE\ (I)\right]^2} \tag{C17}$$

for each state variable and then checking if

$$TOL1 \leq XXX \leq TOL2 \tag{C18}$$

If all XXX's fall within the tolerance band, the matrix is considered "good." For this simulation, TOL1 = 0.001 and TOL2 = 0.01 work well for the operating points.

Scaling of perturbations. - In general, for the initial perturbations at a point the XXX's will not fall in the tolerance band described above. Thus BDINTG scales the perturbations to try to force the XXX's within the band. This is done by calculating

$$YYY = \frac{REF}{XXX} \tag{C19}$$

for each state variable. REF is defined as being the center of the tolerance band:

$$REF = \frac{TOL1 + TOL}{2.0} \tag{C20}$$

Once the set of YYY's has been calculated such that the XXX's fall within the band, the set of YYY's is stored. After this has been done for all N states, the scaling vector YYY is generated. When a new matrix is needed, the scaling vector YYY is applied to the current states to determine first guesses for the perturbations needed to obtain new partial derivatives. If for any state variable the new XXX falls outside the tolerance band, YYY is updated and the new result is stored. This method generally reduces the number of passes required for subsequent matrix generation.

Error Messages

In generating a partial derivative, a situation may arise where XXX never gets within tolerance. When this happens, the program prints out an error message:

CHECK INPUT - BAD PARTIAL DERIVATIVE

prints out a debug output to help the user diagnose the problem, and then stops the simulation. This is the only time when the simulation is stopped except for a normal exit (i.e., ITRAN incremented to its final value, ITRMAX). In general, bad partial derivatives occur when inconsistent coding is added to the simulation.

Another error message occurs when the simulation does not converge. This situation occurs when MPAS (set at 50) is exceeded. A message is printed out, for example

ITERATION FAILURE 15 51 20

The numbers printed out are the number of converged errors (may be any number from 0 to N, 15 is shown here), the number of iteration passes (MPAS + 1), and the point at which the convergence failed (ITRAN).

In this situation, a debug output is printed. This is the same debug output a for the bad partial derivative, and it indicates

I	counter up to system order
VS	current guess variable
VCONV	past converged guess variable
VDOT	current state derivative
VDOTT	averaged state variable derivative between current time point and past time point
E	current errors

After the printout the simulation continues. Note that with the implicit method a convergence failure can occur even if the errors are very close to the tolerance band. Since the simulation may recover after the failure, the simulation is allowed to continue and the user may make a judgment as to the validity of the data after a convergence failure. The occurrence of many convergence failures in a transient, however, usually indicates a need for the user to increase tolerance or to check the input and coding.

The debug output, as described, is generated by BDINTG by setting NOBUG = 1 (table II). The user may want to reprogram the logic to obtain debug output at other times when difficult convergence problems are encountered.

Other error messages are issued in DIGTEM. These are

MAP . NO. INPUTS OUT OF RANGE

XIN = YIN = MATRIX =

and

FUNCTION NO. INPUT OUT OF RANGE

XIN = MATRIX =

These are output from subroutines MOOR and FOOR, respectively. The MAP NO. in the first error message corresponds to the MAPNO described earlier for the component maps. The function out-of-range problem is a little more difficult to debug since the single-valued interpolation routine FUN1 is used in subroutines FLCOND, TRAT, and NOZZL. In either out-of-range case the inputs are printed and the user must locate the map or function in question to debug the problem. Depending on the engine being simulated, maps or functions, or both, may have to be extended. MATRIX is printed out to indicate if a perturbation is being performed to generate a Jacobian matrix since this may cause a map or function to go out of range.

Convergence Aids

BDINTG has some built-in parameters to help the user if convergence problems occur. These are listed in table II. FRAC can be used to force a larger or smaller iteration time step. TOL1 and TOL2 can be shifted depending on the linearity of the system being simulated. TOLSS can be increased if convergence is difficult. MPAS can be increased and finally TOLPCG can be decreased. ISS is set internally to define a steady-state or transient run. MATRIX can be controlled externally by using IHPCNV (from table I). IPRINT is set to obtain the printout described in the test case. If the user desires a more detailed printout for the transient, this can be obtained by resetting the IPRINT from 1 to 0 in BDINTG. Finally VDELTA can be changed to help generate better partial derivatives.

APPENDIX D

ORIGINAL PAGE IS
OF POOR QUALITY

FLOW CHARTS

This appendix contains flow charts for the main program DIGTEM and all of its subroutines.

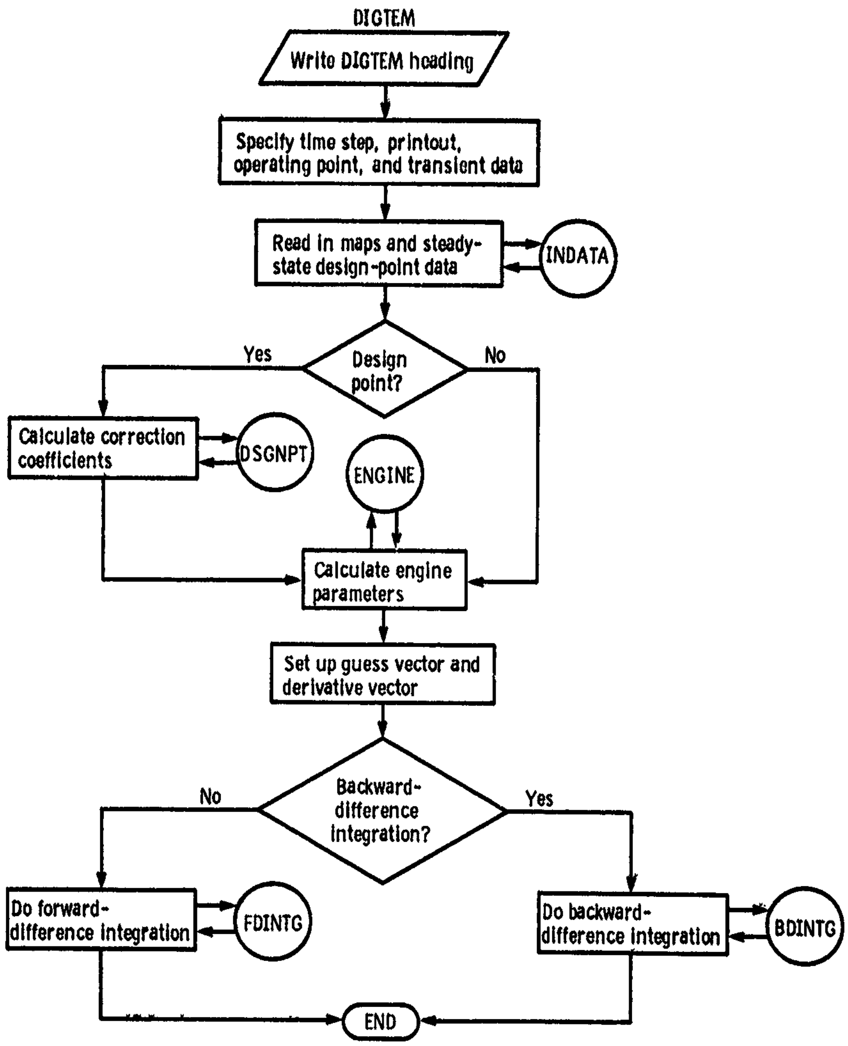

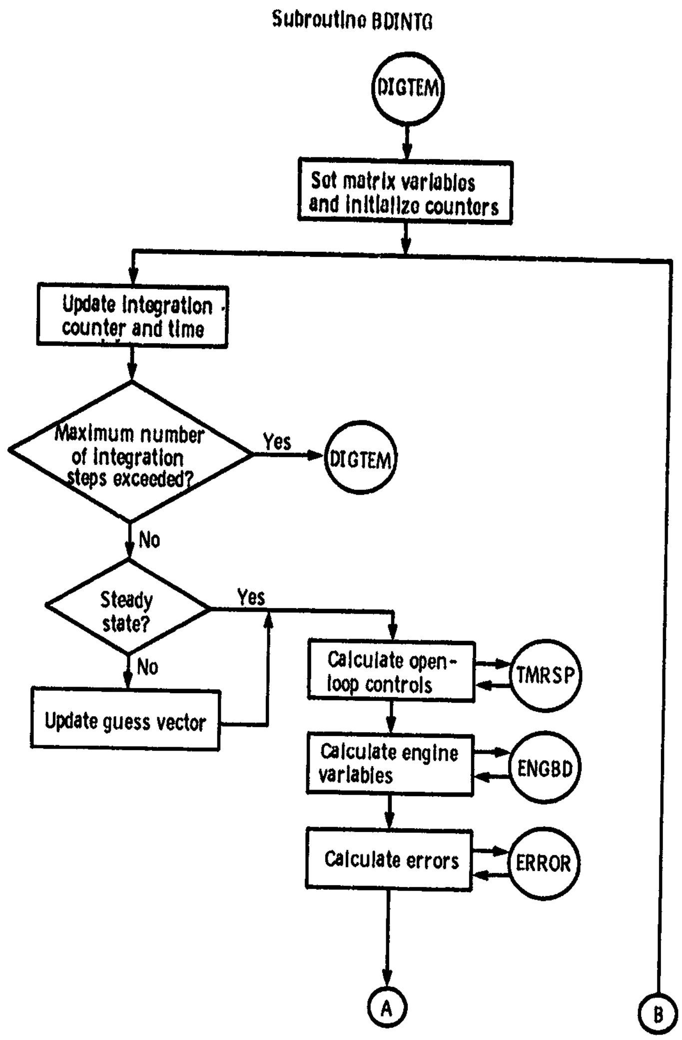
Subroutine BDINTG
DIGTEM
Set matrix variables and initialize counters
Update integration counter and time
Maximum number of integration steps exceeded?
Yes
DIGTEM
No
Steady state?
Yes
No
Update guess vector
Calculate open-loop controls
TMRSP
Calculate engine variables
ENGBD
Calculate errors
ERROR
A
B

ORIGINAL PAGE IS
OF POOR QUALITY

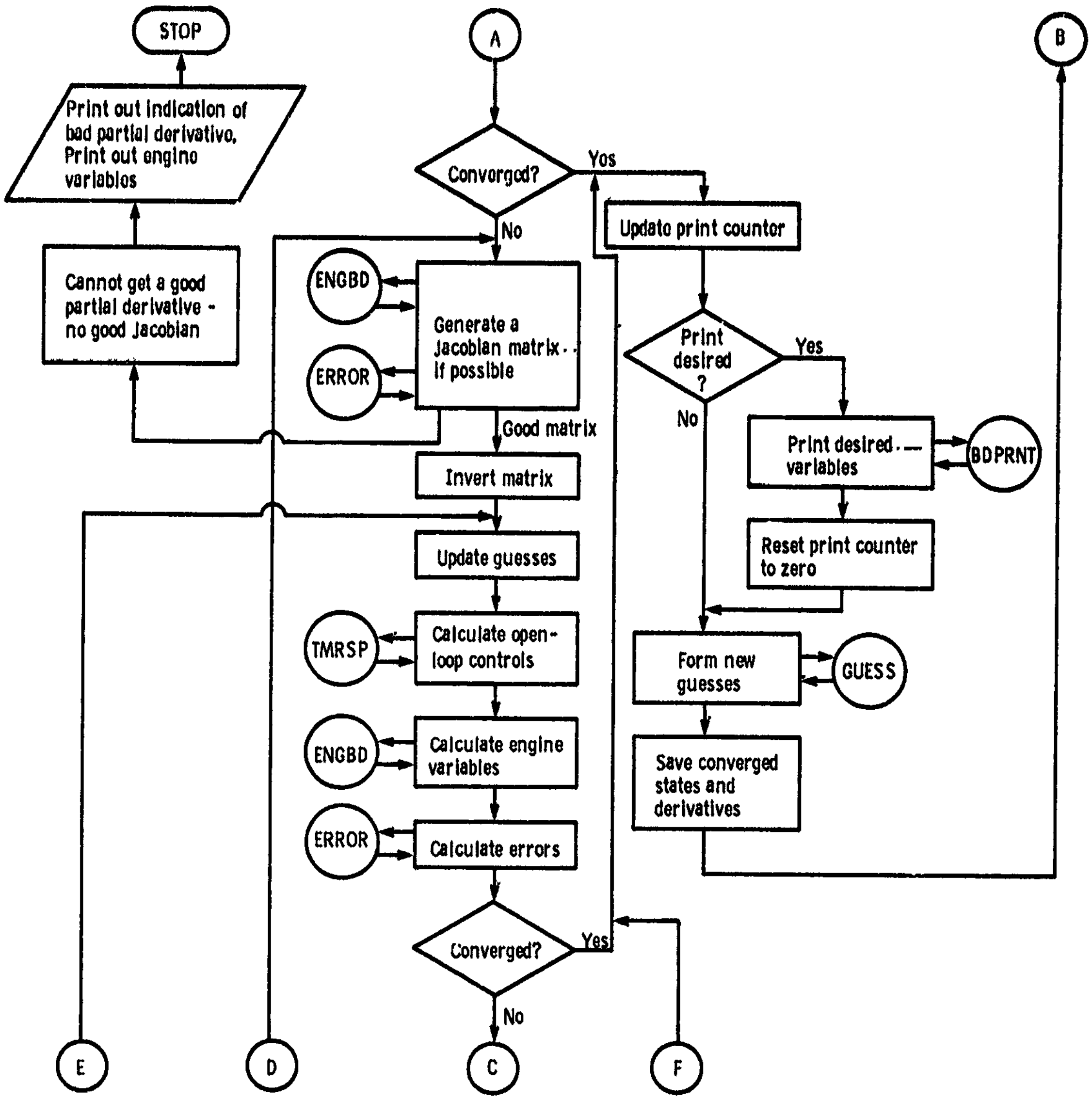

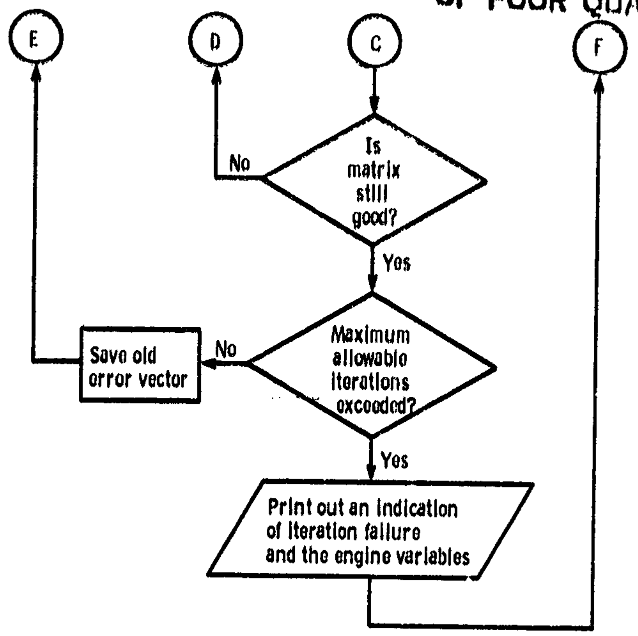

Subroutine BDPRNT

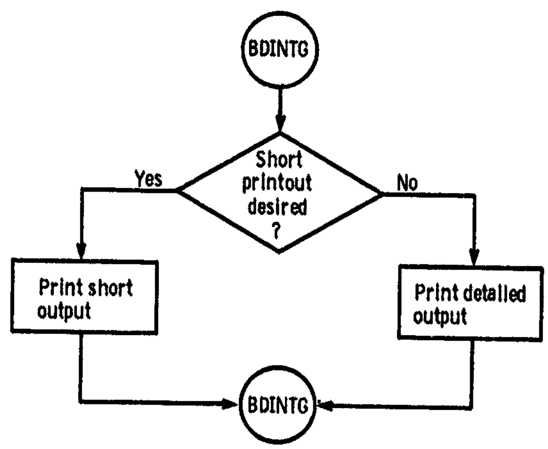

Subroutine DCTINT

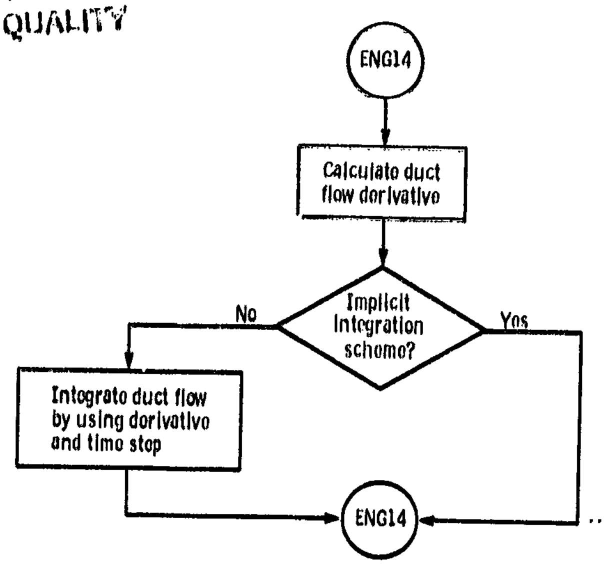

Subroutine DSGNPT

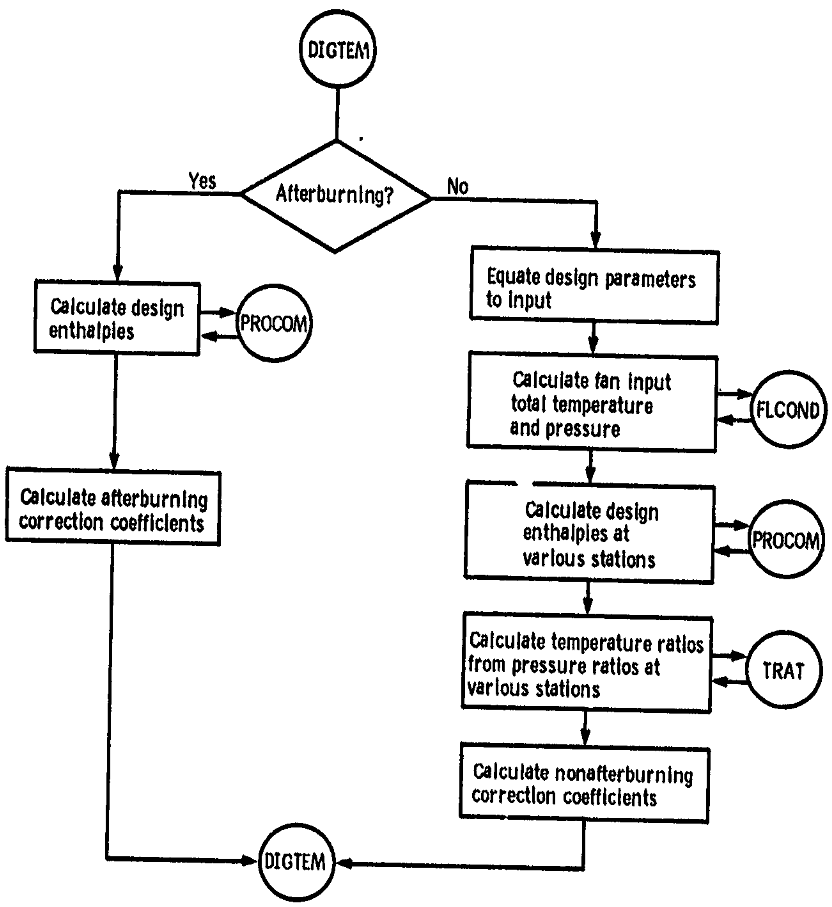

Subroutine DMINV

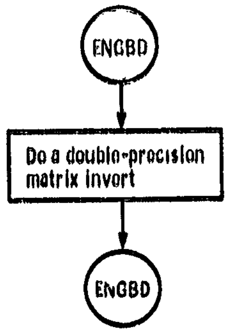

Subroutine DUCT

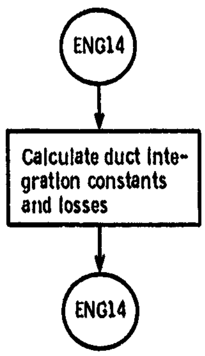

ORIGINAL PAGE IS
OF POOR QUALITY

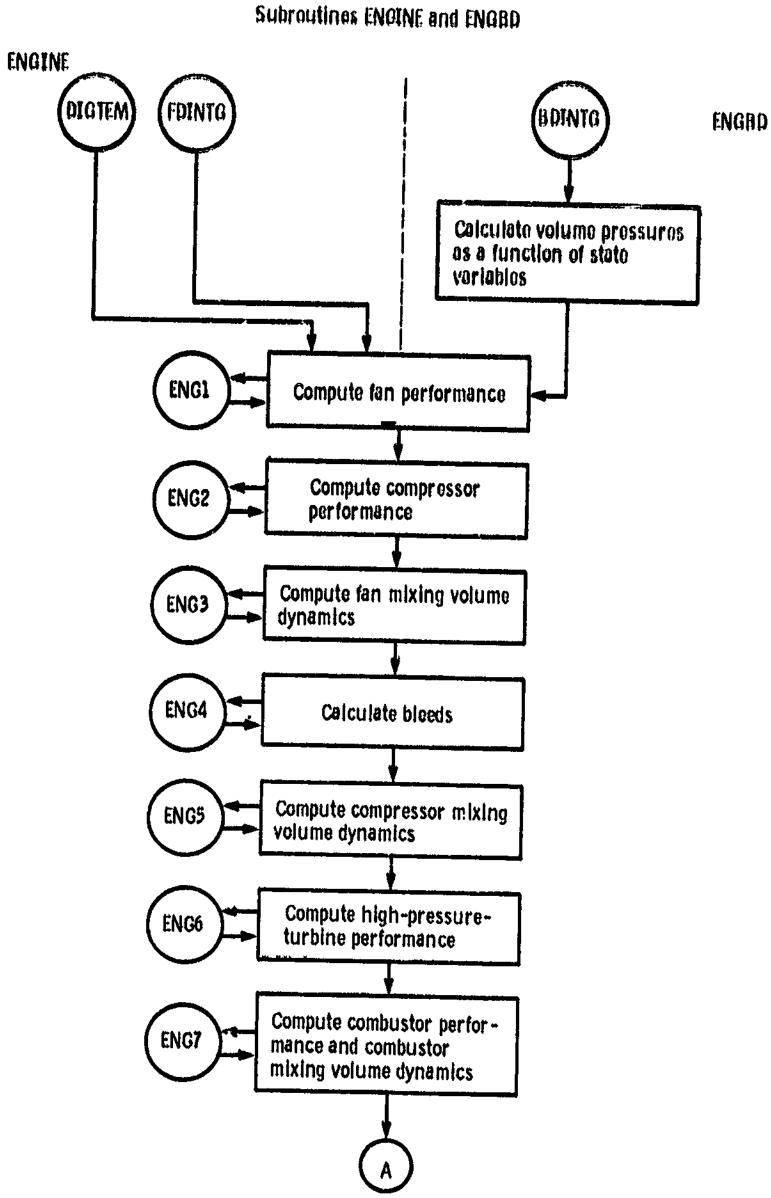

ORIGINAL PAGE IS
OF POOR QUALITY

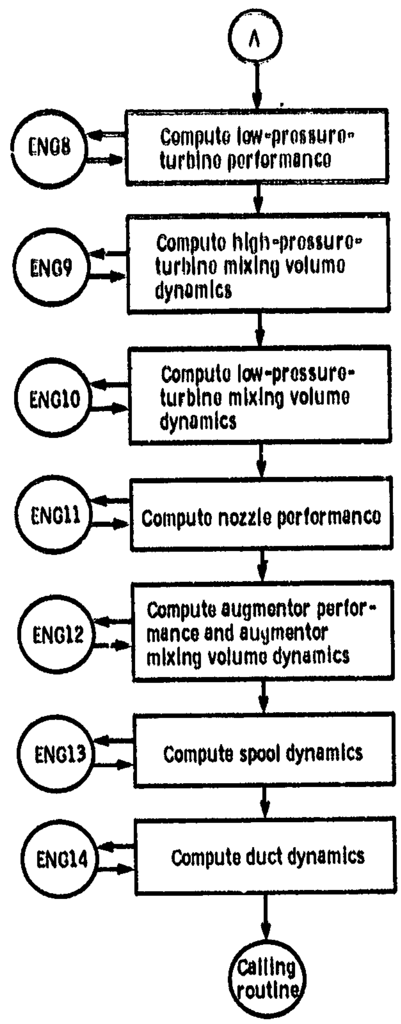

Subroutine ENG1

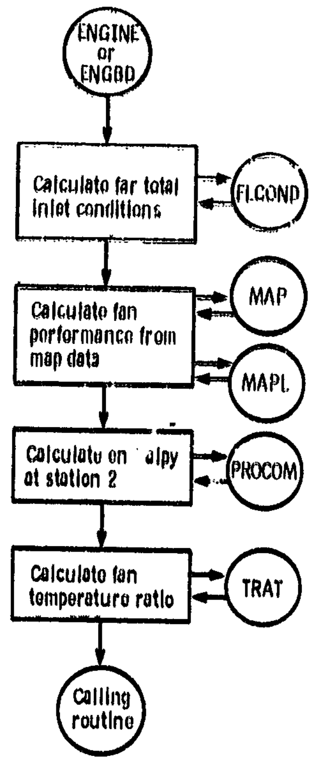

Subroutine ENG2

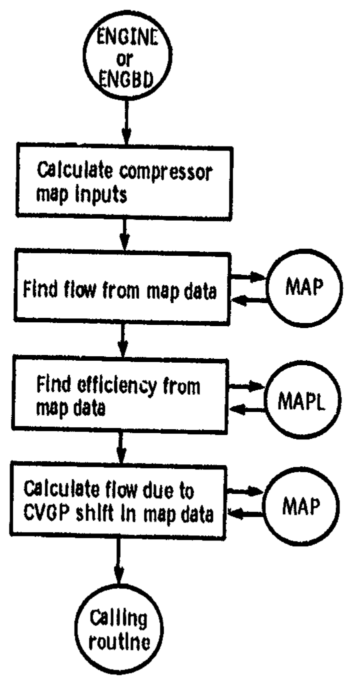

Subroutine ENG3

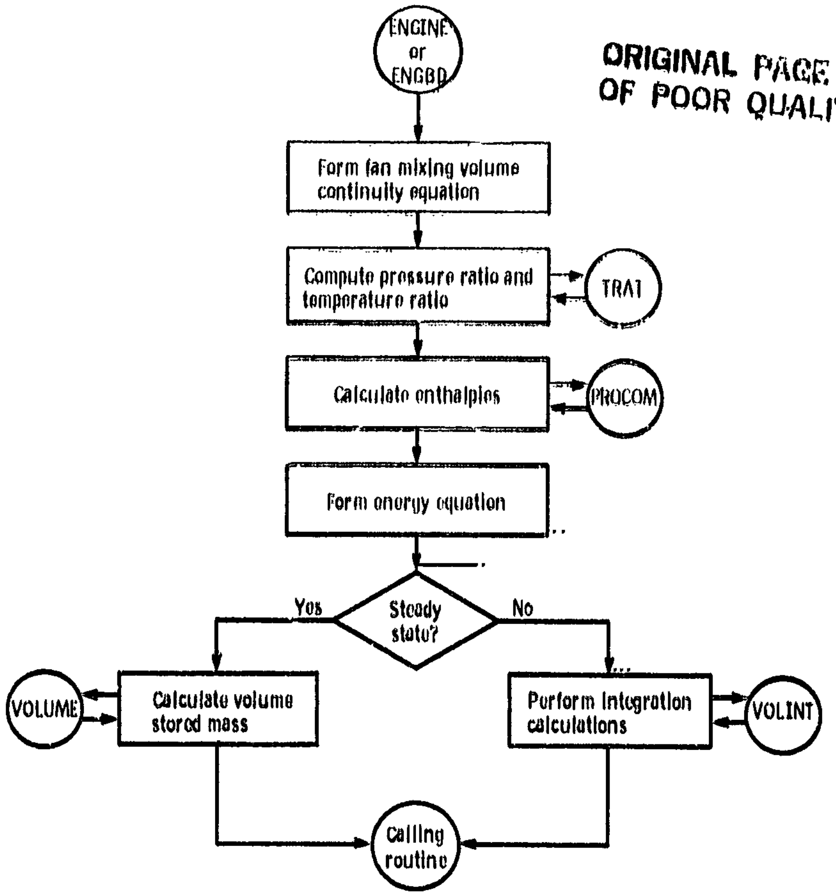

Subroutine ENG4

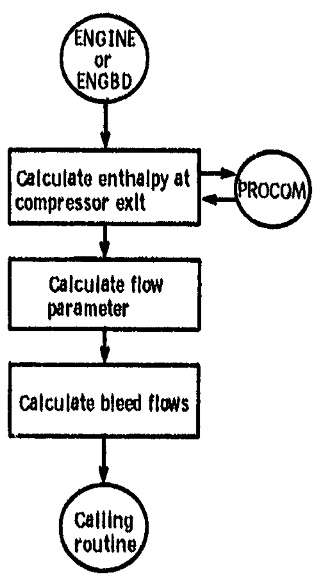

Subroutine ENG5

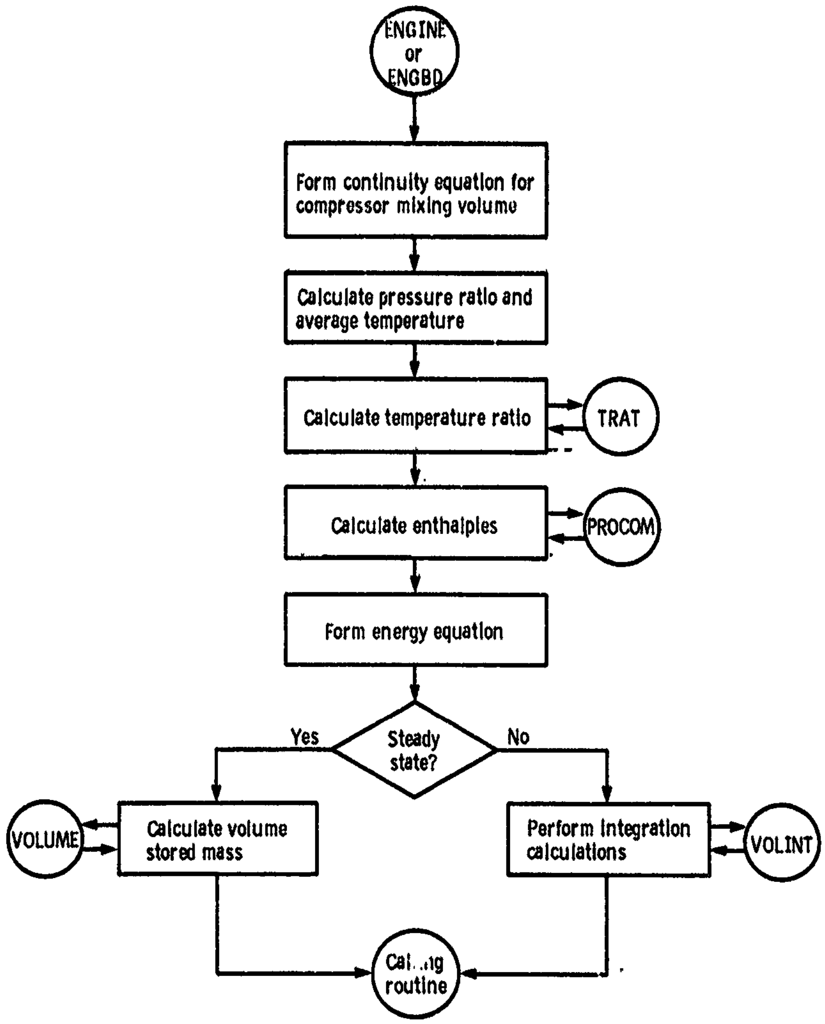

Subroutine ENG6

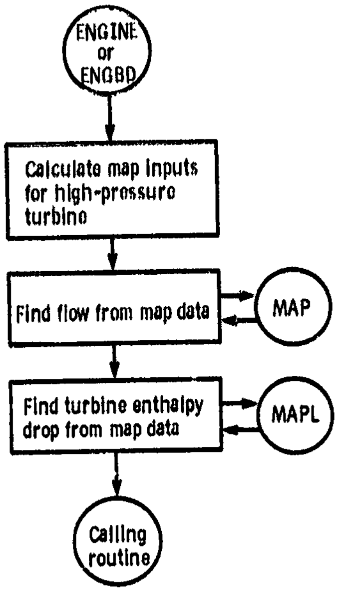

Subroutine ENG7

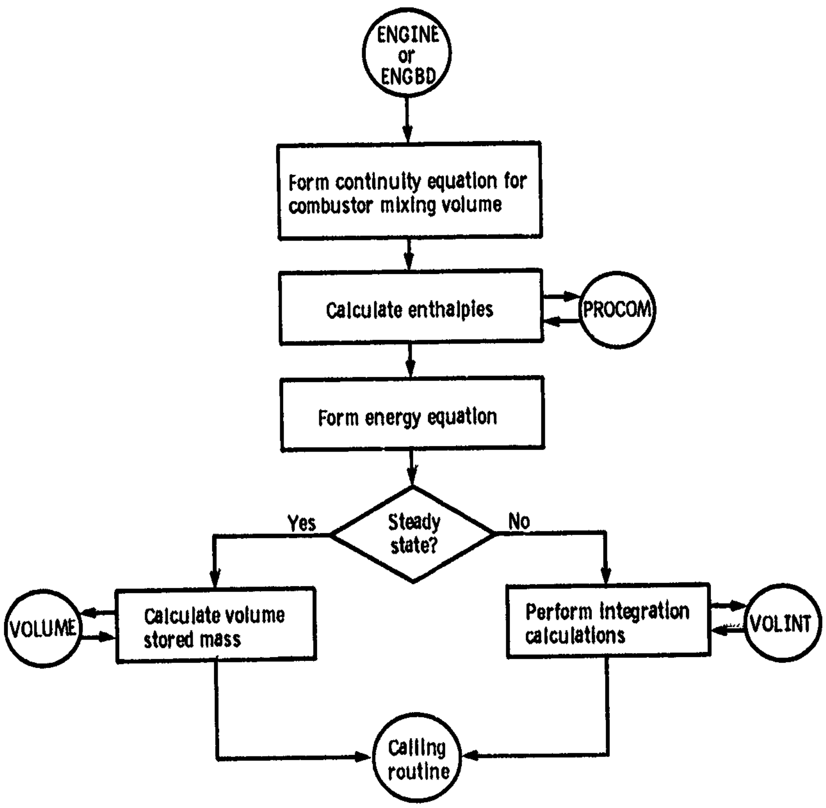

Subroutine ENG8

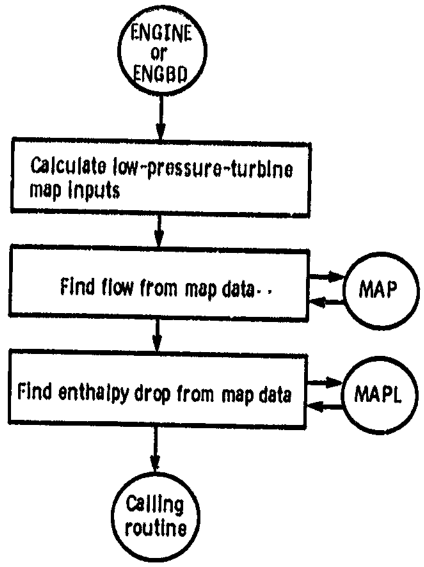

Subroutine ENG9

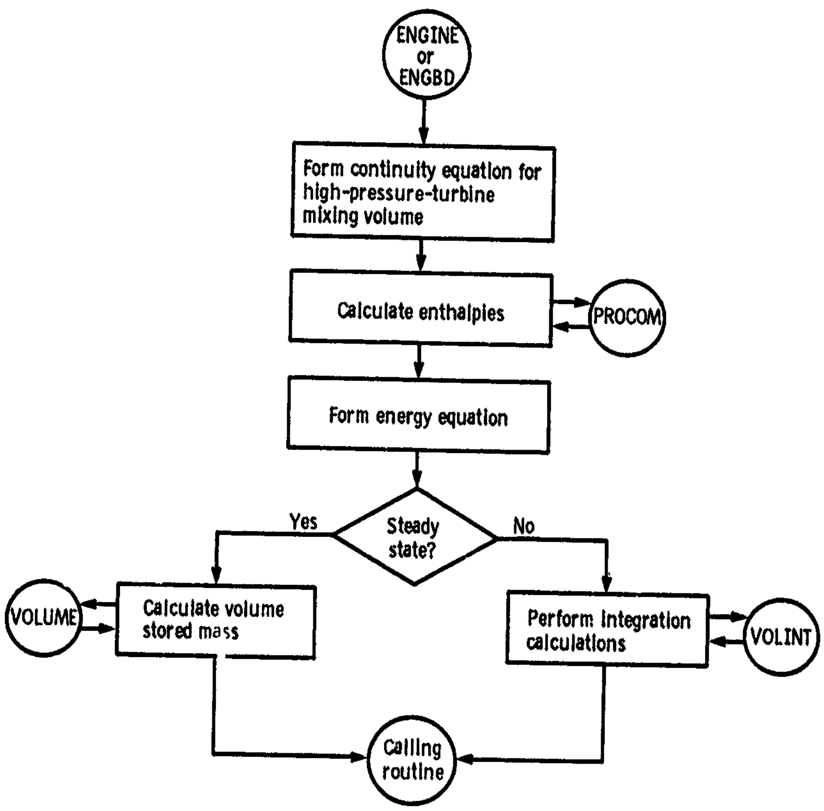

Subroutine ENG10

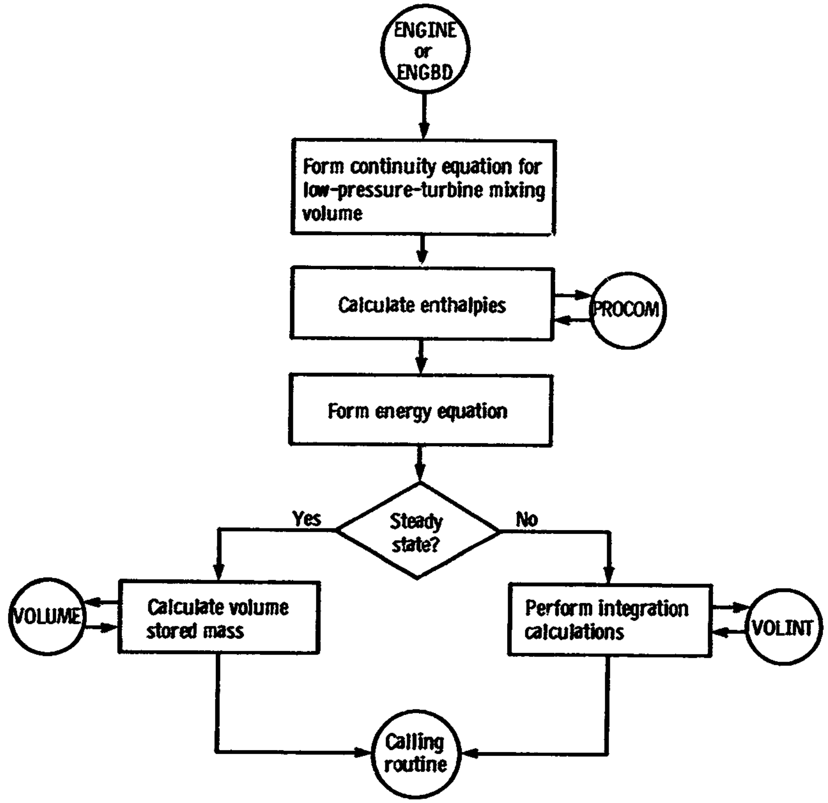

Subroutine ENG11

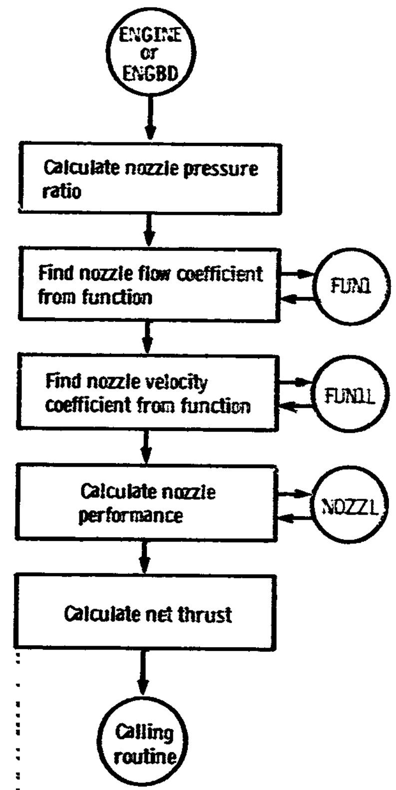

ORIGINAL PAGE IS
OF POOR QUALITY

ORIGINAL PAGE IS
OF POOR QUALITY

Subroutine ENG12

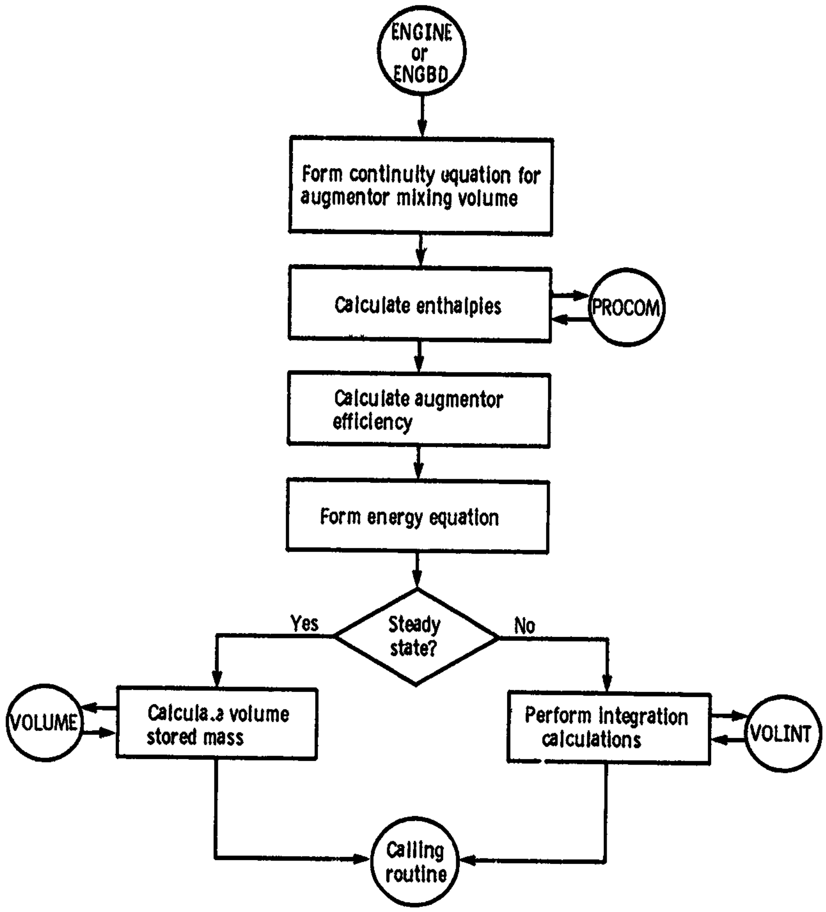

ORIGINAL PAGE IS
OF POOR QUALITY

Subroutine ENG13

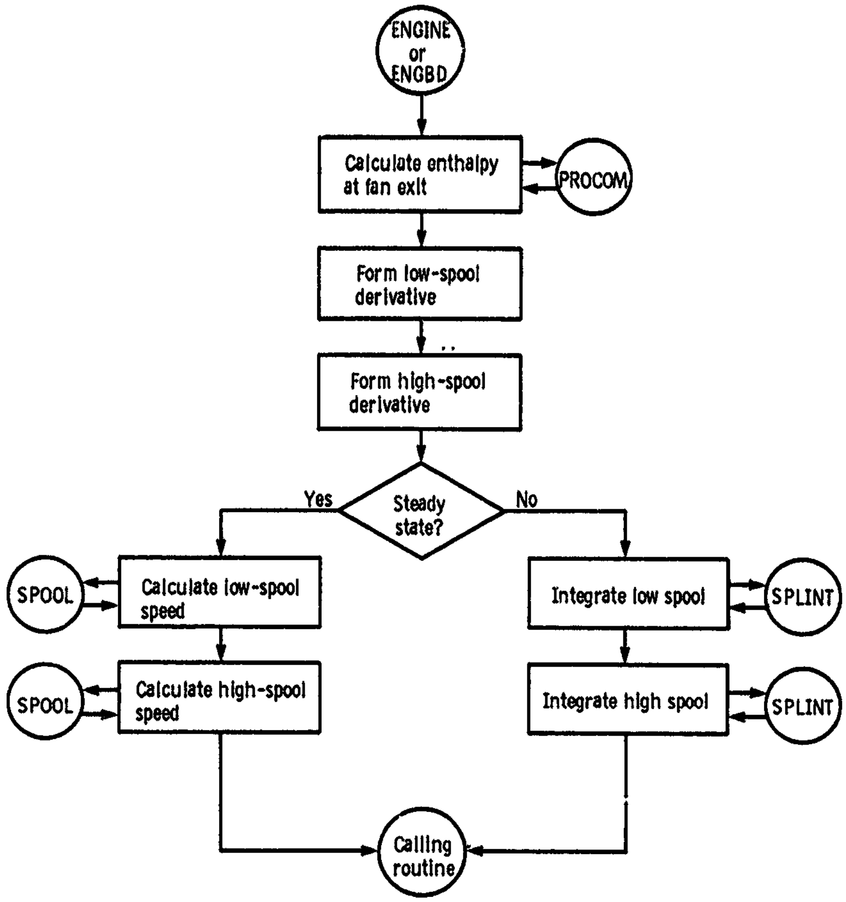

Subroutine ENG14

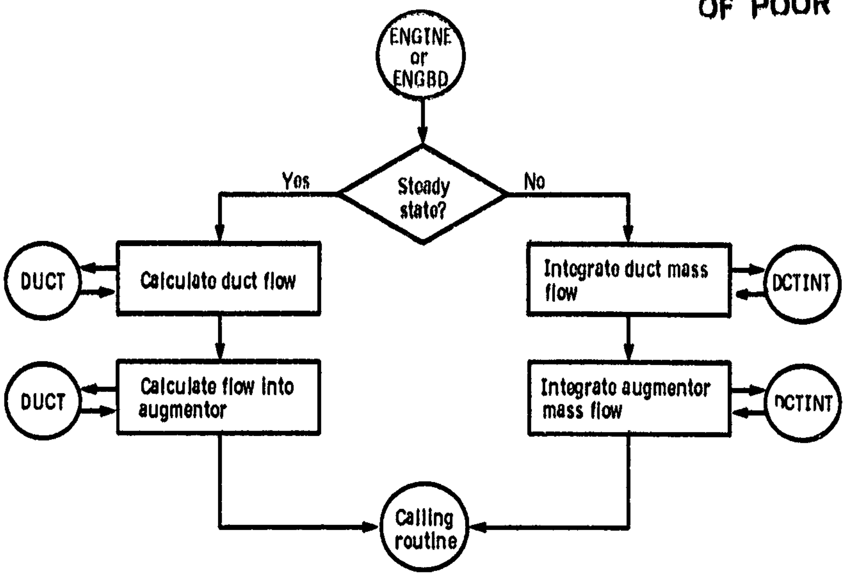

Subroutine ERROR

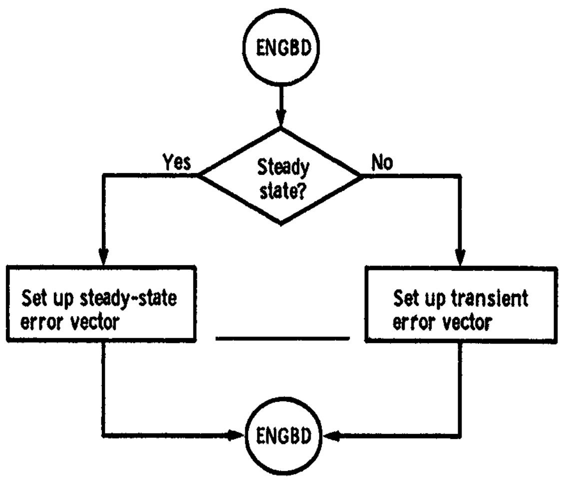

ORIGINAL PAGE IS
OF POOR QUALITY

Subroutine FDINTG

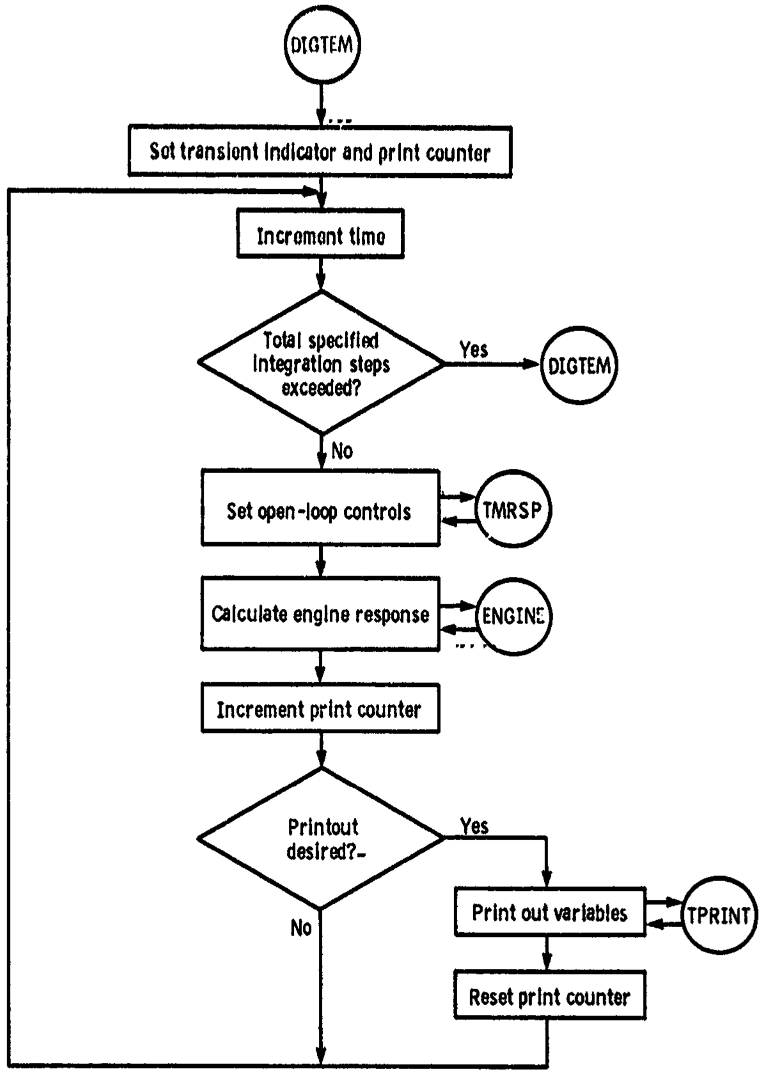

ORIGINAL PAGE IS
OF POOR QUALITY

Subroutine FLCOND

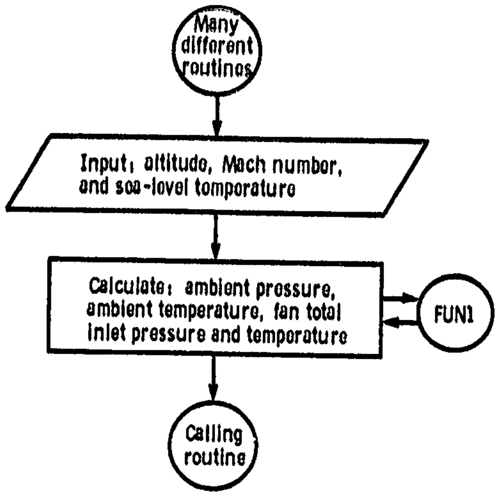

Subroutine FOOR

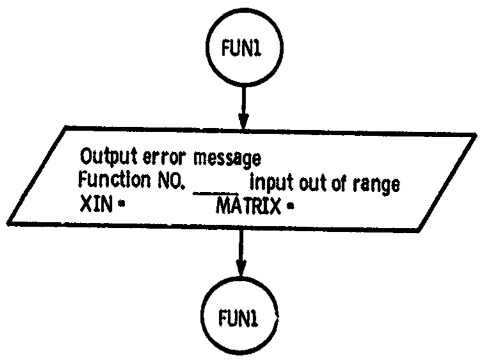

Subroutine FUN1

ORIGINAL PAGE IS
OF POOR QUALITY

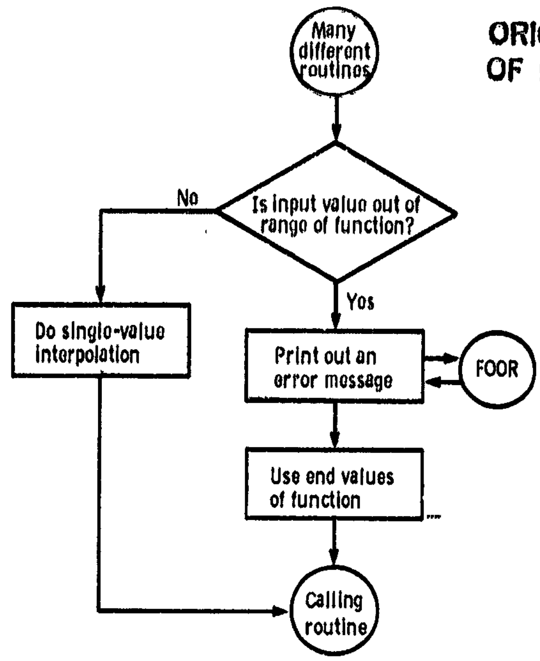

Subroutine FUN1L

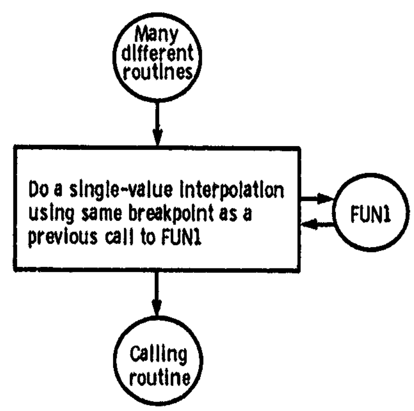

Subroutine GUESS

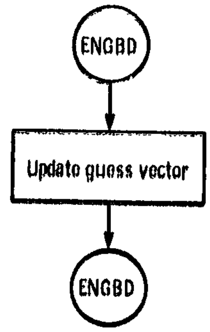

Subroutine INDATA

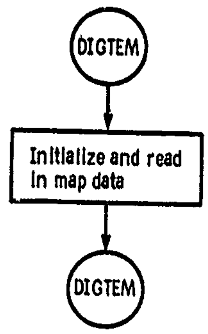

Subroutine MAP

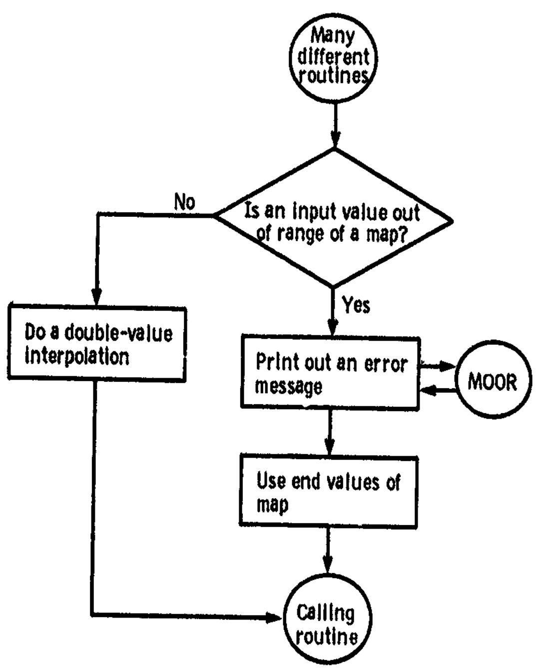

Subroutine MAPL

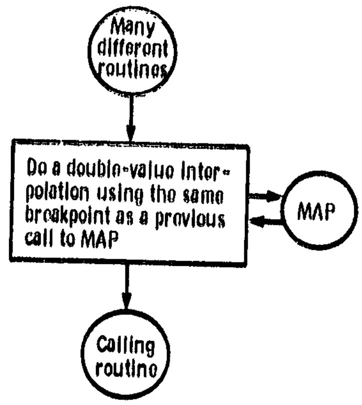

Subroutine MOOR

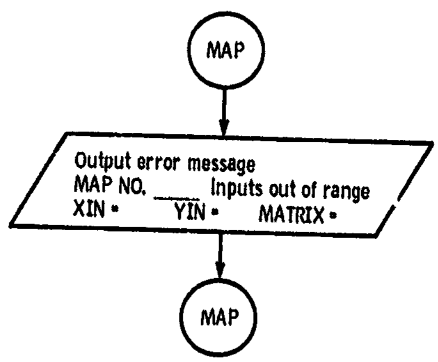

Subroutine NOZZL

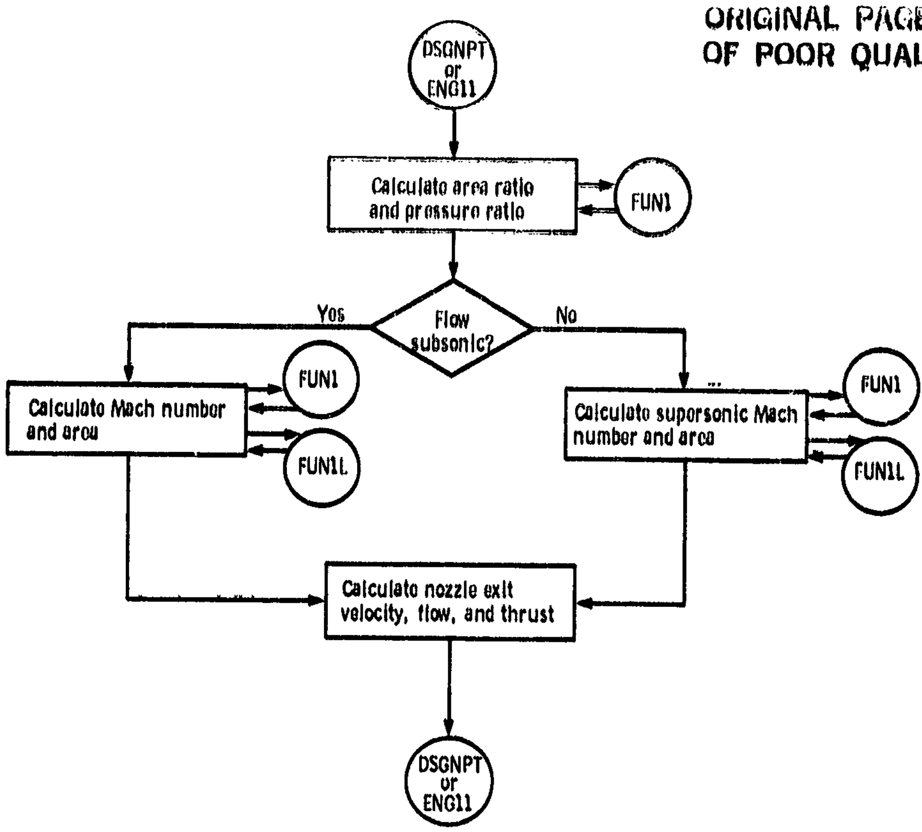

Subroutine PROCOM

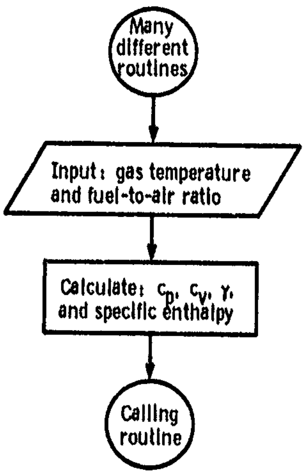

Subroutine SPLINT

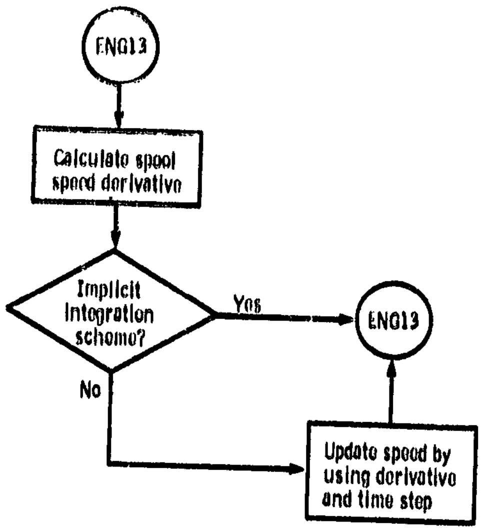

Subroutine SPOOL

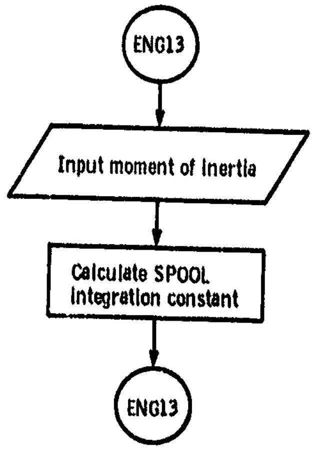

ORIGINAL PAGE IS
OF POOR QUALITY

Subroutine TPRINT

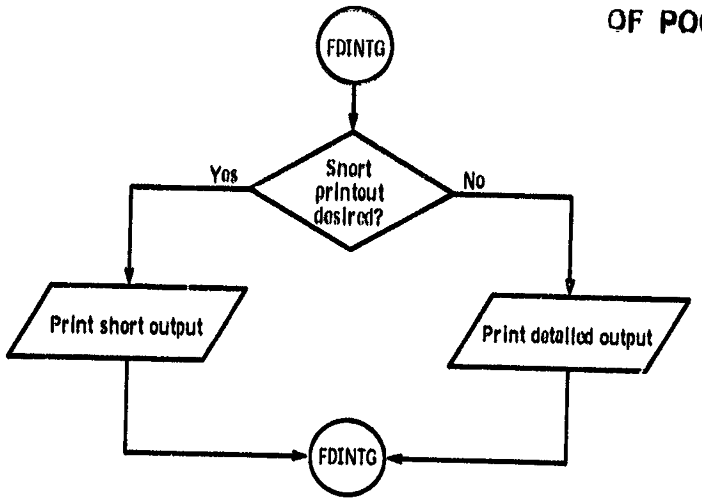

Subroutine TRAT

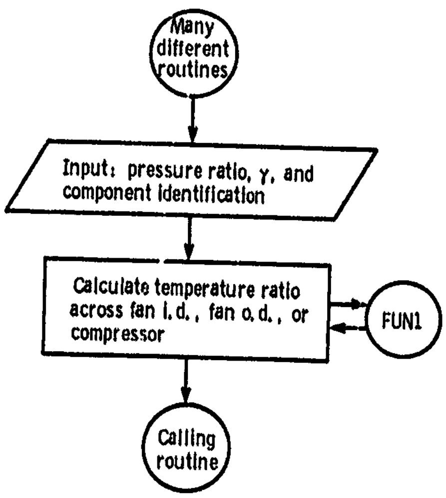

Subroutine VOLINT

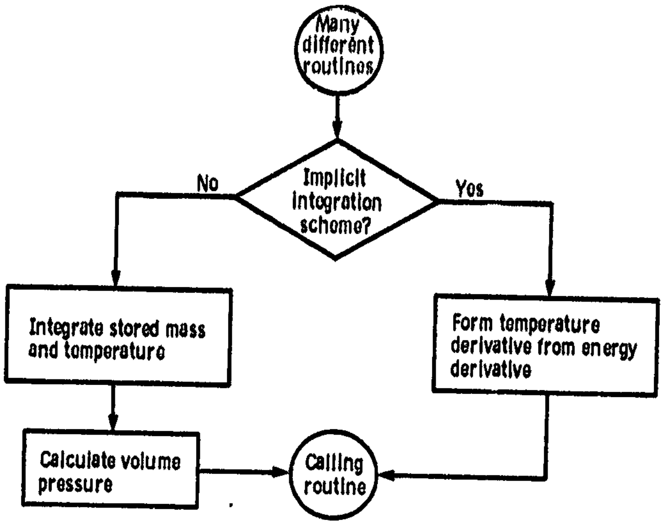

Subroutine VOLUME

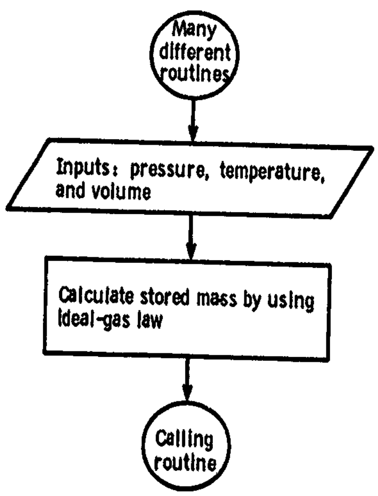

APPENDIX E

DIGTEM STEADY-STATE OPERATING POINTS

DIGTEM was used to generate converged steady-state operating points for the five sets of input data. To obtain these data, NOPER was set to the desired operating-point number and TMAX was set to 0.0 in the main program DIGTEM. In DIGTEM the dry design point is the first operating point read in. These data are used to calculate correction coefficients for balancing the engine equations. These same correction coefficients are then used to scale the model at all other operating points. A similar procedure is used for wet operating points, where the first wet operating point read in is the wet design point. Correction coefficients that only affect wet operating points are calculated at the wet design point and applied to the other wet operating points. The correction coefficients are imbedded in the DIGTEM equations and serve to minimize, if not to eliminate, differences between the DIGTEM model and the input data.

Figure 14 shows printouts of corrected and converged steady-state data for the five operating points. Figure 14(a) contains the dry design-point data. Note that the errors at the dry design point are all close to zero because of the scaling by the correction coefficients. DIGTEM then iterates to try to better the steady-state match and the converged data are shown. Note that the converged data are very close to the input data.

Data for the other dry operating points (figs. 14(b) and (c)) show that the input data (after being scaled by the correction coefficients) do not give as good a steady-state match (large derivative errors) as the design point. This is due in part to the scaling coefficients being calculated at the design point and then used at the off-design points as well. Correction coefficients calculated at the off-design points would be slightly different than those calculated at the design point because of slight inconsistencies in the data from one operating point to the next. These inconsistencies were not eliminated so that DIGTEM's capability for generating a steady-state balance could be tested. For both operating points the converged data have nearly zero errors with the iteration (state) variables being adjusted accordingly.

Data for the wet design point are shown in figure 14(d). Here again the errors are close to zero. DIGTEM iterates to an operating point that is close to the dry design operating point. Figure 14(e) shows data for the wet off-design operating points. The input data do not give as good an engine balance as for the wet design point for the same reason as discussed for the dry off-design points.

Figure 15 shows the correction coefficients calculated by DIGTEM for the dry design point. Since they all are close to 1.0, the modeling equations fairly accurately describe the design point. In fact, one or more large differences from 1.0 would indicate either bad input data or one or more inadequate component models.

APPENDIX F

TURBOSHAFT ENGINE MODEL

DIGTEM is generalized in the aerothermodynamic treatment of components. It also "trims" calculations to match a design point. These features can make it a useful tool for developing simulations of specific engines having the same two-spool, two-stream configuration. Also variations of the turbofan engine configuration such as a turbojet or turboshaft can be simulated with minor modifications to the Fortran coding. With more extensive modifications to the coding, arbitrary configurations can be modeled.

To demonstrate this capability, a turboshaft engine model was implemented by using DIGTEM. A computational flow diagram of the engine is shown in figure 16. Comparing figure 16 with the two-spool, two-stream engine computational flow diagram of DIGTEM in figure 2 indicates the need to make the following changes to the basic DIGTEM model:

(1) The inlet model must be eliminated.
(2) The fan must be eliminated.
(3) The duct must be eliminated.
(4) The low-pressure-turbine cooling bleed must be eliminated.
(5) The low-pressure turbine (i.e., power turbine in the turboshaft) must be disconnected from the fan and connected to a load.
(6) The nozzle must be eliminated.
(7) The back pressure on the power turbine must be fixed (at atmospheric pressure) with turbine flow (and energy) dumped to atmosphere.

The turboshaft engine model was implemented in DIGTEM by

(1) Using the normalized component maps already in DIGTEM
(2) Specifying a new design point with input data satisfying the following conditions:

$$P_{2.2} = P_{13} = P_2 = P_0 \tag{F1}$$

$$T_{2.2} = T_{13} = T_2 \tag{F2}$$

$$\dot{w}_{13} = 0 \tag{F3}$$

$$\dot{w}_7 = \dot{w}_6 = \dot{w}_{4.1} \tag{F4}$$

$$T_7 = T_6 \tag{F5}$$

$$\eta_{AB} = 0 \tag{F6}$$

$$A_8 = A_E = 0 \tag{F7}$$

$$FVGP = CVGP = 0 \tag{F8}$$

$$\dot{w}_{BLLT} = 0 \qquad (F9)$$

(3) Modifying the coding in DIGTEM as follows: For the turboshaft the state variables and derivatives are

VS(1) = XNL	VDOT(1) = DXNL
VS(2) = XNH	VDOT(2) = DXNH
VS(3) = W3	VDOT(3) = DW3
VS(4) = T3	VDOT(4) = DT3
VS(5) = W4	VDOT(5) = DW4
VS(6) = T4	VDOT(6) = DT4
VS(7) = W41	VDOT(7) = DW41
VS(8) = T41	VDOT(8) = DT41

These are the first eight state variables in the state variable list for the turbofan engine, and thus no recoding is needed to set up the state vector and the state derivative vector. By setting N = 8 in the main program DIGTEM, the order of the system is specified and the 8x8 Jacobian error matrix will be generated.

Recoding of DIGTEM routines was required to account for the aforementioned differences in the configurations. A fixed value of load torque Q_{load} was set in DSGNPT and was sized to zero the rotor speed derivative at the design point. Also correction coefficients CC(14) and CC(16) were redefined in DSGNPT to reflect the changed coding in the engine routines. The numerator of CC(16) (eq. (B141)) was set to the load torque. Some coding had to be added in the power turbine discharge. That is, temperature T_6' was calculated implicitly from the calculated turbine discharge enthalpy h_6. Convergence was obtained by guessing T_6', using T_6' to compute the h_6' through PROCOM, and then comparing h_6' with calculated h_6. CC(14) was used to insure a match at the design point.

Finally recoding was done in subroutine TMRSP, where the inputs to the model were specified as functions of time (open-loop control). For the turboshaft engine the inputs are fuel flow $\dot{w}_{F,4}$ to the main combustor and load torque Q_{load} change on the power turbine. TMRSP was set up to give a step change in both fuel flow and load torque.

Figure 17 shows the transient response of the turboshaft engine to simultaneous steps in fuel flow and load torque. Shown are normalized values of fuel flow $\dot{w}_{F,4}$, load torque Q_{load}, low rotor speed N_L, high rotor speed N_H, combustor pressure P_3, and turbine inlet temperature T_4. Note that N_H, P_3, and T_4 all increase with the addition of fuel. Normally N_L would increase also, but the increase in load caused N_L to drop off. For this 2-sec transient the integration time step was 0.01 sec. The printout interval was 0.1 sec. The CPU time was 1.06 sec on the IBM 370/3033 computer.

Thus it is possible to use DIGTEM to model engines other than a two-spool, two-stream turbofan engine. The resultant engine model will have a realistic aerothermodynamic treatment of its components and will be scaled to a user-specified design point.

REFERENCES

1. McKinney, J. S.: Simulation of Turbofan Engine. Part I - Description of Method and Balancing Technique. AFAPL-TR-67-125-Pt.-1, Air Force Aeropropulsion Lab, Air Force Systems Command, Nov. 1967. (AD-825197.)
2. McKinney, J. S.: Simulation of Turbofan Engine. Part II - Users Manual and Computer Program Listing. AFAPL-TP-67-125-Pt.-2, Air Force Aeropropulsion Lab, Air Force Systems Command, Nov. 1967. (AD-825198.)
3. Koenig, R. W.; and Fishbach, L. H.: GENENG - A Program for Calculating Design and Off-Design Performance for Turbojet and Turbofan Engines. NASA TN D-6552, 1972.
4. Fishbach, L. H.; and Koenig, R. W.: GENENG II - A Program for Calculating Design and Off-Design Performance of Two- and Three-Spool Turbofans with as Many as Three Nozzles. NASA TN D-6553, 1972.
5. Fishbach, L. H.; and Caddy, M. J.: NNEP - The Navy NASA Engine Program. NASA TM X-71857, 1975.
6. Sellers, J. F.; and Daniele, C. J.: DYNGEN - A Program for Calculating Steady-State and Transient Performance Of Turbojet and Turbofan Engines. NASA TN D-7901, 1975.
7. Szuch, J. R.: HYDES - A Generalized Hybrid Computer Program for Studying Turbojet or Turbofan Engine Dynamics. NASA TM X-3014, 1974.
8. Szuch, J. R.; Krosel, S. M.; and Bruton, W. M.: Automated Procedure for Developing Hybrid Computer Simulations of Turbofan Engines. Part I - General Description. NASA TP-1851, 1982.
9. Szuch, J. R.; Krosel, S. M.; and Bruton, W. M.: Automated Procedure for Developing Hybrid Computer Simulations of Turbofan Engines. Part II - Computer Printouts. NASA TM-81730, 1981.
10. Shames, I. H.: Mechanics of Fluids. McGraw-Hill, Inc., 1962.
11. Keenan, J. H.; and Kaye, J.: Gas Tables. John Wiley & Sons, Inc., 1948.
12. Shapiro, A. H.: The Dynamics and Thermodynamics of Compressible Fluid Flow. Vol. I, Ronald Press Co., 1953.

TABLE I. - TRANSIENT SPECIFICATIONS IN DIGTEM

Parameter	Setting		Function
	Default	Allowable range	
NOPER	3	1 - NTOTAL	Desired initial operating point
H	0.01	>0.0	Integration time step, sec
TMAX	20.	0.0 for steady state, >0.0 for transient	Desired transient length, sec
TOUT	0.1	>H	Printout interval, sec
IBDINT	1	0 for explicit, 1 for implicit	Integration method selector
IHPCNV	0	0 to use logic to generate a new matrix, 1 to generate a new matrix every time point	Matrix update selector
N	16	>0	System order

TABLE II. - BACKWARD-DIFFERENCE INTEGRATION SETTINGS

Parameter	Setting		Function
	Default	Allowable range	
VDELTA	0.001	>0.0	Initial perturbation of guesses, percent/100
FRAC	0.25	>0	External control of iteration step size
TOL1	0.001	>0	Bottom limit on error tolerance for matrix linearity, percent/100
TOL2	0.01	>TOL1	Top limit on error tolerances for matrix linearity, percent/100
TOLSS	0.0005	>0.0	Solution tolerance, percent/100
MPAS	50	>0	Maximum allowable iteration passes
TOLPCG	0.5	>0.0	Switch for calculating a new matrix
NOBUG	0	0 for no debug, 1 for debug)	Debug selector

ORIGINAL PAGE IS
OF POOR QUALITY

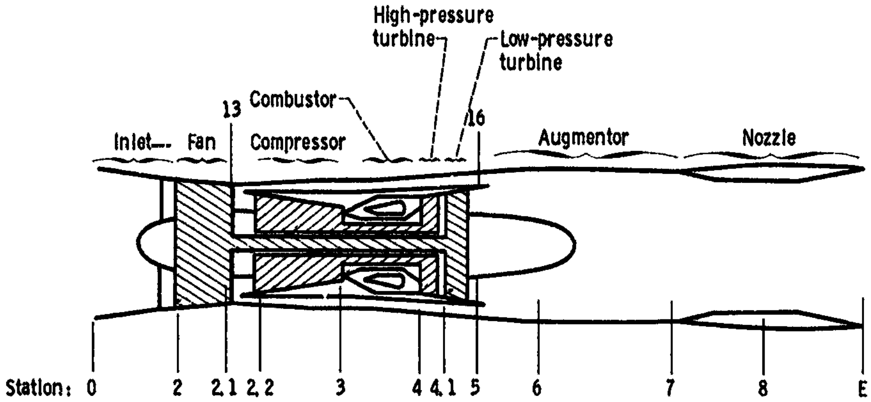

Figure 1. - Schematic of augmented turbofan engine.

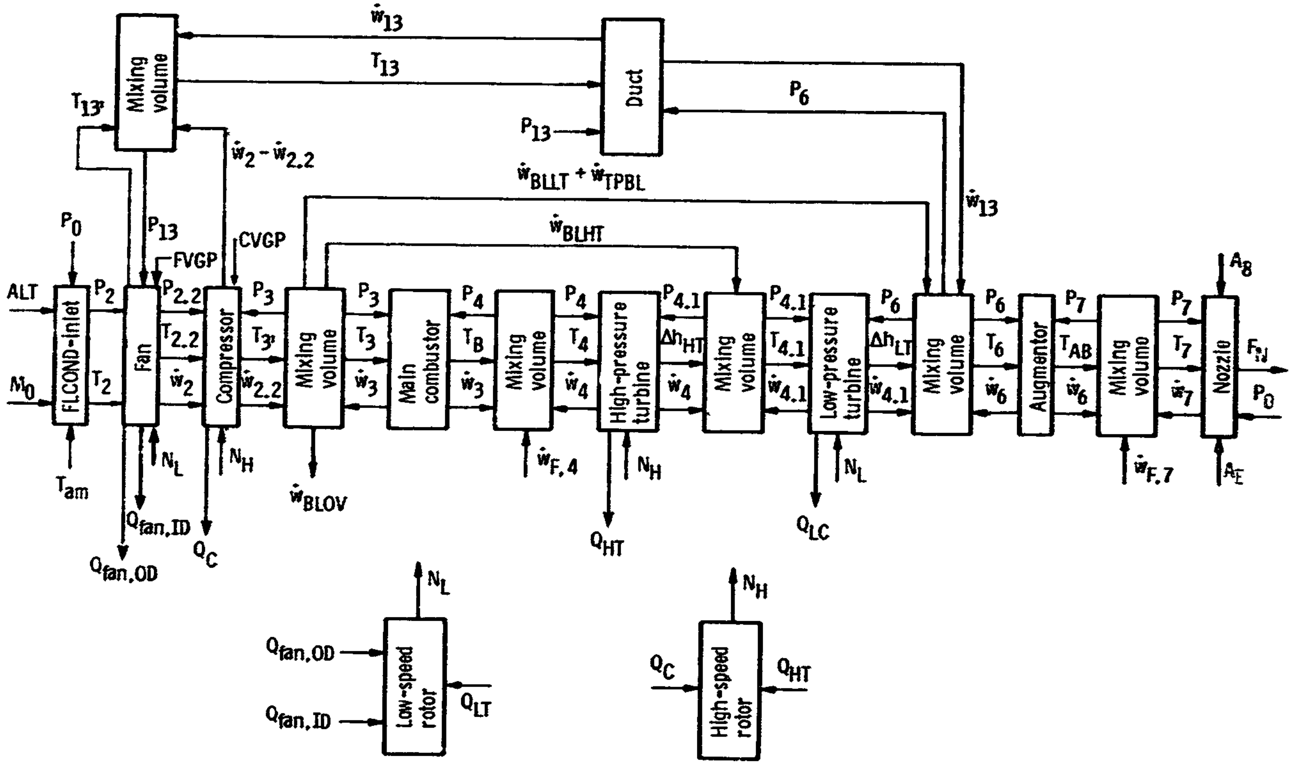

Figure 2. - Computational flow diagram of augmented turbofan engine simulation.

ORIGINAL PAGE IS
OF POOR QUALITY

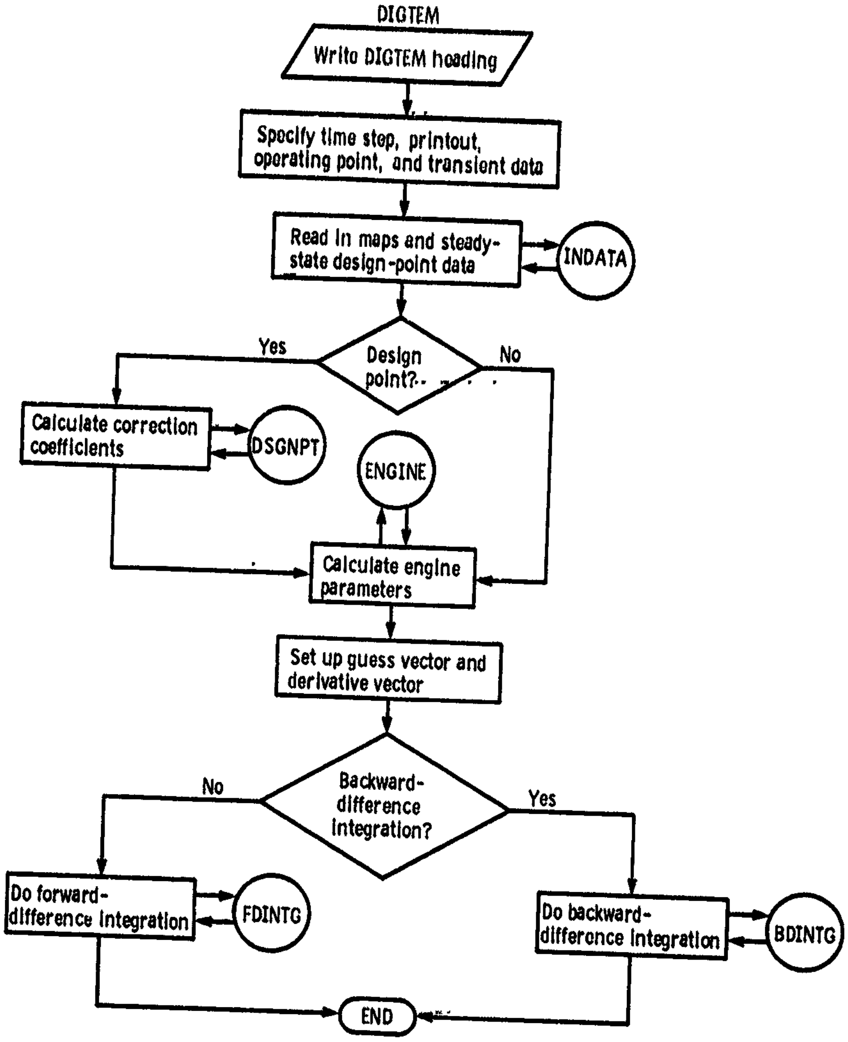

Figure 3. - Overall flow diagram of DIGTEM.

ORIGINAL PAGE IS
OF POOR QUALITY

```
      .60000      .80000                                                              K_BLWHT        KBLWLT
  1 14 11  1                                                                          MAPNO    NCV  NPT  NFCT  NCOM
     (9F8.4) (8F8.4) (9F8.4)                                                                    X    Y   Z formats
  0.3000  0.6500  0.7000  0.7500  0.8000  0.8200  0.8375  0.8500           | N_L/θ_2^1/2
  0.8800  0.9000  0.9400  1.0000  1.0500  1.1999
 15.0000 16.0000 17.0000 18.0000 19.0000 20.0000 21.0000 22.0000 23.0000   | FVGP  }
 24.0000 25.0                                                                      } Speed 1 (0.3000)
  0.0173  0.0155  0.0138  0.0121  0.0104  0.0086  0.0069  0.0052  0.0035   | ΔẆ_2  }
  0.0017  0.0000
 15.0000 16.0000 17.0000 18.0000 19.0000 20.0000 21.0000 22.0000 23.0000   | FVGP  }
 24.0000 25.0                                                                      } Speed 2 (0.6500)
  0.0172  0.0154  0.0137  0.0120  0.0103  0.0086  0.0069  0.0052  0.0034   | ΔẆ_2  }
  0.0017  0.0000
 15.0000 16.0000 17.0000 18.0000 19.0000 20.0000 21.0000 22.0000 23.0000   }
 24.0000 25.0                                                              }
  0.0279  0.0251  0.0223  0.0195  0.0167  0.0139  0.0112  0.0084  0.0056   } Speed 3
  0.0028  0.0000                                                           }
 15.0000 16.0000 17.0000 18.0000 19.0000 20.0000 21.0000 22.0000 23.0000   }
 24.0000 25.0                                                              }
  0.0378  0.0340  0.0302  0.0265  0.0227  0.0189  0.0151  0.0113  0.0076   } Speed 4
  0.0038  0.0000                                                           }
 15.0000 16.0000 17.0000 18.0000 19.0000 20.0000 21.0000 22.0000 23.0000   }
 24.0000 25.0                                                              }
  0.0442  0.0398  0.0354  0.0309  0.0265  0.0221  0.0177  0.0133  0.0088   } Speed 5
  0.0044  0.0000                                                           }
 15.0000 16.0000 17.0000 18.0000 19.0000 20.0000 21.0000 22.0000 23.0000   }
 24.0000 25.0                                                              }
  0.0456  0.0411  0.0365  0.0320  0.0274  0.0228  0.0183  0.0137  0.0091   } Speed 6              Fan variable-
  0.0046  0.0000                                                           }                      geometry effects
 15.0000 16.0000 17.0000 18.0000 19.0000 20.0000 21.0000 22.0000 23.0000   }
 24.0000 25.0                                                              }
  0.0470  0.0423  0.0376  0.0329  0.0282  0.0235  0.0188  0.0141  9.0094   } Speed 7
  0.0047  0.0000                                                           }
 15.0000 16.0000 17.0000 18.0000 19.0000 20.0000 21.0000 22.0000 23.0000   }
 24.0000 25.0                                                              }
  0.0480  0.0432  0.0384  0.0336  0.0288  0.0240  0.0192  0.0144  0.0096   } Speed 8
  0.0048  0.0000                                                           }
 13.0850 14.2765 15.4680 16.6595 17.8510 19.0425 20.2340 21.4255 22.6170   }
 23.8085 25.0                                                              }
  0.0490  0.0432  0.0374  0.0315  0.0256  0.0198  0.0140  0.0081  0.0023   } Speed 9
41100031 -0.0081                                                           }
  9.5164 11.0648 12.6131 14.1615 15.7099 17.2582 18.8066 20.3549 21.9033   }
 23.4516 25.0                                                              }
  0.0484  0.0409  0.0334  0.0259  0.0184  0.0109  0.0034 -0.0037 -0.0105   } Speed 10
 -0.0173 -0.0242                                                           }
  2.3793  4.3793  6.3793  8.3793 10.3793 12.3793 14.3793 16.3793 18.3793   }
 20.3793 22.3793                                                           }
  0.0392  0.0314  0.0236  0.0157  0.0079  0.0000 -0.0093 -0.0187 -0.0280   } Speed 11
 -0.0373 -0.0467                                                           }
  0.0000  1.7004  2.3347  3.5021  4.6695  5.8368  7.0042  8.1715  9.3389   }
 10.5063 11.6736                                                           }
  0.0049  0.0000 -0.0019 -0.0053 -0.0087 -0.0144 -0.0201 -0.0258 -0.0315   } Speed 12
 -0.0372 -0.0429                                                           }
  0.0000  1.0000  2.0000  3.0000  4.0000  5.0000  6.0000  7.0000  8.0000   }
  9.0000 10.0000                                                           }
  0.0000 -0.0026 -0.0051 -0.0077 -0.0103 -0.0129 -0.0178 -0.0228 -0.0278   } Speed 13
 -0.0327 -0.0377                                                           }
  0.0000  1.0000  2.0000  3.0000  4.0000  5.0000  6.0000  7.0000  8.0000   }
  9.0000 10.0000                                                           }
  0.0000 -0.0025 -0.0050 -0.0075 -0.0101 -0.0126 -0.0174 -0.0223 -0.0271   } Speed 14 (1.1999)
 -0.0320 -0.0368                                                           }
  2 14 11  1                                                                          MAPNO    NCV  NPT  NFCT  NCOM
     (9F8.4) (8F8.4) (9F8.4)                                                                    X    Y   Z_1 formats
  0.7000  0.7750  0.8000  0.8250  0.8500  0.8750  0.9000  0.9250           | N_H/θ_2.2^1/2
  0.9500  0.9750  1.0000  1.0250  1.0500  1.0999
 34.0000 35.0000 36.0000 37.0000 38.0000 39.0000 40.0000 41.0000 42.0000   | CVGP    }
 43.0000 44.0                                                                        } Speed 1 (0.7000)
  0.1607  0.1302  0.1029  0.0788  0.0579  0.0402  0.0257  0.0145  0.0064   | ΔẆ_2.2  }
  0.0016  0.0000
 34.0000 35.0000 36.0000 37.0000 38.0000 39.0000 40.0000 41.0000 42.0000   | CVGP    }
 43.0000 44.0                                                                        } Speed 2 (0.7750)
  0.1491  0.1208  0.0955  0.0731  0.0537  0.0373  0.0239  0.0134  0.0060   | ΔẆ_2.2  }
  0.0015  0.0000
 28.6835 30.2152 31.7468 33.2785 34.8101 36.3418 37.8734 39.4051 40.9367   }
 42.4684 44.0                                                              }
  0.1430  0.1160  0.0811  0.0523  0.0297  0.0132  0.0029 -0.0012 -0.0043   } Speed 3
 -0.0159 -0.0362                                                           }
 22.5029 24.5029 26.5029 28.5029 30.5029 32.5029 34.5029 36.5029 38.5029   }
 40.5029 42.5029                                                           }
  0.1255  0.0947  0.0574  0.0292  0.0101  0.0000 -0.0027 -0.0144 -0.0392   } Speed 4
 -0.0772 -0.1283                                                           }
 16.3646 18.3646 20.3646 22.3646 24.3646 26.3646 28.3646 30.3646 32.3646   }
 34.3646 36.3646                                                           }
  0.1113  0.0861  0.0527  0.0272  0.0096  0.0000 -0.0025 -0.0117 -0.0325   } Speed 5
 -0.0650 -0.1092                                                           }
 11.1257 13.1257 15.1257 17.1257 19.1257 21.1257 23.1257 25.1257 27.1257   }
 29.1257 31.1257                                                           }
  0.0899  0.0637  0.0376  0.0184  0.0058  0.0000 -0.0026 -0.0145 -0.0368   } Speed 6              Compressor variable-
 -0.0696 -0.1129                                                           }                      geometry effects
  5.3906  7.3906  9.3906 11.3906 13.3906 15.3906 17.3906 19.3906 21.3906   }
 23.3906 25.3906                                                           }
  0.0594  0.0410  0.0239  0.0114  0.0034  0.0000 -0.0027 -0.0145 -0.0358   } Speed 7
 -0.0666 -0.1068                                                           }
  0.0000  1.9710  3.9421  5.9131  7.8841  9.8551 11.8261 13.7972 15.7682   }
 17.7392 19.7102                                                           }
  0.0529  0.0341  0.0193  0.0087  0.0023  0.0000 -0.0038 -0.0162 -0.0371   } Speed 8
 -0.0666 -0.1046                                                           }
  0.0000  1.4587  2.9173  4.3760  5.8347  7.2933  8.7520 10.2107 11.6693   }
 13.1280 14.5867                                                           }
  0.0127  0.0063  0.0021  0.0001 -0.0008 -0.0053 -0.0140 -0.0270 -0.0443   } Speed 9
 -0.0658 -0.0916                                                           }
  0.0000  1.2001  2.4002  3.6004  4.8005  6.0006  7.2007  8.4009  9.6010   }
 10.8011 12.0012                                                           }
  0.0021  0.0004 -0.0001 -0.0021 -0.0067 -0.0139 -0.0237 -0.0361 -0.0510   } Speed 10
 -0.0685 -0.0886                                                           }
  0.0000  1.0000  2.0000  3.0000  4.0000  5.0000  6.0000  7.0000  8.0000   }
  9.0000 10.0000                                                           }
  0.0000 -0.0008 -0.0032 -0.0072 -0.0128 -0.0200 -0.0288 -0.0392 -0.0512   } Speed 11
 -0.0648 -0.0800                                                           }
  0.0000  1.0000  2.0000  3.0000  4.0000  5.0000  6.0000  7.0000  8.0000   }
  9.0000 10.0000                                                           }
  0.0000 -0.0007 -0.0029 -0.0065 -0.0116 -0.0181 -0.0260 -0.0354 -0.0463   } Speed 12
 -0.0586 -0.0723                                                           }
  0.0000  1.0338  2.0677  3.1015  4.1353  5.1691  6.2030  7.2368  8.2706   }
  9.3045 10.3383                                                           }
  0.0001 -0.0006 -0.0027 -0.0063 -0.0112 -0.0175 -0.0253 -0.0344 -0.0450   } Speed 13
 -0.0569 -0.0680                                                           }
```

Figure 4. - DIGTEM component map and operating-point input data set.

ORIGINAL PAGE IS
OF POOR QUALITY

```
0.0000  1.0000  2.0000  3.0000  4.0000  5.0000  6.0000  7.0000  8.0000
9.0000 10.0000
0.0000 -0.0005 -0.0022 -0.0048 -0.0086 -0.0134 -0.0193 -0.0263 -0.0344      Speed 16 (1.0999)
-0.0435 -0.0537
1 16 12  6                                                                   MAPNO  NCV  NPT  NPCT   NCOH
      (9F8.4) (8F8.4) (9F8.4) (9F8.4) (9F8.4) (9F8.4)                               X    Y    Z1 Z2  Z3 Z4  formats
0.5000  0.5500  0.6000  0.6500  0.7000  0.7500  0.8000  0.8800              N/θ^1/2
0.9000  0.9400  0.9600  1.0000  1.0500  1.0999
0.3215  0.3389  0.3476  0.3563  0.3651  0.3738  0.3825  0.3912  0.3966      P13/P2
0.3999  0.4065  0.4086
0.2615  0.2594  0.2577  0.2561  0.2546  0.2528  0.2505  0.2483  0.2471      (ω_c)fan,M
0.2558  0.2495  0.2455
0.0597  0.6195  0.7077  0.7655  0.7863  0.8390  0.8688  0.8678  0.8619      η fan,OD        Speed 1 (0.3000)
0.8521  0.8315  0.8302
0.3556  0.3667  0.3726  0.3780  0.3836  0.3892  0.3947  0.4001  0.4029      P2,1/P2
0.4056  0.4083  0.4110
0.7466  0.8623  0.9066  0.9284  0.9409  0.9411  0.9393  0.9274  0.9220      η fan,ID
0.9166  0.9113  0.9059
0.3215  0.3547  0.3713  0.3880  0.4046  0.4212  0.4378  0.4544  0.4627      P13/P2
0.4716  0.4793  0.4877
0.4755  0.4749  0.4737  0.4712  0.4679  0.4644  0.4601  0.4558  0.4520      (ω_c)fan,M
0.4487  0.4459  0.4407
0.0456  0.4596  0.6730  0.8725  0.9263  0.9289  0.9529  0.9622  0.9596      η fan,OD        Speed 2 (0.5500)
0.9541  0.9428  0.9219
0.3840  0.4087  0.4223  0.4358  0.4482  0.4602  0.4718  0.4832  0.4889      P2,1/P2
0.4945  0.5002  0.5057
0.5020  0.6599  0.8686  0.9113  0.9893  1.0408  1.0556  1.0509  1.0454      η fan,ID
1.0399  1.0341  1.0284
0.3215  0.3603  0.3797  0.3991  0.4185  0.4379  0.4573  0.4768  0.4865
0.4962  0.5059  0.5156
0.5177  0.5176  0.5165  0.5149  0.5125  0.5097  0.5050  0.4979  0.4934                              Baseline fan map
0.4876  0.4802  0.4716
0.0367  0.4486  0.6683  0.8605  0.9298  0.9580  0.9866  0.9853  0.9804      Speed 3
0.9765  0.9408  0.9108
0.3891  0.4185  0.4349  0.4501  0.4648  0.4791  0.4929  0.5065  0.5132
0.5200  0.5267  0.5332
0.6639  0.6740  0.7869  0.8907  0.9702  1.0247  1.0531  1.0612  1.0593
1.0560  1.0497  1.0327
0.3215  0.3630  0.3851  0.4062  0.4224  0.4486  0.4698  0.4910  0.5016
[illegible]  0.5228  0.5334
0.5599  0.5599  0.5597  0.5595  0.5592  0.5581  0.5538  0.5454  0.5395
0.5312  0.5200  0.4972
0.0285  0.4507  0.5911  0.7565  0.9189  0.9763  1.0129  1.0096  0.9993      Speed 4
0.9860  0.9585  0.9327
0.3936  0.4270  0.4441  0.4611  0.4777  0.4937  0.5093  0.5245  0.5322
0.5397  0.5471  0.5547
0.4312  0.6493  0.7493  0.8397  0.9196  0.9862  1.0422  1.0752  1.0784
1.0741  1.0575  1.0307
0.3215  0.3792  0.4081  0.4370  0.4658  0.4947  0.5236  0.5525  0.5669
0.5813  0.5958  0.6102
0.6148  0.6146  0.6145  0.6143  0.6134  0.6098  0.6022  0.5899  0.5817
0.5707  0.5556  0.5302
0.0042  0.4321  0.6578  0.8553  0.9602  1.0114  1.0218  0.9996  0.9782      Speed 5
0.9484  0.9047  0.8476
0.3989  0.4449  0.4688  0.4920  0.5144  0.5360  0.5569  0.5774  0.5874
0.5972  0.6068  0.6165
0.3742  0.6200  0.7462  0.8581  0.9519  1.0119  1.0577  1.0763  1.0774
1.0597  1.0326  1.0152
0.3215  0.3930  0.4288  0.4646  0.5004  0.5362  0.5719  0.6077  0.6256
0.6435  0.6614  0.6793
0.6749  0.6748  0.6747  0.6745  0.6735  0.6712  0.6637  0.6505  0.6407
0.6283  0.6097  0.5859
-0.0114 0.4769  0.7271  0.8861  0.9685  1.0059  1.0139  0.9953  0.9761      Speed 6
0.9605  0.9501  0.9238
0.4061  0.4663  0.4962  0.5251  0.5530  0.5799  0.6058  0.6312  0.6436
0.6558  0.6677  0.6794
0.3869  0.6682  0.7906  0.8894  0.9680  1.0252  1.0600  1.0699  1.0653
1.0506  1.0317  1.0116
0.3215  0.4055  0.4475  0.4894  0.5314  0.5734  0.6154  0.6574  0.6784
0.6994  0.7204  0.7414
0.7326  0.7324  0.7323  0.7320  0.7316  0.7304  0.7230  0.7093  0.6999
0.6875  0.6717  0.6439
-0.0122 0.4940  0.7419  0.8756  0.9788  1.0183  1.0295  1.0222  1.0104      Speed 7
1.0090  1.0088  1.0087
0.4084  0.4829  0.5190  0.5540  0.5877  0.6203  0.6516  0.6822  0.6971
0.7117  0.7260  0.7400
0.3617  0.6672  0.7880  0.8973  0.9642  1.0249  1.0637  1.0811  1.0807
1.0687  1.0476  1.0188
0.3215  0.4367  0.4944  0.5520  0.6096  0.6672  0.7249  0.7825  0.8113
0.8401  0.8689  0.8977
0.8277  0.8276  0.8275  0.8274  0.8273  0.8270  0.8229  0.8130  0.8051
0.7953  0.7820  0.7613
0.0014  0.6037  0.8380  0.9607  1.0070  1.0386  1.0478  1.0502  1.0504      Speed 8
1.0508  1.0589  1.0791
0.4062  0.5141  0.5662  0.6169  0.6659  0.7127  0.7576  0.8014  0.8227
0.8433  0.8637  0.8835
0.2627  0.5981  0.7428  0.8683  0.9682  1.0297  1.0676  1.0857  1.0881
1.0849  1.0722  1.0550
0.3215  0.4460  0.5083  0.5706  0.6328  0.6951  0.7574  0.8197  0.8508
0.8819  0.9131  0.9442
0.8554  0.8552  0.8551  0.8549  0.8548  0.8545  0.8521  0.8453  0.8402
0.8325  0.8214  0.8058
0.0010  0.6314  0.8562  0.9707  1.0183  1.0382  1.0464  1.0536  1.0550      Speed 9
1.0558  1.0567  1.0571
0.4058  0.5227  0.5797  0.6355  0.6894  0.7409  0.7900  0.8380  0.8611
0.8841  0.9062  0.9277
0.2432  0.5883  0.7361  0.8635  0.9596  1.0271  1.0675  1.0862  1.0899
1.0899  1.0844  1.0777
0.3215  0.4690  0.5427  0.6165  0.6902  0.7640  0.8377  0.9115  0.9483
0.9852  1.0221  1.0590
0.9209  0.9209  0.9208  0.9207  0.9206  0.9205  0.9204  0.9185  0.9155
0.9106  0.8992  0.8782
0.0113  0.5688  0.7937  0.9281  0.9945  1.0244  1.0393  1.0451  1.0458      Speed 10
1.0489  1.0477  1.0467
0.3995  0.5386  0.6085  0.6771  0.7430  0.8059  0.8659  0.9241  0.9521
0.9799  1.0064  1.0323
0.1911  0.5560  0.7164  0.8592  0.9453  1.0084  1.0520  1.0819  1.0927
1.0982  1.0993  1.0805
```

Figure 4. - Continued.

ORIGINAL PAGE IS
OF POOR QUALITY

0.3215	0.4885	0.5656	0.6427	0.7198	0.7969	0.8740	0.9511	0.9896	
1.0282	1.0667	1.1053							
0.9487	0.9486	0.9484	0.9483	0.9482	0.9481	0.9480	0.9472	0.9462	
0.9434	0.9371	0.9274							
0.0000	0.5942	0.7997	0.9166	0.9731	1.0063	1.0265	1.0433	1.0446	Speed 11
1.0410	1.0373	1.0215							
0.3968	0.5559	0.6295	0.7011	0.7699	0.8369	0.8993	0.9605	0.9900	
1.0187	1.0470	1.0746							
0.1644	0.5510	0.7120	0.8384	0.9288	0.9925	1.0360	1.0694	1.0771	
1.0883	1.0962	1.0886							
0.3215	0.5043	0.6833	0.6623	0.7413	0.8203	0.8993	1.0000	1.0673	
1.0968	1.1363	1.1798							
1.0015	1.0012	1.0011	1.0009	1.0008	1.0005	1.0004	1.0000	1.0000	
0.9996	0.9988	0.9964							
0.0000	0.5129	0.6957	0.8159	0.8916	0.9329	0.9669	1.0000	1.0073	Speed 12
1.0023	0.9822	0.8960							
0.3916	0.5688	0.6432	0.7153	0.7857	0.8535	0.9187	1.0000	1.0607	
1.0697	1.0982	1.2486							
0.1156	0.6992	0.6346	0.7503	0.8565	0.8995	0.9495	1.0000	1.0201	
1.0335	1.0432	1.0201							
0.3215	0.5166	0.5931	0.6696	0.7462	0.8609	0.9374	1.0140	1.0905	
1.1287	1.1670	1.2056							
1.0313	1.0310	1.0309	1.0309	1.0308	1.0307	1.0306	1.0305	1.0304	
1.0304	1.0303	1.0300							
0.0000	0.4363	0.6074	0.7327	0.8188	0.8816	0.9109	0.9429	0.9968	Speed 13
0.9292	0.8513	0.7529							
0.3843	0.5788	0.6696	0.7196	0.7877	0.8865	0.9490	1.0088	1.0662	
1.0940	1.1897	1.2861							
0.0674	0.4440	0.5685	0.6784	0.7612	0.8518	0.8967	0.9352	0.9641	
0.9765	0.9968	1.0173							
0.3215	0.5304	0.5986	0.7008	0.7690	0.8712	0.9734	1.0757	1.1098	
1.1438	1.2120	1.2441							
1.0602	1.0571	1.0574	1.0578	1.0581	1.0584	1.0588	1.0592	1.0592	
1.0593	1.0608	1.0602							
0.0000	0.2475	0.3570	0.5436	0.6583	0.7054	0.7517	0.7997	0.8401	Speed 14 (1.1999)
0.8420	0.8449	0.8474							
0.3770	0.5826	0.6469	0.7385	0.8033	0.8919	0.9774	1.0971	1.0827	
1.1140	1.3692	1.2477							
0.0000	0.2535	0.3594	0.4848	0.5773	0.6938	0.7683	0.8329	0.8486	
0.8583	0.7815	0.6394							

4 14 12 2

(9F8.4) (8F8.4) (9F8.4) (9F8.4)

MAPNO	NCV	NPT	NPCT	NCOM
	X	Y	Z_1	Z_2 form on

0.7000	0.7750	0.8000	0.8250	0.8500	0.8750	0.9000	0.9250		$N_H/\theta^{1/2}_{2.2}$
0.9500	0.9750	1.0000	1.0250	1.0500	1.0999				
0.1189	0.2102	0.2193	0.2285	0.2376	0.2467	0.2559	0.2650	0.2741	$P_3/P_{2.2}$
0.2833	0.2924	0.3015							
0.4250	0.4235	0.4226	0.4214	0.4198	0.4179	0.4147	0.4069	0.3966	$(\dot{w}_c)_{C,H}$ Speed 1 (0.7000)
0.3839	0.3709	0.3579							
0.0226	0.6030	0.6184	0.6329	0.6459	0.6574	0.6672	0.6776	0.6866	η_C
0.6952	0.7037	0.7123							
0.1189	0.2390	0.2510	0.2630	0.2751	0.2871	0.2991	0.3111	0.3231	$P_3/P_{2.2}$ Speed 2 (0.7750)
0.3351	0.3471	0.3591							
0.4530	0.4529	0.4528	0.4527	0.4513	0.4495	0.4458	0.4410	0.4336	$(\dot{w}_c)_{C,H}$
0.4223	0.4109	0.3999							
0.0313	0.6759	0.6915	0.7112	0.7233	0.7351	0.7452	0.7550	0.7643	η_C
0.7735	0.7825	0.7916							
0.1189	0.2879	0.3048	0.3217	0.3386	0.3555	0.3724	0.3893	0.4062	
0.4231	0.4400	0.4569							
0.5136	0.5135	0.5131	0.5123	0.5109	0.5093	0.5060	0.5005	0.4922	Speed 3
0.4808	0.4695	0.4582							
0.0471	0.7696	0.7933	0.8121	0.8246	0.8388	0.8488	0.8600	0.8709	
0.8815	0.8922	0.9028							
0.1189	0.3471	0.3699	0.3928	0.4156	0.4384	0.4612	0.4840	0.5069	
0.5297	0.5525	0.5753							
0.5916	0.5912	0.5911	0.5910	0.5909	0.5902	0.5888	v.5842	0.5762	Speed 4
0.5651	0.5540	0.5429							
0.0413	0.8431	0.8693	0.8865	0.9028	0.9198	0.9358	0.9460	0.9563	
0.9630	0.9697	0.9762							
0.1189	0.3921	0.4195	0.4468	0.4741	0.5014	0.5288	0.5561	0.5834	
0.6107	0.6381	0.6654							
0.6741	0.6739	0.6738	0.6738	0.6737	0.6737	0.6733	6 6718	0.6674	Speed 5
0.6597	0.6372	0 6145							
0.0276	0.8394	0.8798	0.9059	0.9298	0.9560	0.9711	0.9824	0.9890	
0.9928	0.9952	0.9975							
0.1189	0.4393	0.4713	0.5034	0.5354	0.5674	0.5995	0.6315	0.6635	
0.6956	0.7276	0.7596							
0.7548	0.7548	0.7548	0.7548	0.7548	0.7548	0.7547	0.7544	0.7510	Speed 6
0.7407	0.7170	0.6925							
0.0238	0.8569	0.9031	0.9296	0.9555	0.9811	0.9942	1.0021	1.0058	
1.0049	1.0002	0.9953							
0.1189	0.4817	0.5180	0.5543	0.5906	0.6269	0.6631	0.6994	0.7357	
0.7720	0.8083	0.8445							
0.8267	0.8266	0.8266	0.8266	0.8266	0.8266	0.8265	0.8256	0.8212	Speed 7
0.8101	0.7888	0.7669							
0.0164	0.8716	0.9078	0.9382	0.9635	0.9850	1.0010	1.0083	1.0107	
1.0065	0.9933	0.9789							
0.1189	0.5161	0.5558	0.5955	0.6352	0.6750	0.7147	0.7544	0.7941	
0.8338	0.8736	0.9133							
0.8783	0.8783	0.8783	0.8783	0.8783	0.8783	0.8783	0.8773	0.8733	Speed 8
0.8626	0.8424	0.8164							
0.0228	0.8442	0.8869	0.9234	0.9514	0.9743	0.9982	1.0100	1.0160	
1.0127	0.9967	0.9761							
0.1189	0.5537	0.5972	0.6406	0.6841	0.7276	0.7711	0.8145	0.8580	
0.9015	0.9450	0.9885							
0.9214	0.9214	0.9214	0.9214	0.9214	0.9214	0.9214	0.9210	0.9173	Speed 9
0.9083	0.8921	0.8687							
0.0222	0.8227	0.8751	0.9097	0.9456	0.9683	0.9885	1.0042	1.0141	
1.0162	1.0017	0.9647							
0.1189	0.5902	0.6373	0.6844	0.7316	0.7787	0.8258	0.8730	0.9201	
0.9672	1.0143	1.0615							
0.9614	0.9614	0.9614	0.9614	0.9614	0.9614	0.9614	0.9610	0.9588	Speed 10
0.9510	0.9365	0.9129							
0.0715	0.8071	0.8597	0.8909	0.9312	0.9547	0.9769	0.9914	1.0049	
1.0117	1.0010	0.9472							
0.1189	0.6246	0.6752	0.7258	0.7764	0.8269	0.8775	0.9281	1.0000	
1.0292	1.0798	1.1304							
1.0035	1.0035	1.0035	1.0035	1.0035	1.0035	1.0035	1.0035	1.0000	Speed 11
0.9950	0.9789	0.9520							
0.1479	0.7680	0.8422	0.8794	0.9190	0.9454	0.9699	0.9857	1.0000	
1.0035	0.9957	0.9118							
0.1189	0.6503	0.7034	0.7566	0.8097	0.8629	0.9160	0.9691	1.0223	
1.0754	1.1286	1.1817							
1.0278	1.0278	1.0278	1.0278	1.0278	1.0278	1.0278	1.0278	1.0267	Speed 12
1.0200	1.0053	0.9805							
0.1548	0.7746	0.8151	0.8624	0.8972	0.9319	0.9483	0.9720	0.9836	
0.9919	0.9769	0.8810							

Baseline compressor map

Figure 4. - Continued.

ORIGINAL PAGE IS OF POOR QUALITY

```
0.1189  0.6621  0.7164  0.7708  0.8251  0.8794  0.9337  0.9880  1.0424 )
1.0967  1.1510  1.2053                                                 |
1.0398  1.0398  1.0398  1.0398  1.0398  1.0398  1.0398  1.0398  1.0395 } Speed 13
1.0330  1.0186  0.9925                                                 |
0.1715  0.7286  0.7959  0.8274  0.8759  0.9036  0.9325  0.9568  0.9721 |
0.9816  0.9729  0.8791                                                 )
0.1189  0.6786  0.7365  0.7905  0.8464  0.9024  0.9584  1.0143  1.0703 )
1.1263  1.1822  1.2382                                                 |
1.0555  1.0555  1.0555  1.0555  1.0555  1.0555  1.0555  1.0555  1.0552 } Speed 14 (1.0000)
1.0477  1.0310  1.0105                                                 |
0.1903  0.6910  0.7479  0.7922  0.8492  0.8822  0.9153  0.9390  0.9539 |
0.9654  0.9685  0.8706                                                 )
```

HAPHO	HCV	HPT	HFCT	HCOH
	X	Y	Z_1	Z_2 formats

```
5   8   9   2   1
    (9F8.4) (8F8.4) (9F8.4) (9F8.4)
 .7129   .7548   .7968   .8807   .9226   .9646  1.0000  1.2499          --> N_H/T_4^(1/2)
0 0      .9188  1.1659  1.3865  1.5402  1.6760  2.0503  2.6646  2.6232 --> P_4,1/P_4
1.6302  1.6302  1.6296  1.6228  1.6046  1.3700  1.2565  1.1122   .9388 --> (W_p)_HT } Speed 1 (0.7129)
1.6286  1.6286  1.1805  1.0020   .9151   .8341   .6499   .4752   .3797 --> (h_p)_HT }
1.3507  1.3507  1.3501  1.3438  1.3265  1.2939  1.1867  1.0506   .9633 --> (W_p)_HT } Speed 2 (0.7548)
1.3493  1.3493  1.1168   .9534   .8712   .7950   .6138   .4488   .3586 --> (h_p)_HT }
1.2796  1.2796  1.2791  1.2730  1.2567  1.2268  1.1262   .9951   .8937 | Speed 3
1.2783  1.2783  1.0630   .9101   .8327   .7602   .5816   .4252   .3397 |
1.1631  1.1631  1.1695  1.1606  1.1256  1.0955  1.0054   .8909   .8052 | Speed 4
1.1615  1.1615   .9731   .8272   .7599   .6879   .5261   .3867   .3076 |
1.0956  1.0956  1.0910  1.0802  1.0625  1.0350   .9507   .8431   .7659 | Speed 5
1.1158  1.1158   .9162   .7992   .7295   .6566   .5022   .3679   .2936 |
1.0519  1.0519  1.0381  1.0288  1.0120   .9859   .9065   .8025   .7322 | Speed 6
1.0783  1.0783   .9059   .7675   .6966   .6309   .4822   .3595   .2816 |
1.0000  1.0000   .9969   .9887   .9726   .9477   .8686   .7705   .7060 | Speed 7
1.0619  1.0619   .8869   .7587   .6786   .6159   .4680   .3612   .2721 |
 .7558   .7558   .7438   .7607   .7287   .7135   .6979   .5759   .5572 | Speed 8 (1.2499)
 .8477   .8477   .6799   .5747   .5176   .4679   .3569   .2699   .2073 |
```

High-pressure turbine map

HAPHO	HCV	HPT	HFCT	HCOH
	X	Z	Z_1	Z_2 formats

```
6   8   9   2   1
    (9F8.4) (8F8.4) (9F8.4) (9F8.4)
 .6076   .6529   .6561   .7267   .8193   .9059   .9965  1.07            --> N_L/T_4,1^(1/2)
0 0      .9016  1.0812  1.2170  1.3922  1.6226  1.7128  1.8680  2.0283 --> P_5/P_4,1
2.3899  2.3899  2.3830  2.3378  2.2402  2.0930  1.9399  1.6762  1.1136 --> (W_p)_LT
2.6999  2.6999  2.0633  1.7191  1.3478   .9406   .7905   .5298   .3173 --> (h_p)_LT } Speed 1 (0.6076)
2.2306  2.2306  2.2291  2.1819  2.0899  1.9161  1.8060  1.5626  1.0392 --> (W_p)_LT } Speed 2 (0.6520)
2.0062  2.0062  1.9081  1.6019  1.2985   .8803   .7405   .5528   .2965 --> (h_p)_LT }
1.5932  1.5932  1.5806  1.5586  1.4926  1.3685  1.2885  1.1161   .7422 | Speed 3
1.2226  1.2226  1.3671  1.1471   .9013   .6391   .5406   .3969   .2122 |
1.3939  1.3939  1.3899  1.3635  1.3060  1.1974  1.1274   .9765   .6499 | Speed 4
1.5095  1.5095  1.1985  1.0056   .7967   .5633   .4738   .3460   .1859 |
1.2391  1.2391  1.2355  1.2120  1.1609  1.0646  1.0021   .8680   .5773 | Speed 5
1.3666  1.3666  1.0781   .9030   .7166   .5019   .4217   .3079   .1654 |
1.1116  1.1116  1.1084  1.0875  1.0409   .9545   .8985   .7748   .5087 | Speed 6
1.2159  1.2159   .9755   .8233   .6670   .4521   .3801   .2773   .1487 |
1.0002  1.0002   .9975   .9788   .9365   .8583   .8076   .6896   .4399 | Speed 7
1.1189  1.1189   .8986   .7524   .5896   .4113   .3455   .2516   .1369 |
 .9310   .9310   .9281   .9100   .8702   .7977   .7505   .6381   .4036 | Speed 8 (1.07)
 .8916   .8916   .7093   .5933   .4649   .3243   .2724   .1984   .1060 |
                        Blank line must be left here
0.0000      4.0000
   3    2
          1
```

Low-pressure turbine map

BSFVGP	BSCVGP
NDRY	NAUG

Operating point

P0	P2	P13	P22	P3
P4	P41	P5	P6	P7
TAM	T2	T13	T22	T3
T4	T41	T6	T7	WA2
WA13	WA22	WA3	WG4	WG41
WG6	WG7	DH4	DH41	ETAB
ETAAB	FN	XNL	XNH	WF4
WF7	AB	AE	ALT	XMN
CON	CVN	FVGP	CVGP	FG
V13	V3	V4	V41	V6 V7
AQL13	AQL6	XIH	XIL	
ETAOF	ETAIF	ETAHC		

Dry operating point 1 (design)

```
14.696      14.696      34.500      36.000      267.00                    OPER1- 1
256.00      70.000      32.400      31.800      30.600                    OPER1- 2
518.67      518.67      696.00      698.00      1325.0                    OPER1- 3
2520.0      1780.0      1160.0      1160.0      193.50                    OPER1- 4
86.500      107.00      88.100      87.800      107.00                    OPER1- 5
194.94      195.00      167.00      75.500      1.0000                    OPER1- 6
.66000      9500.0      9200.0      11900.      1.7000                    OPER1- 7
.0000       430.0.      492.00      .0000       .0000                     OPER1- 8
.95200      .98000      -1.7094     4.0000      9900.0                    OPER1- 9
      87000.      2900.       2900.       40000.      52000.      43000.
      5.1800      5.1800      40.0        60.
      0.8112      0.8427      0.8298
```

```
14.696      14.696      24.200      26.180      158.70                    OPER2- 1
151.50      41.240      22.400      21.700      21.210                    OPER2- 2
518.67      518.67      614.00      621.00      1106.0                    OPER2- 3
1918.0      1353.0      831.00      891.00      140.00                    OPER2- 4
75.000      72.500      60.200      60.900      72.110                    OPER2- 5
148.00      148.00      129.00      58.200      1.0000                    OPER2- 6
.61000      5900.0      7706.0      10434.      .72800                    OPER2- 7
.0000       430.00      492.00      .0000       .0000                     OPER2- 8
.88000      .95000      -24.990     -4.8000     5900.0                    OPER2- 9
      87000.      2900.       2900.       40000.      52000.      43000.
      5.1800      5.1800      40.0        60.
      0.7785      0.8408      0.8249
```

Dry operating point 2

```
14.696      14.696      19.100      20.500      99.400                    OPER3- 1
94.600      27.100      25.400      17.500      17.300                    OPER3- 2
518.67      518.67      571.00      577.80      966.00                    OPER3- 3
1580.0      1117.0      785.00      785.00      100.00                    OPER3- 4
54.000      50.000      41.500      41.900      49.000                    OPER3- 5
104.00      104.00      102.33      28.000      1.0000                    OPER3- 6
.58409      1130.0      6175.0      9439.0      .37000                    OPER3- 7
.0000       430.00      492.00      .0000       .0000                     OPER3- 8
.90700      .96000      -24.990     -20.000     1130.0                    OPER3- 9
      87000.      2900.       2900.       40000.      52000.      43000.
      5.1800      5.1800      40.0        60.
      0.6584      0.7612      0.7582
```

Dry operating point 3

```
14.696      14.696      34.500      36.000      267.00                    OPER4- 1
256.00      70.000      32.400      31.800      30.600                    OPER4- 2
518.67      518.67      696.00      698.00      1325.0                    OPER4- 3
2520.0      1780.0      1160.0      2682.9      193.50                    OPER4- 4
86.500      107.00      88.100      89.800      107.00                    OPER4- 5
194.94      199.94      167.00      75.500      1.0000                    OPER4- 6
.99000      12500.      9200.0      11900.      1.7000                    OPER4- 7
5.0000      660.00      880.00      0.0000      0.0000                    OPER4- 8
.96100      .97000      -2.5004     4.0000      12500.                    OPER4- 9
      87000.      2900.       2900.       40000.      52000.      43000.
      5.1800      5.1800      40.0        60.
      0.7739      0.7867      0.8189
```

Wet operating point 1 (design)

```
14.696      14.696      34.500      36.000      267.00                    OPER5- 1
256.00      70.000      32.400      31.800      30.600                    OPER5- 2
518.67      518.67      696.00      698.00      1325.0                    OPER5- 3
2520.0      1780.0      1160.0      1971.4      193.50                    OPER5- 4
86.500      107.00      88.100      89.800      107.00                    OPER5- 5
194.94      197.74      167.00      75.500      1.0000                    OPER5- 6
.99000      10300.      9200.0      11900.      1.7000                    OPER5- 7
2.8000      560.00      780.00      0.0000      0.0000                    OPER5- 8
.96100      .97000      -2.5000     4.0000      10300.                    OPER5- 9
      87000.      2900.       2900.       40000.      52000.      43000.
      5.1800      5.1800      40.0        60.
      0.7742      0.7871      0.8189
```

Wet operating point 2

Figure 4. - Concluded.

2 3 5 3						MAPNO, NCV, NPT, NFCT, NCOM
	(5F8.1)	(3F8.1)	(5F8.1)	(5F8.2)	(5F8.3)	X, Y, Z1, Z2, Z3, FORMATS
0.2	0.4	0.6			Y	VALUES
0	0.2	0.3	0.4	0.5	X	VALUES - CURVE 1
0.3	0.3	0.2	0.1	0.0	Z1	VALUES - CURVE 1
0.15	0.15	0.10	0.05	0.00	Z2	VALUES - CURVE 1
.225	0.225	0.150	0.075	0.000	Z3	VALUES - CURVE 1
0.0	0.4	0.5	0.6	0.7	X	VALUES - CURVE 2
0.6	0.6	0.4	0.2	0.0	Z1	VALUES - CURVE 2
0.30	0.30	0.20	0.10	0.00	Z2	VALUES - CURVE 2
0.450	0.450	0.300	0.150	0.000	Z3	VALUES - CURVE 2
0.0	0.6	0.7	0.8	0.9	X	VALUES - CURVE 3
0.9	0.9	0.6	0.3	0.0	Z1	VALUES - CURVE 3
0.45	0.45	0.30	0.15	0.00	Z2	VALUES - CURVE 3
0.675	0.675	0.450	0.225	0.000	Z3	VALUES - CURVE 3

NCV - NUMBER OF CURVES IN MAP

NPT - NUMBER OF POINTS PER CURVE

NFCT - NUMBER OF COMMON FUNCTIONS OF X, Y

NCOM - SWITCH FOR COMMON CURVE BREAKPOINTS

Figure 5. - Example of map input data.

ORIGINAL PAGE IS
OF POOR QUALITY

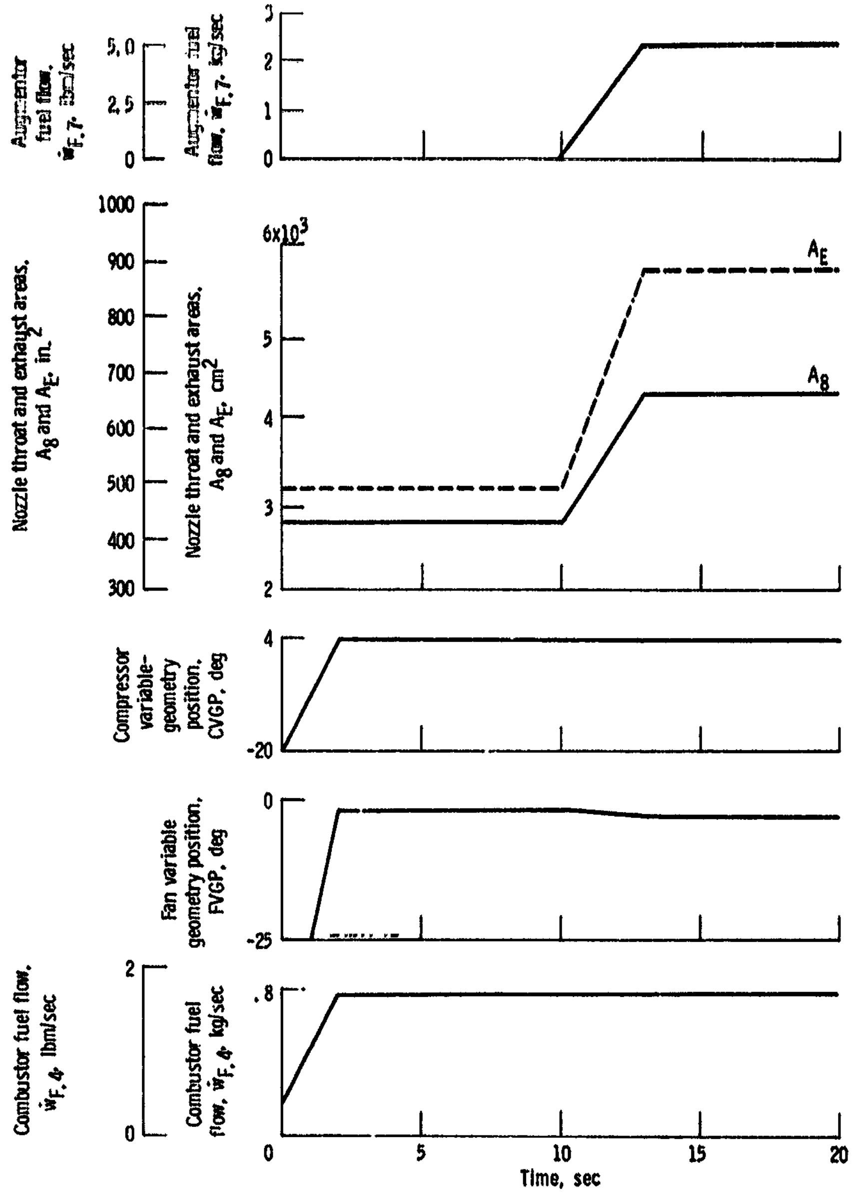

Figure 6. - Open-loop controls for DIGTEM test case.

ORIGINAL PAGE IS
OF POOR QUALITY

```
      SUBROUTINE TMRSP(WF4,WF7,CVGP,FVGP,AE,  -
     * A8,TIME,JSS)
C
C*********************************************************************
C
      COMMON /CONST/ AQL13,AQL6,V13,V3,V4,V41,V6,V7,XIH,XIL,BSFVGP,BSCVGP,  -
     * CC(50),BETAHC,BETAB,BETAAB
C
C*********************************************************************
C
      IF (JSS .EQ. 0) RETURN
      IF (TIME .GT. 10.0) GO TO 100
      WF4=.37+TIME*(1.7-.37)/2.0
      IF (WF4 .GT. 1.7) WF4=1.7
      WF7=0.0
      FVGP=-24.99+(TIME-1.0)*(24.99-1.7)/1.00
      IF (FVGP .LT. -24.99) FVGP=-24.99
      IF (FVGP .GT. -1.7) FVGP=-1.7
      FVGP=BSFVGP-FVGP
      CVGP=-20.0+TIME*(20.+4.)/2.0
      IF (CVGP .GT. 4.0) CVGP=4.0
      CVGP=BSCVGP-CVGP
      A8=430.0
      AE=492.0
      RETURN
  100 CONTINUE
      WF4=1.7
      WF7=0.0+(TIME-10.0)*(5.0-0.0)/3.0
      IF (WF7 .GT. 5.0) WF7=5.0
      FVGP=-1.7-(TIME-10.0)*(2.5-1.7)/3.0
      IF (FVGP .LT. -2.5) FVGP=-2.5
      CVGP=4.0
      CVGP=BSCVGP-CVGP
      FVGP=BSFVGP-FVGP
      A8=430.+(TIME-10.0)*(660.-430.)/3.0
      IF (A8 .GT. 660.) A8=660.
      AE=492.+(TIME-10.0)*(880.-492.)/3.0
      IF (AE .GT. 880.) AE=880.
      RETURN
      END
```

Figure 7. - Subroutine TMRSP for test case.

```
C       MAIN PROGRAM FOR D I G T E M
C
        DOUBLE PRECISION EMAT,DETERM
C
        REAL KBLWHT,KBLWLT
C
        DIMENSION LW(16),MW(16),VMAT(16),YYY(16),DELE(16),RR(16)
C
        COMMON /HELP/ MATRIX
        COMMON/OUTPT/MATTOT
        COMMON/SYTORD/N,IHPCNV
C
        COMMON /BDINT/ VS(16),VDOT(16),VDOTT(16),E(16),DELTA(16),  -
       * VSAVE(16),VDOTSV(16),VCONV(16),VGUESS(16),VWS(16),VNIM(16), -
       * ERRDSE(16),EMAT(16,16),ISS
C
        COMMON /NMAPS/F1(322),F2(322),F3(894),F4(518),F5(224),F6(224),  -
       1             N1(5),N2(5),N3(5),N4(5),N5(5),N6(5)
C
        COMMON /CONST/ AQL13,AQL6,V13,V3,V4,V41,V6,V7,XIH,XIL,BSFVGP,BSCVGP,  -
       * CC(50),BETAHC,BETAB,BETAAB
C
        COMMON /DESIGN/ P0D,P2D,P13D,P22D,P3D,P4D,P41D,P5D,P6D,P7D,TAMD,T2D,T13D,  -
       1 T22D,T3D,T4D,T41D,T6D,T7D,WA2D,WA13D,WA22D,WA3D,WG4D,WG41D,WG6D,WG7D,DH4D,-
       2 DH41D,ETABD,FND,XNLD,XNHD,WF4D,WF7D,A8D,AED,ALTD,XMND,CDND,CVND,FVGPD,  -
       3 CVGPD,FGD,CP3D,CV3D,GM3D,H3D,WBLHTD,WBLLTD,WBLOVD,WP4D,HP4D,WP41D,HP41D,  -
       4 ETAOFD,ETAIFD,ETAHCD
C
         COMMON /VARS/ A8,AE,ALT,ALTM,CD7,CDN,FVGP,CP13,CP13P,CP2,CP22,CP3,CP3P, -
       2 CP4,CP41,CP6,CP7,CPAB,CPB,CPHC,CSHIFT,CV13,CV13P,CV2,CV22,CV3,CV3P,CV4, -
       3 CV41,CV6,CV7,CV8,CVAB,CVB,CVHC,CVN,DH4,DH41,DTQW13,DTQW3,DTQW4,DTQW41,  -
       4 DTQW6,DTQW7,DT13,DT3,DT4,DT41,DT6,DT7,                                  -
       5 DWA13,DWG6,DW13,DW3,DW4,DW41,DW6,DW7,DXNH,DXNL,ETAAB,ETAB,ETAHCM,-
       6 ETAIFM,ETAOFM,FAR4M,FAR41M,FAR6M,FAR7M,FG,FGM3,FGPT3,FN,FNET,FNM,FSHIFT,-
       7 GM13,GM13M,GM13P,GM2,GM22,GM3,GM3M,GM3P,GM4,GM41,GM4M, -
       8 GM41M,GM6,GM6M,GM7,GM7M,GMAB,GMB,GMHC,H13,H13M,H13P,H13PM,H2,H22,H2M,  -
       9 H22M,H3,H3M,H3P,H3PM,H4,H41,H4M,H41M,H6,H6M,H7,H7M,HAB,HABM,HB,HBM,   -
       A HHCM,HP4,HP41,KBLWHT,KBLWLT,PE,P0,P0A,P0QT7,P13,P2,P2A,P22,P22Q2M,P3,  -
       B P4,P41,P5,P6,P7,PRHC,PRIF,PROF,CVGP,RTT2,RTT22,RTT4,RTT41,T0A,T13,T13M, -
       C T13P,T13PM,T2,T2A,T2M,T22,T22M,T3,T3M,T3P,T3PM,T4,T4M,T41,T41M,T6,T6M,  -
       D T7,T7M,TAM,TAVAB,TAVB,TAVHC,TRHCM1,TRIFM1,TROFM1,WA13,WA2,WA22,WA3,WAR2,-
       E WAR2M,WAR22,WAR22M,WBLHT,WBLLT,WBLOV,WF4,WF7,WG4,WG41,WG6,WG7,WG7M,WP4, -
       F WP41,W13,W3,W4,W41,W6,W7,X3,X4,X5,X6,XF,XMN,XMNM,XNH,XNL,Y3,Y4,Y5
C
        COMMON /TRNS/ ITRANS,NOPER,IBDINT,H,TMAX,TOUT,NOBUG,TIME
        WRITE(6,1008)
 1008   FORMAT(1H1)
        WRITE(6,1005)
        WRITE(6,1006)
 1005   FORMAT(40X,'************** D I G T E M **************')
 1006   FORMAT(50X,'TURBOFAN ENGINE MODEL')
        WRITE(6,502)
        WRITE(6,1007)
 1007   FORMAT(10X,'INPUT DATA')
  502   FORMAT(/)
        NOPER=3
        IBDINT=1
        H=.01
        TMAX=20.0
        TOUT=.1
        N=16
        IHPCNV=0
C*****READ MAP DATA
        READ(5,504) KBLWHT,KBLWLT
        CALL INDATA(N1,F1)
        READ (5,505) BSFVGP,BSCVGP
C*****READ OPERATING POINT DATA (IP=1 DRY DESIGN,IP=NDRY+1 WET DESIGN)
        READ(5,508) NDRY,NAUG
        NTOTAL=NDRY+NAUG
        DO 100 IP=1,NOPER
        READ(5,507) POINT
        READ(5,504) P0,P2,P13,P22,P3,P4,P41,P5,P6,P7,TAM,T2,T13,T22,T3,  -
       1 T4,T41,T6,T7,WA2,WA13,WA22,WA3,WG4,WG41,WG6,WG7,DH4,DH41,ETAB,   -
       2 ETAAB,FN,XNL,XNH,WF4,WF7,A8,AE,ALT,XMN,CDN,CVN,FVGP,CVGP,FG
        READ(5,510) V13,V3,V4,V41,V6,V7,AQL13,AQL6,XIH,XIL
        READ(5,511) ETAOF,ETAIF,ETAHC
C
C*************************************
C
C...    ACCOUNT FOR BIAS ON VANE GEOMETRY
        FVGP=BSFVGP-FVGP
        CVGP=BSCVGP-CVGP
C
        IF (IP .EQ. 1) GOTO 49
        IWET=NDRY+1
        IF (IP .EQ. IWET) GOTO 49
        GOTO 50
C
   49 CALL DSGNPT(P0,P2,P13,P22,P3,P4,P41,P5,P6,P7,TAM,T2,T13,T22,T3,  -
       1 T4,T41,T6,T7,WA2,WA13,WA22,WA3,WG4,WG41,WG6,WG7,DH4,DH41,ETAB,   -
       2 ETAAB,FN,XNL,XNH,WF4,WF7,A8,AE,ALT,XMN,CDN,CVN,FVGP,CVGP,FG,  -
       3 KBLWLT,KBLWHT,IP,ETAOF,ETAIF,ETAHC)
C
   50 CONTINUE
C
C.....STEADY-STATE
        ITRANS=0
C
        CALL ENGINE
C
```

Figure 8. - Main routine DIGTEM for the output test case.

```
      IF(IP .NE. NOPER) GOTO 100
      WRITE(6,514) POINT
C
  100 CONTINUE
C
CXXXXXXXXXXXXXXXXXXXXXXXXXXXXXXXXXXXXXXXXXXXXXXXXXXXXXXXXXXXXXXXXXXXXXXXX
C
C... INITIALIZE STATE AND DERIVATIVE VARIABLES
C
      VS(1) = XNL
      VS(2) = XNH
      VS(3) = W3
      VS(4) = T3
      VS(5) = W4
      VS(6) = T4
      VS(7) = W41
      VS(8) = T41
      VS(9) = W6
      VS(10) = T6
      VS(11) = W7
      VS(12) = T7
      VS(13) = WA13
      VS(14) = WG6
      VS(15) = W13
      VS(16) = T13
      VDOT(1) = DXNL
      VDOT(2) = DXNH
      VDOT(3) = DW3
      VDOT(4) = DT3
      VDOT(5) = DW4
      VDOT(6) = DT4
      VDOT(7) = DW41
      VDOT(8) = DT41
      VDOT(9) = DW6
      VDOT(10) = DT6
      VDOT(11) = DW7
      VDOT(12) = DT7
      VDOT(13) = DWA13
      VDOT(14) = DWG6
      VDOT(15) = DW13
      VDOT(16) = DT13
C
      IF (IBDINT .EQ. 1) GOTO 2000
      CALL FDINTG
      GO TO 3000
C
 2000 CONTINUE
      CALL BDINTG
 3000 CONTINUE
  504 FORMAT(5F12.5)
  505 FORMAT(2F10.0)
  507 FORMAT(9X,I3)
  508 FORMAT((1X,2(I2,2X)))
  510 FORMAT(6F12.5)
  511 FORMAT(3F12.5)
  514 FORMAT(/,' OPERATING POINT NUMBER ',I4)
      STOP
      END
```

Figure 8. - Concluded.

INPUT DATA

OPERATING POINT NUMBER 3

ORIGINAL PAGE IS
OF POOR QUALITY

TIME = 0.0000 SECONDS

	STA 2	STA 13	STA 2.2	STA 3	STA 4	STA 4.1	STA 6	STA 7
PRESSURE	14.6960	19.1000	20.6036	99.3999	94.5999	27.0999	17.5000	17.3000
TEMPERATURE	518.670	571.000	578.205	966.000	1580.00	1117.00	785.000	785.000
DERIVATIVE		1.52573		53.3228	-23.8950	-.416268	10.5138	-93.3126
MASS FLOW	103.567	54.0000	49.7557	41.5867	41.8824	49.3406	104.000	104.451
DERIVATIVE		0.244141E-03					0.268595E-02	
STORED MASS		4.54641		0.466186	0.271259	1.51610	1.81102	1.48046
DERIVATIVE		-.158446		-.771942E-01	0.742999E-01	0.462494E-01	-.311279E-01	-.490562
ENERGY DER.		6.93660		24.8983	-6.48174	-.631104	19.0407	-138.146
DELTA H					101.309	27.1968		

LOW SPEED SPOOL = 6175.00 RPM
DERIVATIVE = -25.4913 RPM/SEC

HIGH SPEED SPOOL = 9439.00 RPM
DERIVATIVE = 16.1629 RPM/SEC

MAIN COMBUSTOR FUEL FLOW =0.370000

AFTERBURNER FUEL FLOW =0.000000

BLEED MASS FLOWS--
LOW PRESSURE =0.628276
HIGH PRESSURE = 7.50448
OVERBOARD =0.113444

VARIABLE GEOMETRY --
FVGP = -24.9900
CVGP = -20.0000
THROAT AREA = 430.000

FSHIFT =0.216844E-04
CSHIFT =-.339364E-02

CONVERGED STEADY STATE POINT

TIME = 0.0000 SECONDS

	STA 2	STA 13	STA 2.2	STA 3	STA 4	STA 4.1	STA 6	STA 7
PRESSURE	14.6960	19.0887	20.6006	99.6367	94.8361	27.1478	17.4849	17.2840
TEMPERATURE	518.670	571.375	578.098	966.401	1578.93	1115.84	784.934	784.934
DERIVATIVE		-.461090E-02		-.133642	0.244831	-.870769E-01	-.525365E-01	0.221378E-01
MASS FLOW	103.927	54.0319	49.8948	41.6306	42.0007	49.5215	104.183	104.183
DERIVATIVE		-.166016E-01					-.131836E-01	
STORED MASS		4.54076		0.467103	0.272121	1.52035	1.80961	1.47922
DERIVATIVE		-.915527E-04		0.305176E-04	-.562072E-04	-.152588E-04	-.152588E-04	0.106812E-03
ENERGY DER.		-.209370E-01		-.624246E-01	0.666237E-01	-.132387	-.950707E-01	0.327466E-01
DELTA H					101.306	27.3107		

LOW SPEED SPOOL = 6181.22 RPM
DERIVATIVE = 0.151318E-01 RPM/SEC

HIGH SPEED SPOOL = 9444.84 RPM
DERIVATIVE = 0.264081E-01RPM/SEC

MAIN COMBUSTOR FUEL FLOW =0.370000

AFTERBURNER FUEL FLOW =0.000000

BLEED MASS FLOWS--
LOW PRESSURE =0.629642
HIGH PRESSURE = 7.52079
OVERBOARD =0.113691

VARIABLE GEOMETRY --
FVGP = -24.9900
CVGP = -20.0000
THROAT AREA = 430.000

FSHIFT =0.218332E-04
CSHIFT =-.415303E-02

TIME	P0 TAM XNL	P2 T2 XNH	P13 T13 WF4	P22 T22 WF7	P3 T3 A8	P4 T4 AE	P41 T41 FVGP	P6 T6 CVGP	P7 T7 MATTOT
0.000	14.696 518.67 6181.2	14.696 518.67 9444.8	19.089 571.37 0.37000	20.601 578.10 0.00000	99.637 966.40 430.00	94.836 1578.9 492.00	27.148 1115.8 -24.990	17.485 784.93 -20.000	17.284 784.93 1
0.100	14.696 518.67 6192.8	14.696 518.67 9463.2	19.198 572.50 0.43650	20.687 578.98 0.00000	102.31 973.21 430.00	97.634 1684.0 492.00	27.936 1171.0 -24.990	17.630 805.78 -18.800	17.420 801.58 2
0.200	14.696 518.67 6235.3	14.696 518.67 9513.4	19.359 574.29 0.50300	20.835 580.22 0.00000	106.24 983.78 430.00	101.57 1786.0 492.00	28.922 1245.0 -24.990	17.792 839.86 -17.600	17.568 835.75 2
0.300	14.696 518.67 6309.9	14.696 518.67 9597.1	19.580 576.45 0.56950	21.053 581.93 0.00000	111.44 997.52 430.00	106.67 1875.5 492.00	30.059 1308.1 -24.990	17.989 869.95 -16.400	17.748 866.61 3
0.400	14.696 518.67 6416.2	14.696 518.67 9704.8	19.893 579.21 0.63600	21.365 584.41 0.00000	117.80 1014.4 430.00	112.86 1952.8 492.00	31.467 1362.7 -24.990	18.268 896.98 -15.200	18.006 894.28 3
0.500	14.696 518.67 6551.8	14.696 518.67 9828.6	20.296 582.74 0.70250	21.812 587.76 0.00000	125.16 1032.5 430.00	119.97 2017.4 492.00	33.104 1408.3 -24.990	18.610 920.44 -14.000	18.327 918.49 3

Figure 9. - DIGTEM output for test case.

0.600	14.696 518.67 6711.3	14.696 518.67 9966.1	20.791 587.07 0.76900	22.367 592.02 0.00000	132.56 1049.9 430.00	127.14 2076.2 492.00	34.865 1449.1 -24.990	19.001 939.49 -12.800	18.691 938.10 3
0.700	14.696 518.67 6892.1	14.696 518.67 10114.	21.352 591.86 0.83550	22.992 597.16 0.00000	140.48 1067.8 430.00	134.79 2127.3 492.00	36.792 1485.7 -24.990	19.456 956.51 -11.600	19.181 955.45 3
0.800	14.696 518.67 7091.7	14.696 518.67 10269.	21.974 596.81 0.90200	23.703 602.48 0.00000	149.08 1085.2 430.00	143.05 2169.5 492.00	38.801 1515.6 -24.990	20.081 972.63 -10.400	19.667 971.48 3
0.900	14.696 518.67 7297.1	14.696 518.67 10429.	22.846 603.69 0.96850	24.604 608.87 0.00000	158.73 1103.4 430.00	152.31 2201.9 492.00	41.113 1539.8 -24.990	20.846 990.63 -9.2000	20.472 990.15 3
1.000	14.696 518.67 7508.0	14.696 518.67 10587.	23.680 610.07 1.0350	25.521 615.56 0.00000	168.43 1122.5 430.00	161.61 2233.6 492.00	43.485 1561.4 -24.990	21.570 1003.9 -8.0000	21.173 1003.3 3
1.100	14.696 518.67 7711.9	14.696 518.67 10739.	24.694 617.92 1.1015	26.572 623.38 0.00000	178.47 1143.2 430.00	171.23 2263.6 492.00	46.029 1583.6 -22.661	22.416 1014.1 -6.8000	21.979 1014.2 3
1.200	14.696 518.67 7905.7	14.696 518.67 10877.	25.727 625.14 1.1680	27.680 630.68 0.00000	188.40 1162.8 430.00	180.76 2292.7 492.00	48.683 1606.3 -20.332	23.311 1025.6 -5.6000	22.891 1025.4 3
1.300	14.696 518.67 8091.2	14.696 518.67 11000.	26.732 632.52 1.2345	28.635 637.71 0.00000	197.90 1181.3 430.00	189.88 2322.7 492.00	51.205 1628.7 -18.003	24.197 1038.4 -4.4000	23.719 1038.2 3
1.400	14.696 518.67 8267.0	14.696 518.67 11115.	27.699 639.45 1.3010	29.681 645.08 0.00000	207.19 1199.1 430.00	198.77 2352.2 492.00	53.648 1650.9 -15.674	25.092 1052.2 -3.2000	24.596 1051.9 3
1.500	14.696 518.67 8427.6	14.696 518.67 11221.	28.715 647.04 1.3675	30.733 652.65 0.00000	216.30 1216.4 430.00	207.49 2381.2 492.00	56.081 1672.5 -13.345	26.019 1066.0 -2.0000	25.498 1065.7 3
1.600	14.696 518.67 8566.8	14.696 518.67 11321.	29.719 654.86 1.4340	31.741 659.87 0.00000	225.12 1232.9 430.00	215.99 2410.3 492.00	58.466 1694.3 -11.016	26.953 1080.8 -.80002	26.422 1080.3 3
1.700	14.696 518.67 8688.7	14.696 518.67 11415.	30.651 661.95 1.5005	32.653 666.56 0.00000	233.44 1248.6 430.00	223.98 2440.8 492.00	60.753 1716.7 -8.6870	27.842 1096.1 0.39998	27.303 1095.5 3
1.800	14.696 518.67 8796.8	14.696 518.67 11504.	31.519 668.55 1.5670	33.473 672.92 0.00000	241.13 1263.5 430.00	231.39 2473.1 492.00	62.879 1740.7 -6.3580	28.693 1112.7 1.6000	28.134 1112.0 3
1.900	14.696 518.67 8892.2	14.696 518.67 11589.	32.339 675.00 1.6335	34.187 679.00 0.00000	248.27 1278.0 430.00	238.25 2507.0 492.00	64.875 1765.6 -4.0291	29.494 1129.5 2.8000	28.919 1128.6 3
2.000	14.696 518.67 8974.5	14.696 518.67 11673.	33.081 681.19 1.7000	34.807 684.50 0.00000	254.93 1291.8 430.00	244.69 2542.0 492.00	66.708 1791.6 -1.7000	30.218 1146.7 4.0000	29.636 1145.7 3
2.100	14.696 518.67 9046.5	14.696 518.67 11744.	33.461 685.12 1.7000	35.126 688.51 0.00000	258.55 1302.5 430.00	248.07 2536.6 492.00	67.714 1793.1 -1.7000	30.588 1151.5 4.0000	30.011 1151.7 4
2.200	14.696 518.67 9105.6	14.696 518.67 11794.	33.662 687.90 1.7000	35.295 691.52 0.00000	260.55 1309.8 430.00	249.96 2534.7 492.00	68.309 1791.4 -1.7000	30.780 1152.3 4.0000	30.204 1152.4 4
2.300	14.696 518.67 9152.0	14.696 518.67 11829.	33.817 690.19 1.7000	35.425 693.93 0.00000	261.92 1315.2 430.00	251.23 2534.0 492.00	68.719 1790.9 -1.7000	30.925 1153.2 4.0000	30.346 1153.2 4
2.400	14.696 518.67 9187.3	14.696 518.67 11854.	33.935 692.01 1.7000	35.524 695.80 0.00000	262.88 1319.3 430.00	252.13 2533.8 492.00	69.012 1790.9 -1.7000	31.039 1154.0 4.0000	30.450 1154.0 4
2.500	14.696 518.67 9212.1	14.696 518.67 11872.	34.020 693.37 1.7000	35.594 696.93 0.00000	263.61 1321.9 430.00	252.81 2533.2 492.00	69.193 1790.6 -1.7000	31.119 1155.2 4.0000	30.533 1155.1 4
2.600	14.696 518.67 9227.2	14.696 518.67 11885.	34.064 694.15 1.7000	35.628 697.47 0.00000	264.18 1323.5 430.00	253.35 2532.3 492.00	69.317 1789.6 -1.7000	31.164 1156.1 4.0000	30.580 1156.1 4
2.700	14.696 518.67 9236.8	14.696 518.67 11895.	34.090 694.63 1.7000	35.649 697.81 0.00000	264.61 1324.7 430.00	253.75 2531.6 492.00	69.409 1788.9 -1.7000	31.192 1156.7 4.0000	30.610 1156.7 4
2.800	14.696 518.67 9243.3	14.696 518.67 11903.	34.108 694.94 1.7000	35.662 698.03 0.00000	264.90 1325.6 430.00	254.02 2531.2 492.00	69.475 1788.4 -1.7000	31.215 1157.1 4.0000	30.630 1157.1 4
2.900	14.696 518.67 9247.4	14.696 518.67 11909.	34.120 695.15 1.7000	35.672 698.18 0.00000	265.08 1326.2 430.00	254.19 2531.0 492.00	69.513 1788.1 -1.7000	31.229 1157.3 4.0000	30.640 1157.3 4
3.000	14.696 518.67 9250.1	14.696 518.67 11913.	34.129 695.29 1.7000	35.678 698.28 0.00000	265.22 1326.7 430.00	254.32 2530.9 492.00	69.541 1787.9 -1.7000	31.234 1157.5 4.0000	30.653 1157.5 4
3.100	14.696 518.67 9252.0	14.696 518.67 11917.	34.134 695.37 1.7000	35.682 698.34 0.00000	265.33 1327.0 430.00	254.42 2530.8 492.00	69.563 1787.7 -1.7000	31.239 1157.6 4.0000	30.660 1157.6 4
3.200	14.696 518.67 9253.3	14.696 518.67 11920.	34.135 695.42 1.7000	35.683 698.39 0.00000	265.42 1327.3 430.00	254.50 2530.7 492.00	69.580 1787.6 -1.7000	31.251 1157.7 4.0000	30.660 1157.7 4

Figure 9. - Continued.

ORIGINAL PAGE IS
OF POOR QUALITY

3.300	14.696 518.67 9254.3	14.696 518.67 11923.	34.138 695.47 1.7000	35.685 698.42 0.00000	265.48 1327.5 430.00	254.57 2530.7 492.00	69.594 1787.5 -1.7000	31.253 1157.8 4.0000	30.662 1157.7 4
3.400	14.696 518.67 9255.1	14.696 518.67 11925.	34.140 695.50 1.7000	35.687 698.45 0.00000	265.54 1327.7 430.00	254.62 2530.6 492.00	69.605 1787.4 -1.7000	31.252 1157.8 4.0000	30.665 1157.8 4
3.500	14.696 518.67 9255.7	14.696 518.67 11927.	34.143 695.53 1.7000	35.689 698.47 0.00000	265.58 1327.8 430.00	254.66 2530.5 492.00	69.615 1787.4 -1.7000	31.248 1157.8 4.0000	30.674 1157.9 4
3.600	14.696 518.67 9256.2	14.696 518.67 11928.	34.143 695.55 1.7000	35.689 698.49 0.00000	265.61 1327.9 430.00	254.69 2530.5 492.00	69.622 1787.4 -1.7000	31.255 1157.9 4.0000	30.673 1157.9 4
3.700	14.696 518.67 9256.6	14.696 518.67 11929.	34.144 695.57 1.7000	35.690 698.50 0.00000	265.63 1328.0 430.00	254.71 2530.5 492.00	69.627 1787.3 -1.7000	31.259 1158.0 4.0000	30.672 1157.9 4
3.800	14.696 518.67 9256.9	14.696 518.67 11929.	34.144 695.58 1.7000	35.690 698.51 0.00000	265.65 1328.1 430.00	254.72 2530.5 492.00	69.631 1787.3 -1.7000	31.259 1158.0 4.0000	30.672 1158.0 4
3.900	14.696 518.67 9257.2	14.696 518.67 11930.	34.146 695.60 1.7000	35.692 698.52 0.00000	265.66 1328.1 430.00	254.73 2530.4 492.00	69.634 1787.3 -1.7000	31.254 1158.0 4.0000	30.676 1158.0 4
4.000	14.696 518.67 9257.3	14.696 518.67 11930.	34.146 695.60 1.7000	35.692 698.53 0.00000	265.66 1328.1 430.00	254.74 2530.5 492.00	69.636 1787.3 -1.7000	31.256 1158.0 4.0000	30.677 1158.0 4
4.100	14.696 518.67 9257.4	14.696 518.67 11930.	34.146 695.60 1.7000	35.692 698.53 0.00000	265.67 1328.1 430.00	254.74 2530.4 492.00	69.637 1787.3 -1.7000	31.259 1158.0 4.0000	30.676 1158.0 4
4.200	14.696 518.67 9257.6	14.696 518.67 11930.	34.146 695.60 1.7000	35.691 698.53 0.00000	265.67 1328.1 430.00	254.74 2530.6 492.00	69.638 1787.3 -1.7000	31.263 1158.0 4.0000	30.672 1158.0 4
4.300	14.696 518.67 9257.6	14.696 518.67 11930.	34.147 695.61 1.7000	35.692 698.54 0.00000	265.68 1328.2 430.00	254.75 2530.4 492.00	69.639 1787.3 -1.7000	31.259 1158.0 4.0000	30.674 1158.0 4
4.400	14.696 518.67 9257.7	14.696 518.67 11930.	34.147 695.62 1.7000	35.693 698.54 0.00000	265.68 1328.2 430.00	254.75 2530.4 492.00	69.639 1787.3 -1.7000	31.258 1158.0 4.0000	30.676 1158.0 4
4.500	14.696 518.67 9257.7	14.696 518.67 11931.	34.147 695.62 1.7000	35.693 698.54 0.00000	265.68 1328.2 430.00	254.75 2530.4 492.00	69.640 1787.3 -1.7000	31.259 1158.0 4.0000	30.677 1158.0 4
4.600	14.696 518.67 9257.7	14.696 518.67 11931.	34.146 695.61 1.7000	35.692 698.54 0.00000	265.68 1328.2 430.00	254.76 2530.4 492.00	69.640 1787.3 -1.7000	31.263 1158.0 4.0000	30.674 1158.0 4
4.700	14.696 518.67 9257.7	14.696 518.67 11931.	34.147 695.61 1.7000	35.692 698.54 0.00000	265.68 1328.2 430.00	254.76 2530.4 492.00	69.640 1787.3 -1.7000	31.262 1158.0 4.0000	30.674 1158.0 4
4.800	14.696 518.67 9257.7	14.696 518.67 11931.	34.147 695.62 1.7000	35.692 698.54 0.00000	265.68 1328.2 430.00	254.76 2530.4 492.00	69.640 1787.3 -1.7000	31.260 1158.0 4.0000	30.675 1158.0 4
4.900	14.696 518.67 9257.7	14.696 518.67 11931.	34.147 695.62 1.7000	35.693 698.54 0.00000	265.68 1328.2 430.00	254.76 2530.4 492.00	69.641 1787.3 -1.7000	31.259 1158.0 4.0000	30.676 1158.0 4
5.000	14.696 518.67 9257.7	14.696 518.67 11931.	34.147 695.62 1.7000	35.693 698.54 0.00000	265.68 1328.2 430.00	254.76 2530.4 492.00	69.640 1787.3 -1.7000	31.261 1158.0 4.0000	30.676 1158.1 4
5.100	14.696 518.67 9257.8	14.696 518.67 11931.	34.147 695.62 1.7000	35.692 698.54 0.00000	265.68 1328.2 430.00	254.76 2530.4 492.00	69.640 1787.3 -1.7000	31.262 1158.0 4.0000	30.675 1158.0 4
5.200	14.696 518.67 9257.8	14.696 518.67 11931.	34.147 695.62 1.7000	35.692 698.54 0.00000	265.68 1328.2 430.00	254.76 2530.4 492.00	69.640 1787.3 -1.7000	31.261 1158.0 4.0000	30.675 1158.0 4
5.300	14.696 518.67 9257.8	14.696 518.67 11931.	34.148 695.62 1.7000	35.693 698.54 0.00000	265.68 1328.2 430.00	254.76 2530.4 492.00	69.640 1787.3 -1.7000	31.257 1158.0 4.0000	30.678 1158.0 4
5.400	14.696 518.67 9257.7	14.696 518.67 11931.	34.146 695.61 1.7000	35.692 698.54 0.00000	265.68 1328.2 430.00	254.76 2530.4 492.00	69.641 1787.3 -1.7000	31.265 1158.1 4.0000	30.674 1158.0 4
5.500	14.696 518.67 9257.8	14.696 518.67 11931.	34.146 695.61 1.7000	35.692 698.54 0.00000	265.68 1328.2 430.00	254.75 2530.5 492.00	69.641 1787.3 -1.7000	31.264 1158.1 4.0000	30.673 1158.0 4
5.600	14.696 518.67 9257.8	14.696 518.67 11931.	34.147 695.62 1.7000	35.692 698.54 0.00000	265.68 1328.2 430.00	254.76 2530.4 492.00	69.640 1787.3 -1.7000	31.261 1158.0 4.0000	30.674 1158.0 4
5.700	14.696 518.67 9257.8	14.696 518.67 11931.	34.147 695.62 1.7000	35.693 698.54 0.00000	265.68 1328.2 430.00	254.76 2530.4 492.00	69.641 1787.3 -1.7000	31.259 1158.0 4.0000	30.676 1158.0 4
5.800	14.696 518.67 9257.8	14.696 518.67 11931.	34.147 695.62 1.7000	35.693 698.54 0.00000	265.68 1328.2 430.00	254.76 2530.5 492.00	69.640 1787.3 -1.7000	31.259 1158.0 4.0000	30.677 1158.0 4
5.900	14.696 518.67 9257.8	14.696 518.67 11931.	34.147 695.62 1.7000	35.692 698.54 0.00000	265.68 1328.2 430.00	254.76 2530.4 492.00	69.641 1787.3 -1.7000	31.262 1158.0 4.0000	30.675 1158.0 4

Figure 9. - Continued.

ORIGINAL PAGE IS
OF POOR QUALITY

6.000	14.696 518.67 9257.8	14.696 518.67 11931.	34.147 695.62 1.7000	35.692 698.54 0.00000	265.68 1328.2 430.00	254.76 2530.4 492.00	69.640 1787.3 -1.7000	31.259 1158.0 4.0000	30.674 1158.0 4
6.100	14.696 518.67 9257.8	14.696 518.67 11931.	34.148 695.62 1.7000	35.693 698.54 0.00000	265.68 1328.2 430.00	254.76 2530.4 492.00	69.640 1787.3 -1.7000	31.256 1158.0 4.0000	30.678 1158.0 4
6.200	14.696 518.67 9257.8	14.696 518.67 11931.	34.148 695.62 1.7000	35.693 698.54 0.00000	265.68 1328.2 430.00	254.76 2530.4 492.00	69.641 1787.3 -1.7000	31.257 1158.0 4.0000	30.678 1158.1 4
6.300	14.696 518.67 9257.8	14.696 518.67 11931.	34.147 695.62 1.7000	35.693 698.54 0.00000	265.68 1328.2 430.00	254.76 2530.4 492.00	69.641 1787.3 -1.7000	31.260 1158.0 4.0000	30.677 1158.1 4
6.400	14.696 518.67 9257.8	14.696 518.67 11931.	34.147 695.62 1.7000	35.692 698.54 0.00000	265.68 1328.2 430.00	254.76 2530.4 492.00	69.641 1787.3 -1.7000	31.261 1158.0 4.0000	30.676 1158.0 4
6.500	14.696 518.67 9257.8	14.696 518.67 11931.	34.147 695.62 1.7000	35.692 698.54 0.00000	265.69 1328.2 430.00	254.76 2530.4 492.00	69.641 1787.3 -1.7000	31.260 1158.0 4.0000	30.675 1158.0 4
6.600	14.696 518.67 9257.8	14.696 518.67 11931.	34.148 695.62 1.7000	35.693 698.54 0.00000	265.68 1328.2 430.00	254.76 2530.4 492.00	69.640 1787.3 -1.7000	31.258 1158.0 4.0000	30.677 1158.0 4
6.700	14.696 518.67 9257.8	14.696 518.67 11931.	34.147 695.62 1.7000	35.693 698.54 0.00000	265.68 1328.2 430.00	254.76 2530.4 492.00	69.640 1787.3 -1.7000	31.259 1158.0 4.0000	30.677 1158.0 4
6.800	14.696 518.67 9257.8	14.696 518.67 11931.	34.147 695.61 1.7000	35.692 698.54 0.00000	265.68 1328.2 430.00	254.76 2530.4 492.00	69.641 1787.3 -1.7000	31.264 1158.1 4.0000	30.674 1158.0 4
6.900	14.696 518.67 9257.8	14.696 518.67 11931.	34.148 695.62 1.7000	35.693 698.54 0.00000	265.68 1328.2 430.00	254.76 2530.4 492.00	69.640 1787.3 -1.7000	31.256 1158.0 4.0000	30.676 1158.0 4
7.000	14.696 518.67 9257.8	14.696 518.67 11931.	34.148 695.62 1.7000	35.693 698.54 0.00000	265.68 1328.2 430.00	254.76 2530.4 492.00	69.640 1787.3 -1.7000	31.254 1158.0 4.0000	30.680 1158.1 4
7.100	14.696 518.67 9257.8	14.696 518.67 11931.	34.148 695.62 1.7000	35.693 698.54 0.00000	265.68 1328.2 430.00	254.76 2530.4 492.00	69.641 1787.3 -1.7000	31.258 1158.0 4.0000	30.679 1158.1 4
7.200	14.696 518.67 9257.8	14.696 518.67 11931.	34.147 695.62 1.7000	35.693 698.54 0.00000	265.68 1328.2 430.00	254.76 2530.4 492.00	69.641 1787.3 -1.7000	31.261 1158.0 4.0000	30.677 1158.1 4
7.300	14.696 518.67 9257.8	14.696 518.67 11931.	34.147 695.62 1.7000	35.692 698.54 0.00000	265.68 1328.2 430.00	254.76 2530.4 492.00	69.640 1787.3 -1.7000	31.262 1158.0 4.0000	30.675 1158.0 4
7.400	14.696 518.67 9257.8	14.696 518.67 11931.	34.147 695.62 1.7000	35.693 698.54 0.00000	265.68 1328.2 430.00	254.76 2530.4 492.00	69.641 1787.3 -1.7000	31.258 1158.0 4.0000	30.676 1158.0 4
7.500	14.696 518.67 9257.8	14.696 518.67 11931.	34.148 695.62 1.7000	35.693 698.54 0.00000	265.68 1328.2 430.00	254.76 2530.4 492.00	69.641 1787.3 -1.7000	31.257 1158.0 4.0000	30.678 1158.0 4
7.600	14.696 518.67 9257.8	14.696 518.67 11931.	34.147 695.61 1.7000	35.692 698.54 0.00000	265.68 1328.2 430.00	254.76 2530.4 492.00	69.641 1787.3 -1.7000	31.265 1158.1 4.0000	30.675 1158.0 4
7.700	14.696 518.67 9257.8	14.696 518.67 11931.	34.146 695.61 1.7000	35.692 698.54 0.00000	265.68 1328.2 430.00	254.76 2530.4 492.00	69.641 1787.3 -1.7000	31.264 1158.1 4.0000	30.673 1158.0 4
7.800	14.696 518.67 9257.8	14.696 518.67 11931.	34.147 695.62 1.7000	35.692 698.54 0.00000	265.68 1328.2 430.00	254.76 2530.4 492.00	69.640 1787.3 -1.7000	31.262 1158.0 4.0000	30.674 1158.0 4
7.900	14.696 518.67 9257.8	14.696 518.67 11931.	34.147 695.62 1.7000	35.693 698.54 0.00000	265.68 1328.2 430.00	254.76 2530.4 492.00	69.641 1787.3 -1.7000	31.259 1158.0 4.0000	30.676 1158.0 4
8.000	14.696 518.67 9257.8	14.696 518.67 11931.	34.148 695.62 1.7000	35.693 698.54 0.00000	265.68 1328.2 430.00	254.76 2530.4 492.00	69.641 1787.3 -1.7000	31.259 1158.0 4.0000	30.677 1158.0 4
8.100	14.696 518.67 9257.8	14.696 518.67 11931.	34.147 695.62 1.7000	35.692 698.54 0.00000	265.68 1328.2 430.00	254.76 2530.4 492.00	69.640 1787.3 -1.7000	31.262 1158.0 4.0000	30.676 1158.0 4
8.200	14.696 518.67 9257.8	14.696 518.67 11931.	34.147 695.62 1.7000	35.692 698.54 0.00000	265.68 1328.2 430.00	254.76 2530.4 492.00	69.641 1787.3 -1.7000	31.262 1158.0 4.0000	30.674 1158.0 4
8.300	14.696 518.67 9257.8	14.696 518.67 11931.	34.148 695.62 1.7000	35.693 698.54 0.00000	265.68 1328.2 430.00	254.76 2530.4 492.00	69.641 1787.3 -1.7000	31.256 1158.0 4.0000	30.677 1158.0 4
8.400	14.696 518.67 9257.8	14.696 518.67 11931.	34.148 695.62 1.7000	35.693 698.54 0.00000	265.68 1328.2 430.00	254.76 2530.4 492.00	69.641 1787.3 -1.7000	31.257 1158.0 4.0000	30.679 1158.1 4
8.500	14.696 518.67 9257.8	14.696 518.67 11931.	34.147 695.62 1.7000	35.693 698.54 0.00000	265.68 1328.2 430.00	254.76 2530.4 492.00	69.641 1787.3 -1.7000	31.259 1158.0 4.0000	30.677 1158.1 4
8.600	14.696 518.67 9257.8	14.696 518.67 11931.	34.147 695.62 1.7000	35.692 698.54 0.00000	265.68 1328.2 430.00	254.76 2530.4 492.00	69.641 1787.3 -1.7000	31.261 1158.0 4.0000	30.676 1158.0 4

Figure 9. - Continued.

ORIGINAL PAGE IS
OF POOR QUALITY

8.700	14.696 518.67 9257.8	14.696 518.67 11931.	34.147 695.62 1.7000	35.692 698.54 0.00000	265.69 1328.2 430.00	254.76 2530.4 492.00	69.641 1787.3 -1.7000	31.260 1158.0 4.0000	30.674 1158.0 4
8.800	14.696 518.67 9257.8	14.696 518.67 11931.	34.148 695.62 1.7000	35.693 698.54 0.00000	265.68 1328.2 430.00	254.76 2530.4 492.00	69.640 1787.3 -1.7000	31.258 1158.0 4.0000	30.677 1158.0 4
8.900	14.696 518.67 9257.8	14.696 518.67 11931.	34.147 695.62 1.7000	35.693 698.54 0.00000	265.68 1328.2 430.00	254.76 2530.5 492.00	69.640 1787.3 -1.7000	31.258 1158.0 4.0000	30.677 1158.0 4
9.000	14.696 518.67 9257.8	14.696 518.67 11931.	34.147 695.61 1.7000	35.692 698.54 0.00000	265.68 1328.2 430.00	254.76 2530.4 492.00	69.641 1787.3 -1.7000	31.264 1158.1 4.0000	30.674 1158.0 4
9.100	14.696 518.67 9257.8	14.696 518.67 11931.	34.147 695.62 1.7000	35.692 698.54 0.00000	265.68 1328.2 430.00	254.76 2530.4 492.00	69.640 1787.3 -1.7000	31.262 1158.0 4.0000	30.674 1158.0 4
9.200	14.696 518.67 9257.8	14.696 518.67 11931.	34.147 695.62 1.7000	35.692 698.54 0.00000	265.68 1328.2 430.00	254.76 2530.4 492.00	69.641 1787.3 -1.7000	31.260 1158.0 4.0000	30.675 1158.0 4
9.300	14.696 518.67 9257.8	14.696 518.67 11931.	34.147 695.62 1.7000	35.693 698.54 0.00000	265.68 1328.2 430.00	254.76 2530.4 492.00	69.641 1787.3 -1.7000	31.259 1158.0 4.0000	30.676 1158.0 4
9.400	14.696 518.67 9257.8	14.696 518.67 11931.	34.147 695.62 1.7000	35.693 698.54 0.00000	265.68 1328.2 430.00	254.76 2530.4 492.00	69.641 1787.3 -1.7000	31.261 1158.0 4.0000	30.677 1158.1 4
9.500	14.696 518.67 9257.8	14.696 518.67 11931.	34.147 695.62 1.7000	35.692 698.54 0.00000	265.68 1328.2 430.00	254.76 2530.4 492.00	69.640 1787.3 -1.7000	31.262 1158.0 4.0000	30.675 1158.0 4
9.600	14.696 518.67 9257.8	14.696 518.67 11931.	34.147 695.62 1.7000	35.692 698.54 0.00000	265.68 1328.2 430.00	254.76 2530.4 492.00	69.641 1787.3 -1.7000	31.261 1158.0 4.0000	30.675 1158.0 4
9.700	14.696 518.67 9257.8	14.696 518.67 11931.	34.148 695.62 1.7000	35.693 698.54 0.00000	265.68 1328.2 430.00	254.76 2530.4 492.00	69.640 1787.3 -1.7000	31.257 1158.0 4.0000	30.678 1158.0 4
9.800	14.696 518.67 9257.8	14.696 518.67 11931.	34.147 695.62 1.7000	35.692 698.54 0.00000	265.68 1328.2 430.00	254.76 2530.4 492.00	69.640 1787.3 -1.7000	31.264 1158.1 4.0000	30.676 1158.1 4
9.900	14.696 518.67 9257.8	14.696 518.67 11931.	34.146 695.61 1.7000	35.692 698.54 0.00000	265.68 1328.2 430.00	254.76 2530.4 492.00	69.640 1787.3 -1.7000	31.265 1158.1 4.0000	30.673 1158.0 4
10.000	14.696 518.67 9257.8	14.696 518.67 11931.	34.147 695.62 1.7000	35.692 698.54 0.00000	265.68 1328.2 430.00	254.76 2530.4 492.00	69.641 1787.3 -1.7000	31.262 1158.0 4.0000	30.674 1158.0 4
10.100	14.696 518.67 9256.4	14.696 518.67 11930.	34.179 695.78 1.7000	35.720 698.60 0.16666	265.83 1328.2 437.67	254.89 2529.7 504.93	69.669 1786.9 -1.7267	31.304 1158.5 4.0000	30.717 1194.8 4
10.200	14.696 518.67 9255.2	14.696 518.67 11930.	34.184 695.77 1.7000	35.724 698.58 0.33333	265.85 1328.1 445.33	254.91 2529.5 517.87	69.682 1786.7 -1.7533	31.309 1158.4 4.0000	30.726 1235.7 4
10.300	14.696 518.67 9254.3	14.696 518.67 11929.	34.191 695.78 1.7000	35.730 698.57 0.50000	265.87 1328.1 453.00	254.93 2529.4 530.80	69.686 1786.6 -1.7800	31.318 1158.5 4.0000	30.737 1278.1 4
10.400	14.696 518.67 9253.2	14.696 518.67 11929.	34.202 695.81 1.7000	35.740 698.58 0.66666	265.91 1328.0 460.67	254.98 2529.0 543.73	69.696 1786.4 -1.8067	31.335 1158.7 4.0000	30.757 1321.8 4
10.500	14.696 518.67 9251.8	14.696 518.67 11928.	34.219 695.87 1.7000	35.754 698.58 0.83333	265.98 1328.0 468.33	255.04 2528.6 556.67	69.712 1786.1 -1.8333	31.359 1158.9 4.0000	30.779 1366.6 4
10.600	14.696 518.67 9250.0	14.696 518.67 11927.	34.238 695.93 1.7000	35.770 698.59 1.00000	266.06 1327.9 476.00	255.12 2528.0 569.60	69.732 1785.8 -1.8600	31.388 1159.1 4.0000	30.803 1412.9 4
10.700	14.696 518.67 9247.8	14.696 518.67 11926.	34.261 696.00 1.7000	35.790 698.60 1.1667	266.16 1327.8 483.67	255.20 2527.5 582.53	69.756 1785.4 -1.8867	31.417 1159.3 4.0000	30.833 1460.1 4
10.800	14.696 518.67 9245.3	14.696 518.67 11925.	34.285 696.06 1.7000	35.810 698.60 1.3333	266.25 1327.7 491.33	255.29 2526.9 595.47	69.781 1785.0 -1.9133	31.448 1159.5 4.0000	30.865 1508.3 4
10.900	14.696 518.67 9242.6	14.696 518.67 11924.	34.309 696 13 1.7000	35.831 698.60 1.5000	266.35 1327.5 499.00	255.38 2526.3 608.40	69.805 1784.5 -1.9400	31.479 1159.7 4.0000	30.896 1557.3 4
11.000	14.696 518.67 9239.7	14.696 518.67 11922.	34.334 696.19 1.7000	35.853 698.59 1.6667	266.45 1327.4 506.67	255.47 2525.6 621.33	69.831 1784.1 -1.9667	31.509 1159.8 4.0000	30.933 1607.3 4
11.100	14.696 518.67 9236.6	14.696 518.67 11920.	34.358 696.23 1.7000	35.873 698.57 1.8333	266.54 1327.2 514.33	255.56 2524.9 634.27	69.857 1783.6 -1.9933	31.546 1160.0 4.0000	30.960 1658.2 4
11.200	14.696 518.67 9233.5	14.696 518.67 11919.	34.381 696.28 1.7000	35.894 698.56 2.0000	266.63 1327.1 522.00	255.65 2524.2 647.20	69.882 1783.1 -2.0200	31.578 1160.2 4.0000	31.006 1710.0 4
11.300	14.696 518.67 9230.4	14.696 518.67 11917.	34.406 696.33 1.7000	35.915 698.54 2.1667	266.72 1326.9 529.67	255.73 2523.6 660.13	69.905 1782.7 -2.0467	31.604 1160.3 4.0000	31.033 1761.8 4

Figure 9. - Continued.

ORIGINAL PAGE IS
OF POOR QUALITY

11.400	14.696 518.67 9227.3	14.696 518.67 11915.	34.427 696.36 1.7000	35.933 698.62 2.3333	266.80 1326.7 537.33	255.81 2523.0 675.07	69.928 1782.2 -2.0733	31.637 1160.5 4.0000	31.068 1816.9 5
11.500	14.696 518.67 9224.3	14.696 518.67 11913.	34.446 696.38 1.7000	35.950 698.50 2.5000	266.87 1326.5 545.00	255.88 2522.4 688.00	69.948 1781.8 -2.1000	31.671 1160.6 4.0000	31.088 1868.4 5
11.600	14.696 518.67 9221.6	14.696 518.67 11911.	34.466 696.40 1.7000	35.967 698.48 2.6667	266.94 1326.4 552.67	255.94 2521.9 698.93	69.966 1781.4 -2.1267	31.69[illegible] 1160.7 4.0000	31.116 1922.2 5
11.700	14.696 518.67 9218.8	14.696 518.67 11910.	34.485 696.42 1.7000	35.982 698.45 2.8333	267.00 1326.2 560.33	255.99 2521.6 711.87	69.982 1781.1 -2.1533	31.714 1160.8 4.0000	31.139 1976.8 5
11.800	14.696 518.67 9216.3	14.696 518.67 11908.	34.498 696.43 1.7000	35.995 698.43 3.0000	267.05 1326.1 568.00	256.03 2521.0 724.80	69.996 1780.8 -2.1800	31.730 1160.9 4.0000	31.162 2031.0 5
11.900	14.696 518.67 9214.0	14.696 518.67 11907.	34.510 696.44 1.7000	36.006 698.41 3.1667	267.08 1325.9 575.67	256.08 2520.6 737.73	70.008 1780.5 -2.2067	31.750 1161.0 4.0000	31.179 2086.0 5
12.000	14.696 518.67 9212.0	14.696 518.67 11905.	34.520 696.44 1.7000	36.014 698.38 3.3333	267.11 1325.8 583.33	256.10 2520.3 750.67	70.017 1780.3 -2.2333	31.768 1161.0 4.0000	31.193 2141.3 5
12.100	14.696 518.67 9210.2	14.696 518.67 11904.	34.529 696.44 1.7000	36.021 698.36 3.5000	267.12 1325.7 591.00	256.12 2520.1 763.60	70.023 1780.1 -2.2600	31.777 1161.1 4.0000	31.208 2196.7 5
12.200	14.696 518.67 9208.7	14.696 518.67 11903.	34.539 696.44 1.7000	36.029 698.33 3.6667	267.13 1325.6 598.67	256.12 2520.0 776.53	70.027 1780.0 -2.2867	31.785 1161.1 4.0000	31.215 2252.1 5
12.300	14.696 518.67 9207.5	14.696 518.67 11902.	34.538 696.42 1.7000	36.028 698.31 3.8333	267.13 1325.5 606.33	256.12 2519.9 789.47	70.027 1780.0 -2.3133	31.790 1161.1 4.0000	31.219 2307.8 5
12.400	14.696 518.67 9206.5	14.696 518.67 11901.	34.539 696.40 1.7000	36.028 698.29 4.0000	267.12 1325.4 614.00	256.11 2519.8 802.40	70.026 1779.9 -2.3400	31.793 1161.1 4.0000	31.223 2363.7 5
12.500	14.696 518.67 9205.9	14.696 518.67 11901.	34.539 696.38 1.7000	36.028 698.27 4.1667	267.11 1325.3 621.67	256.09 2519.8 815.33	70.023 1779.9 -2.3667	31.792 1161.1 4.0000	31.221 2419.6 5
12.600	14.696 518.67 9205.6	14.696 518.67 11901.	34.536 696.35 1.7000	36.026 698.26 4.3333	267.09 1325.3 629.33	256.08 2519.9 828.27	70.019 1779.9 -2.3933	31.791 1161.1 4.0000	31.219 2475.6 5
12.700	14.696 518.67 9205.7	14.696 518.67 11900.	34.527 696.29 1.7000	36.019 698.23 4.5000	267.06 1325.3 637.00	256.05 2520.0 841.20	70.014 1780.0 -2.4200	31.779 1160.9 4.0000	31.207 2529.5 5
12.800	14.696 518.67 9207.3	14.696 518.67 11900.	34.494 696.12 1.7000	35.994 698.18 4.6667	266.93 1325.3 644.67	255.93 2520.6 854.13	69.989 1780.4 -2.4467	31.738 1160.6 4.0000	31.167 2579.0 5
12.900	14.696 518.67 9210.1	14.696 518.67 11901.	34.458 695.97 1.7000	35.963 698.15 4.8333	266.76 1325.3 652.33	255.78 2521.5 867.07	69.951 1781.0 -2.4733	31.692 1160.3 4.0000	31.117 2627.7 5
13.000	14.696 518.67 9213.7	14.696 518.67 11902.	34.421 695.85 1.7000	35.931 698.14 5.0000	266.59 1325.4 660.00	255.61 2522.5 880.00	69.909 1781.7 -2.5000	31.648 1160.1 4.0000	31.072 2676.9 5
13.100	14.696 518.67 9217.3	14.696 518.67 11903.	34.402 695.85 1.7000	35.914 698.18 5.0000	266.48 1325.5 660.00	255.51 2523.2 880.00	69.872 1782.3 -2.5000	31.624 1160.3 4.0000	31.050 2679.2 6
13.200	14.696 518.67 9219.4	14.696 518.67 11904.	34.405 695.94 1.7000	35.916 698.25 5.0000	266.50 1325.7 660.00	255.53 2523.3 880.00	69.871 1782.4 -2.5000	31.622 1160.4 4.0000	31.055 2679.1 6
13.300	14.696 518.67 9220.7	14.696 518.67 11905.	34.407 696.00 1.7000	35.917 698.29 5.0000	266.53 1325.8 660.00	255.56 2523.3 880.00	69.875 1782.4 -2.5000	31.626 1160.5 4.0000	31.055 2679.1 6
13.400	14.696 518.67 9221.5	14.696 518.67 11906.	34.408 696.03 1.7000	35.918 698.31 5.0000	266.55 1325.9 660.00	255.58 2523.3 880.00	69.879 1782.3 -2.5000	31.628 1160.5 4.0000	31.055 2679.2 6
13.500	14.696 518.67 9222.1	14.696 518.67 11907.	34.408 696.06 1.7000	35.919 698.33 5.0000	266.58 1326.0 660.00	255.60 2523.3 880.00	69.883 1782.3 -2.5000	31.630 1160.5 4.0000	31.056 2679.2 6
13.600	14.696 518.67 9222.4	14.696 518.67 11908.	34.409 696.07 1.7000	35.919 698.34 5.0000	266.59 1326.0 660.00	255.61 2523.3 880.00	69.886 1782.3 -2.5000	31.631 1160.6 4.0000	31.054 2679.3 6
13.700	14.696 518.67 9222.7	14.696 518.67 11908.	34.409 696.08 1.7000	35.919 698.35 5.0000	266.60 1326.1 660.00	255.63 2523.2 880.00	69.889 1782.3 -2.5000	31.630 1160.6 4.0000	31.056 2679.2 6
13.800	14.696 518.67 9222.9	14.696 518.67 11908.	34.410 696.09 1.7000	35.920 698.35 5.0000	266.61 1326.1 660.00	255.63 2523.2 880.00	69.891 1782.3 -2.5000	31.630 1160.6 4.0000	31.057 2679.1 6
13.900	14.696 518.67 9223.1	14.696 518.67 11909.	34.410 696.10 1.7000	35.920 698.36 5.0000	266.62 1326.1 660.00	255.64 2523.3 880.00	69.892 1782.3 -2.5000	31.630 1160.6 4.0000	31.059 2679.0 6
14.000	14.696 518.67 9223.2	14.696 518.67 11909.	34.409 696.10 1.7000	35.919 698.36 5.0000	266.62 1326.1 660.00	255.64 2523.2 880.00	69.893 1782.3 -2.5000	31.636 1160.6 4.0000	31.054 2679.4 6

Figure 9. - Continued.

ORIGINAL PAGE IS
OF POOR QUALITY

14.100	14.696 518.67 9223.5	14.696 518.67 11909.	34.610 696.10 1.7000	35.919 698.36 5.0000	266.63 1326.2 660.00	255.65 2523.2 880.00	69.896 1782.3 -2.5000	31.634 1160.6 4.0000	31.055 2679.3 6
14.200	14.696 518.67 9223.6	14.696 518.67 11909.	34.610 696.11 1.7000	35.920 698.37 5.0000	266.63 1326.2 660.00	255.65 2523.2 880.00	69.895 1782.3 -2.5000	31.632 1160.6 4.0000	31.056 2679.2 6
14.300	14.696 518.67 9223.6	14.696 518.67 11909.	34.611 696.11 1.7000	35.920 698.37 5.0000	266.63 1326.2 660.00	255.65 2523.2 880.00	69.895 1782.3 -2.5000	31.631 1160.6 4.0000	31.057 2679.1 6
14.400	14.696 518.67 9223.6	14.696 518.67 11909.	34.611 696.11 1.7000	35.920 698.37 5.0000	266.63 1326.2 660.00	255.65 2523.2 880.00	69.896 1782.3 -2.5000	31.631 1160.6 4.0000	31.058 2679.1 6
14.500	14.696 518.67 9223.5	14.696 518.67 11909.	34.611 696.11 1.7000	35.920 698.37 5.0000	266.63 1326.2 660.00	255.65 2523.2 880.00	69.896 1782.3 -2.5000	31.631 1160.6 4.0000	31.059 2679.1 6
14.600	14.696 518.67 9223.5	14.696 518.67 11909.	34.611 696.11 1.7000	35.920 698.37 5.0000	266.63 1326.2 660.00	255.65 2523.2 880.00	69.896 1782.3 -2.5000	31.632 1160.6 4.0000	31.058 2679.1 6
14.700	14.696 518.67 9223.5	14.696 518.67 11909.	34.611 696.11 1.7000	35.920 698.37 5.0000	266.63 1326.2 660.00	255.65 2523.2 880.00	69.896 1782.3 -2.5000	31.632 1160.6 4.0000	31.058 2679.1 6
14.800	14.696 518.67 9223.5	14.696 518.67 11909.	34.411 696.11 1.7000	35.920 698.37 5.0000	266.64 1326.2 660.00	255.65 2523.2 880.00	69.896 1782.3 -2.5000	31.632 1160.6 4.0000	31.057 2679.2 6
14.900	14.696 518.67 9223.5	14.696 518.67 11909.	34.411 696.11 1.7000	35.920 698.37 5.0000	266.63 1326.2 660.00	255.66 2523.2 880.00	69.896 1782.3 -2.5000	31.631 1160.6 4.0000	31.058 2679.1 6
15.000	14.694 518.67 9223.5	14.696 518.67 11909.	34.411 696.12 1.7000	35.920 698.37 5.0000	266.63 1326.2 660.00	255.65 2523.2 880.00	69.896 1782.3 -2.5000	31.631 1160.6 4.0000	31.058 2679.1 6
15.100	14.696 518.67 9223.5	14.696 518.67 11909.	34.411 696.12 1.7000	35.920 698.37 5.0000	266.63 1326.2 660.00	255.65 2523.2 880.00	69.896 1782.3 -2.5000	31.631 1160.6 4.0000	31.059 2679.1 6
15.200	14.696 518.67 9223.5	14.696 518.67 11909.	34.411 696.11 1.7000	35.920 698.37 5.0000	266.63 1326.2 660.00	255.66 2523.2 880.00	69.896 1782.3 -2.5000	31.632 1160.6 4.0000	31.058 2679.1 6
15.300	14.696 518.67 9223.5	14.696 518.67 11909.	34.411 696.11 1.7000	35.920 698.37 5.0000	266.63 1326.2 660.00	255.65 2523.2 880.00	69.896 1782.3 -2.5000	31.632 1160.6 4.0000	31.058 2679.1 6
15.400	14.696 518.67 9223.5	14.696 518.67 11909.	34.411 696.11 1.7000	35.920 698.37 5.0000	266.64 1326.2 660.00	255.65 2523.2 880.00	69.896 1782.3 -2.5000	31.632 1160.6 4.0000	31.057 2679.2 6
15.500	14.696 518.67 9223.5	14.696 518.67 11909.	34.411 696.12 1.7000	35.920 698.37 5.0000	266.63 1326.2 660.00	255.66 2523.2 880.00	69.896 1782.3 -2.5000	31.631 1160.6 4.0000	31.058 2679.1 6
15.600	14.696 518.67 9223.5	14.696 518.67 11909.	34.411 696.12 1.7000	35.920 698.37 5.0000	266.63 1326.2 660.00	255.65 2523.2 880.00	69.896 1782.3 -2.5000	31.631 1160.6 4.0000	31.058 2679.1 6
15.700	14.696 518.67 9223.5	14.696 518.67 11909.	34.411 696.12 1.7000	35.920 698.37 5.0000	266.63 1326.2 660.00	255.65 2523.2 880.00	69.896 1782.3 -2.5000	31.631 1160.6 4.0000	31.059 2679.1 6
15.800	14.696 518.67 9223.5	14.696 518.67 11909.	34.411 696.11 1.7000	35.920 698.37 5.0000	266.63 1326.2 660.00	255.66 2523.2 880.00	69.896 1782.3 -2.5000	31.632 1160.6 4.0000	31.058 2679.1 6
15.900	14.696 518.67 9223.5	14.696 518.67 11909.	34.410 696.11 1.7000	35.920 698.37 5.0000	266.63 1326.2 660.00	255.66 2523.2 880.00	69.896 1782.3 -2 5000	31.633 1160.6 4.0000	31.056 2679.3 6
16.000	14.696 518.67 9223.5	14.696 518.67 11909.	34.411 696.11 1.7000	35.920 698.37 5.0000	266.64 1326.2 660.00	255.65 2523.2 880.00	69.896 1782.3 -2.5000	31.632 1160.6 4.0000	31.057 2679.2 6
16.100	14.696 518.67 9223.5	14.696 518.67 11909.	34.411 696.12 1.7000	35.920 698.37 5.0000	266.63 1326.2 660.00	255.66 2523.2 880.00	69.896 1782.3 -2.5000	31.631 1160.6 4.0000	31.058 2679.1 6
16.200	14.696 518.67 9223.5	14.696 518.67 11909.	34.411 696.12 1.7000	35.921 698.37 5.0000	266.63 1326.2 660.00	255.65 2523.2 880.00	69.896 1782.3 -2.5000	31.630 1160.6 4.0000	31.060 2679.0 6
16.300	14.696 518.67 9223.5	14.696 518.67 11909.	34.411 696.12 1.7000	35.920 698.37 5.0000	266.63 1326.2 660.00	255.65 2523.2 880.00	69.896 1782.3 -2.5000	31.632 1160.6 4.0000	31.059 2679.1 6
16.400	14.696 518.67 9223.6	14.696 518.67 11909.	34.410 696.11 1.7000	35.920 698.37 5.0000	266.64 1326.2 660.00	255.65 2523.2 880.00	69.896 1782.3 -2.5000	31.635 1160.6 4.0000	31.055 2679.3 6
16.500	14.696 518.67 9223.5	14.696 518.67 11909.	34.410 696.11 1.7000	35.920 698.37 5.0000	266.64 1326.2 660.00	255.66 2523.2 880.00	69.896 1782.3 -2.5000	31.633 1160.6 4.0000	31.056 2679.2 6
16.600	14.696 518.67 9223.5	14.696 518.67 11909.	34.411 696.12 1.7000	35.920 698.37 5.0000	266.64 1326.2 660.00	255.65 2523.2 880.00	69.896 1782.3 -2.5000	31.631 1160.6 4.0000	31.057 2679.2 6
16.700	14.696 518.67 9223.5	14.696 518.67 11909.	34.411 696.12 1.7000	35.921 698.38 5.0000	266.64 1326.2 660.00	255.65 2523.3 880.00	69.896 1782.3 -2.5000	31.628 1160.6 4.0000	31.061 2678.9 6

Figure 9. - Continued.

ORIGINAL PAGE IS
OF POOR QUALITY

16.800	14.696 518.67 9223.5	14.696 518.67 11909.	34.411 696.12 1.7000	35.921 698.37 5.0000	266.63 1326.2 660.00	255.66 2523.2 880.00	69.897 1782.3 -2.5000	31.631 1160.6 4.0000	31.060 2679.0 6
16.900	14.696 518.67 9223.5	14.696 518.67 11909.	34.411 696.11 1.7000	35.920 698.37 5.0000	266.64 1326.2 660.00	255.65 2523.2 880.00	69.897 1782.3 -2.5000	31.632 1160.6 4.0000	31.059 2679.1 6
17.000	14.696 518.67 9223.5	14.696 518.67 11909.	34.411 696.11 1.7000	35.920 698.37 5.0000	266.63 1326.2 660.00	255.66 2523.2 880.00	69.896 1782.3 -2.5000	31.632 1160.6 4.0000	31.058 2679.1 6
17.100	14.696 518.67 9223.5	14.696 518.67 11909.	34.411 696.11 1.7000	35.920 698.37 5.0000	266.64 1326.2 660.00	255.66 2523.2 880.00	69.896 1782.3 -2.5000	31.632 1160.6 4.0000	31.058 2679.1 6
17.200	14.696 518.67 9223.5	14.696 518.67 11909.	34.411 696.12 1.7000	35.920 698.37 5.0000	266.64 1326.2 660.00	255.65 2523.2 880.00	69.896 1782.3 -2.5000	31.631 1160.6 4.0000	31.057 2679.2 6
17.300	14.696 518.67 9223.5	14.696 518.67 11909.	34.411 696.12 1.7000	35.920 698.37 5.0000	266.63 1326.2 660.00	255.66 2523.2 880.00	69.896 1782.3 -2.5000	31.631 1160.6 4.0000	31.058 2679.1 6
17.400	14.696 518.67 9223.5	14.696 518.67 11909.	34.411 696.12 1.7000	35.921 698.37 5.0000	266.63 1326.2 660.00	255.66 2523.2 880.00	69.896 1782.3 -2.5000	31.631 1160.6 4.0000	31.060 2679.0 6
17.500	14.696 518.67 9223.5	14.696 518.67 11909.	34.411 696.11 1.7000	35.920 698.37 5.0000	266.63 1326.2 660.00	255.65 2523.2 880.00	69.896 1782.3 -2.5000	31.632 1160.6 4.0000	31.059 2679.1 6
17.600	14.696 518.67 9223.5	14.696 518.67 11909.	34.411 696.11 1.7000	35.920 698.37 5.0000	266.63 1326.2 660.00	255.66 2523.2 880.00	69.896 1782.3 -2.5000	31.632 1160.6 4.0000	31.058 2679.1 6
17.700	14.696 518.67 9223.5	14.696 518.67 11909.	34.411 696.11 1.7000	35.920 698.37 5.0000	266.63 1326.2 660.00	255.66 2523.2 880.00	69.896 1782.3 -2.5000	31.632 1160.6 4.0000	31.057 2679.2 6
17.800	14.696 518.67 9223.5	14.696 518.67 11909.	34.411 696.11 1.7000	35.920 698.37 5.0000	266.64 1326.2 660.00	255.65 2523.2 880.00	69.897 1782.3 -2.5000	31.631 1160.6 4.0000	31.058 2679.1 6
17.900	14.696 518.67 9223.5	14.696 518.67 11909.	34.411 696.12 1.7000	35.920 698.37 5.0000	266.63 1326.2 660.00	255.66 2523.2 880.00	69.896 1782.3 -2.5000	31.631 1160.6 4.0000	31.058 2679.1 6
18.000	14.696 518.67 9223.5	14.696 518.67 11909.	34.411 696.12 1.7000	35.920 698.37 5.0000	266.63 1326.2 660.00	255.66 2523.2 880.00	69.896 1782.3 -2.5000	31.631 1160.6 4.0000	31.059 2679.0 6
18.100	14.696 518.67 9223.5	14.696 518.67 11909.	34.411 696.11 1.7000	35.920 698.37 5.0000	266.64 1326.2 660.00	255.65 2523.2 880.00	69.896 1782.3 -2.5000	31.632 1160.6 4.0000	31.059 2679.1 6
18.200	14.696 518.67 9223.5	14.696 518.67 11909.	34.411 696.11 1.7000	35.920 698.37 5.0000	266.63 1326.2 660.00	255.66 2523.2 880.00	69.896 1782.3 -2.5000	31.632 1160.6 4.0000	31.058 2679.1 6
18.300	14.696 518.67 9223.5	14.696 518.67 11909.	34.411 696.11 1.7000	35.920 698.37 5.0000	266.63 1326.2 660.00	255.65 2523.2 880.00	69.896 1782.3 -2.5000	31.632 1160.6 4.0000	31.058 2679.1 6
18.400	14.696 518.67 9223.5	14.696 518.67 11909.	34.411 696.12 1.7000	35.920 698.37 5.0000	266.64 1326.2 660.00	255.65 2523.2 880.00	69.896 1782.3 -2.5000	31.631 1160.6 4.0000	31.058 2679.1 6
18.500	14.696 518.67 9223.5	14.696 518.67 11909.	34.411 696.12 1.7000	35.920 698.37 5.0000	266.63 1326.2 660.00	255.66 2523.2 880.00	69.896 1782.3 -2.5000	31.631 1160.6 4.0000	31.058 2679.1 6
18.600	14.696 518.67 9223.5	14.696 518.67 11909.	34.411 696.12 1.7000	35.920 698.37 5.0000	266.63 1326.2 660.00	255.66 2523.2 880.00	69.896 1782.3 -2.5000	31.631 1160.6 4.0000	31.059 2679.1 6
18.700	14.696 518.67 9223.5	14.696 518.67 11909.	34.411 696.11 1.7000	35.920 698.37 5.0000	266.64 1326.2 660.00	255.65 2523.2 880.00	69.896 1782.3 -2.5000	31.632 1160.6 4.0000	31.058 2679.1 6
18.800	14.696 518.67 9223.5	14.696 518.67 11909.	34.411 696.11 1.7000	35.920 698.37 5.0000	266.63 1326.2 660.00	255.66 2523.2 880.00	69.896 1782.3 -2.5000	31.632 1160.6 4.0000	31.058 2679.1 6
18.900	14.696 518.67 9223.5	14.696 518.67 11909.	34.411 696.11 1.7000	35.920 698.37 5.0000	266.63 1326.2 660.00	255.65 2523.2 880.00	69.896 1782.3 -2.5000	31.632 1160.6 4.0000	31.058 2679.1 6
19.000	14.696 518.67 9223.5	14.696 518.67 11909.	34.411 696.12 1.7000	35.920 698.37 5.0000	266.64 1326.2 660.00	255.65 2523.2 880.00	69.896 1782.3 -2.5000	31.631 1160.6 4.0000	31.058 2679.1 6
19.100	14.696 518.67 9223.5	14.696 518.67 11909.	34.411 696.12 1.7000	35.920 698.37 5.0000	266.63 1326.2 660.00	255.66 2523.2 880.00	69.896 1782.3 -2.5000	31.631 1160.6 4.0000	31.058 2679.1 6
19.200	14.696 518.67 9223.5	14.696 518.67 11909.	34.411 696.12 1.7000	35.920 698.37 5.0000	266.63 1326.2 660.00	255.65 2523.2 880.00	69.896 1782.3 -2.5000	31.631 1160.6 4.0000	31.059 2679.1 6
19.300	14.696 518.67 9223.5	14.696 518.67 11909.	34.411 696.12 1.7000	35.920 698.37 5.0000	266.63 1326.2 660.00	255.65 2523.2 880.00	69.896 1782.3 -2.5000	31.632 1160.6 4.0000	31.058 2679.1 6

Figure 9. - Continued.

ORIGINAL PAGE IS
OF POOR QUALITY

19.400	14.696	14.696	34.410	35.920	266.64	255.65	69.896	31.634	31.056
	518.67	518.67	696.11	698.37	1326.2	2523.2	1782.3	1162.6	2579.2
	9223.6	11909.	1.7000	5.0000	660.00	880.00	-2.5000	4.0000	6
19.500	14.696	14.696	34.411	35.920	266.65	255.65	69.895	31.632	31.057
	518.67	518.67	696.11	698.37	1326.2	2523.2	1782.3	1160 6	2579.2
	9223.5	11909.	1.7000	5.0000	660.00	880.00	-2.5000	4.0000	6
19.600	14.696	14.696	34.411	35.921	266.63	255.65	69.895	31.628	31.031
	518.67	518.67	696.12	698.38	1326.2	2523.2	1782.3	1160.6	2578.9
	9223.5	11909.	1.7000	5.0000	660.00	880.00	-2.5000	4.0000	5
19.700	14.696	14.696	34.411	35.921	266.63	255.65	69.895	31.630	31.030
	518.67	518.67	696.12	698.37	1326.2	2523.2	1782.3	1160.6	2579.0
	9223.5	11909.	1.7000	5.0000	660.00	880.00	-2.5000	4.0000	6
19.800	14.696	14.696	34.410	35.920	266.64	255.65	69 896	31.537	31.055
	518.67	518.67	696.11	698.37	1326.2	2523.2	1732.3	1160.7	2579.3
	9223.5	11909.	1.7000	5.0000	660.00	880.00	-2.5000	4.0000	6
19.900	14.696	14.696	34.410	35.920	266.63	255.66	69.896	31.535	31 055
	518.67	518.67	696.11	698.37	1326.2	2523.2	1782.3	1160.6	2579.3
	9223.5	11909.	1.7000	5.0000	660.00	880.00	-2.5000	4.0000	6
20.000	14.696	14.696	34.410	35.920	266.64	255.65	69.896	31.633	31.056
	518.67	518.67	696.11	698.37	1326.2	2523.2	1782.3	1160.6	2579.2
	9223.5	11909.	1.7000	5.0000	660.00	880.00	-2.5000	4.0000	6

TIME = 20.0000 SECONDS

	STA 2	STA 13	STA 2.2	STA 3	STA 4	STA 4.1	STA 6	STA 7
PRESSURE	14.6960	34.4104	35.9200	266.635	255.652	69.8953	31.6333	31.0561
TEMPERATURE	518.670	696.113	698.373	1326.19	2523.23	1782.29	1160.63	2579.24
DERIVATIVE		-.445407		8.57182	-18.5339	-.310210	3.02837	8.55375
MASS FLOW	193.302	86.5275	106.786	87.9336	89.6204	106.789	194.721	199.703
DERIVATIVE		-5.58203					7.35327	
STORED MASS		6.71864		0.910883	0.459032	2.45069	2.21414	1.778575
DERIVATIVE		-.113983E-01		-.137634E-01	0.132322E-01	-.320435E-03	0.127813E-01	-.424174E-02
ENERGY DER.		-2.99253		7.80793	-8.50767	-.760229	6.70555	6.55435
DELTA H					167.231	75.6776		

LOW SPEED SPOOL = 9223.55 RPM
DERIVATIVE = -.528816 RPM/SEC

MAIN COMBUSTOR FUEL FLOW = 1.70000

BLEED MASS FLOWS—
LOW PRESSURE = 1.43737
HIGH PRESSURE = 17.1688
OVERBOARD =0.259538

HIGH SPEED SPOOL = 11909.4 RPM
DERIVATIVE = -.698108E-01RPM/SEC

AFTERBURNER FUEL FLOW = 5.00000

VARIABLE GEOMETRY --
FVGP = -2.50000
CVGP = 4.00000
THROAT AREA = 660.000

FSHIFT =-.259255E-02
CSHIFT =2.000000

Figure 9. - Concluded.

ORIGINAL PAGE IS
OF POOR QUALITY

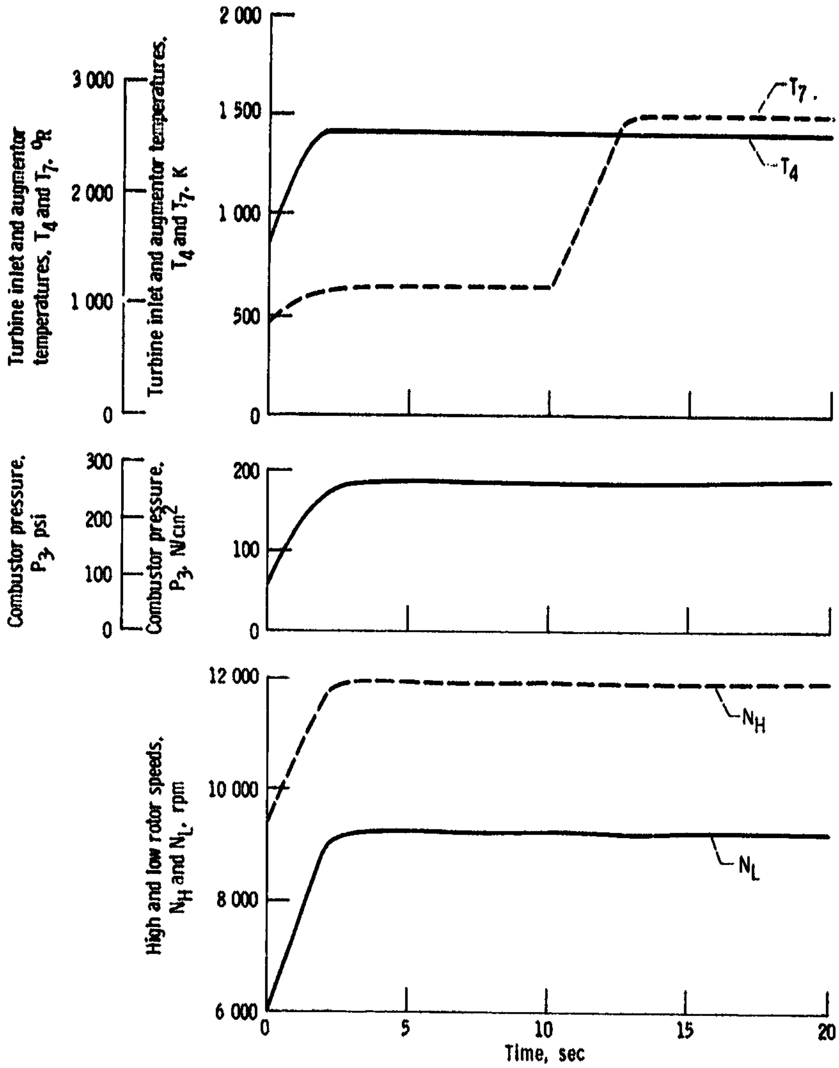

Figure 10. - Turbofan engine response for DIGTEM test case.

C-2

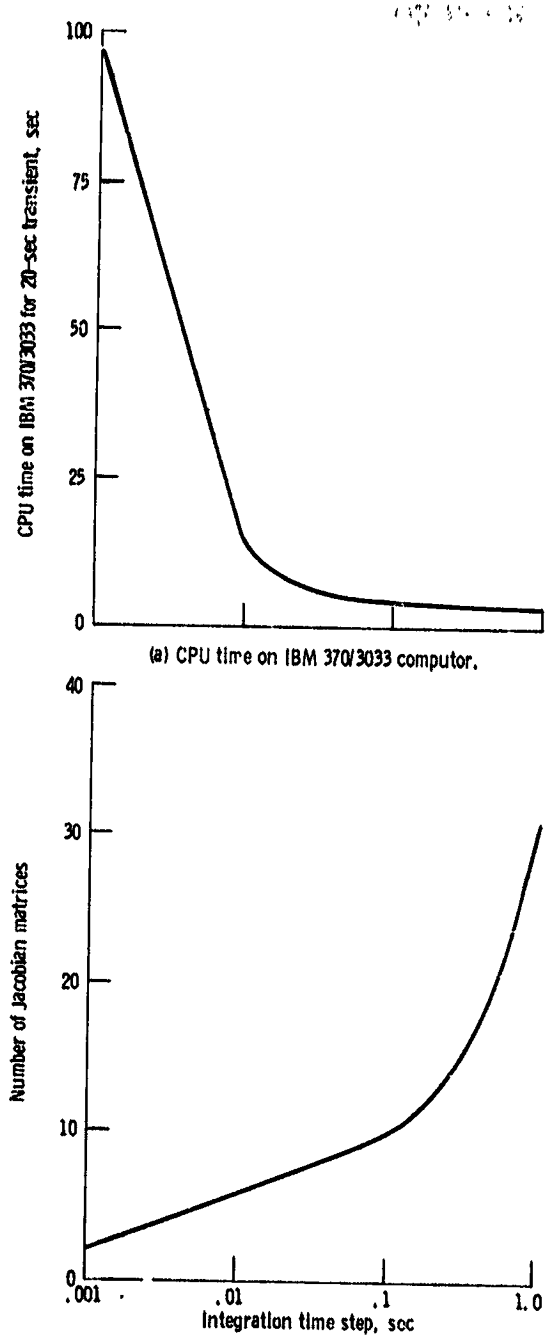

(a) CPU time on IBM 370/3033 computor.

(b) Number of Jacobian matrices.

Figure 11. - Integration time step study for DIGTEM 20-sec test case transient.

ORIGINAL PAGE IS
OF POOR QUALITY

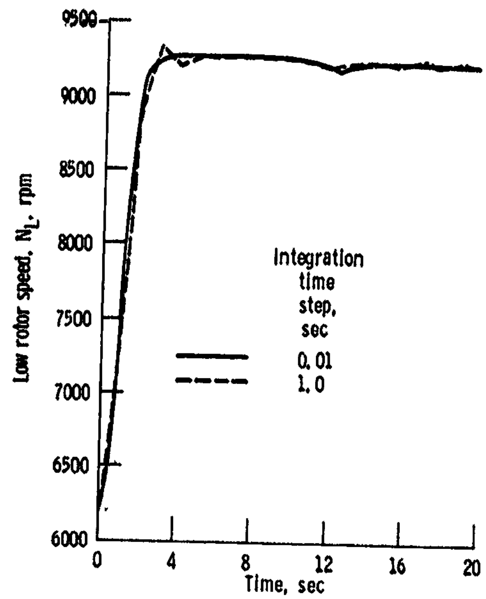

(a) Low rotor speed.

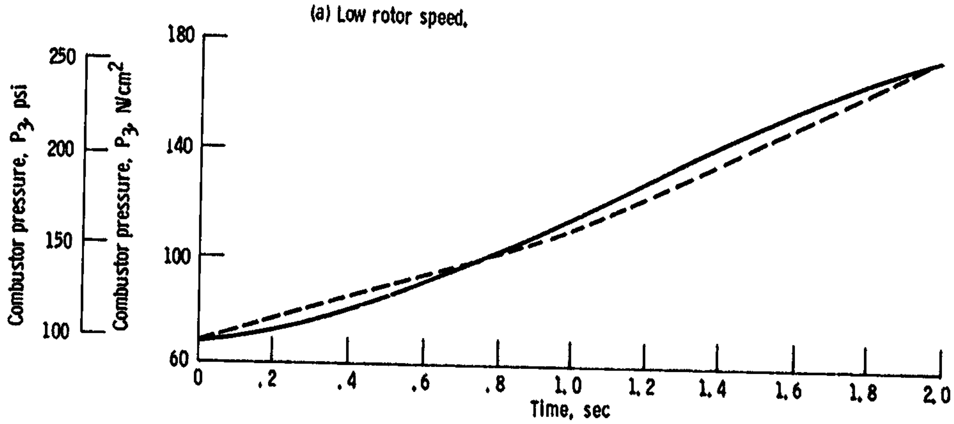

(b) Combustor pressure.

Figure 12. - Comparison of low rotor speed and combustor pressure responses for the DIGTEM test case with different integration time steps.

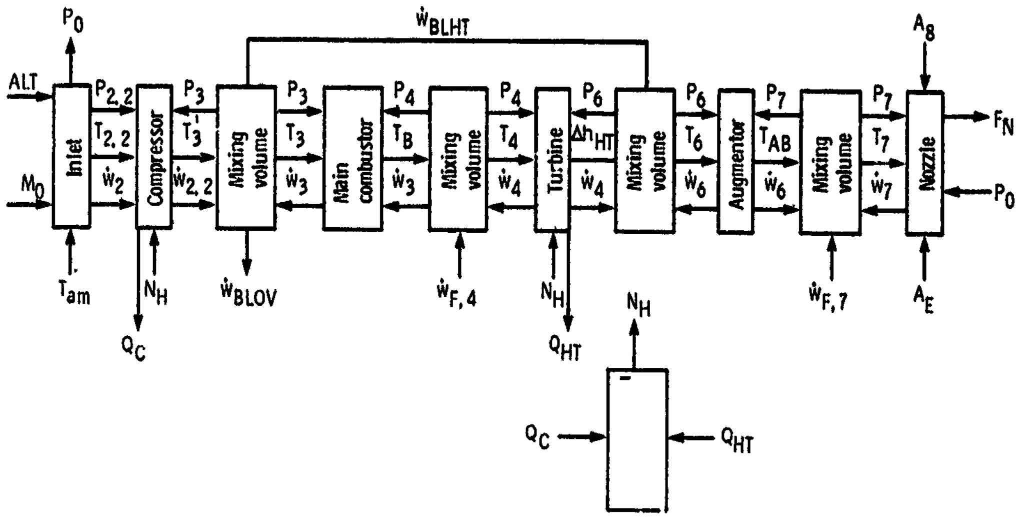

Figure 13. - Computational flow diagram of a turbojet engine.

ORIGINAL PAGE IS
OF POOR QUALITY

INPUT DATA

OPERATING POINT NUMBER 1

TIME = 0.0000 SECONDS

	STA 2	STA 13	STA 2.2	STA 3	STA 4	STA 4.1	STA 6	STA 7
PRESSURE	14.6960	34.9000	36.0000	267.000	256.000	70.0000	31.8000	30.5999
TEMPERATURE	518.670	696.000	697.999	1325.00	2520.00	1780.00	1160.00	1160.00
DERIVATIVE		-.268704E-01		-.484254	0.595337	0.193774E-01	-.144589	-.503200
MASS FLOW	193.500	86.5000	107.000	88.0995	89.7999	107.000	194.940	194.942
DERIVATIVE		0.390625E-01					0.273438E-01	
STORED MASS		6.73723		0.912947	0.460246	2.45748	2.22702	1.77208
DERIVATIVE		-.213623E-03		0.350952E-03	-.317574E-03	-.457764E-04	-.122070E-03	-.210571E-02
ENERGY DER.		-.181032		-.442098	0.255592	0.476195E-01	-.322003	-.891712
DELTA H					167.000	75.5001		

LOW SPEED SPOOL = 9200.00 RPM
DERIVATIVE = 0.722958E-01 RPM/SEC

HIGH SPEED SPOOL = 11900.0 RPM
DERIVATIVE = 0.349328E-01RPM/SEC

MAIN COMBUSTOR FUEL FLOW = 1.70000

AFTERBURNER FUEL FLOW =0.000000

BLEED MASS FLOWS--
LOW PRESSURE = 1.43999
HIGH PRESSURE = 17.2000
OVERBOARD =0.260009

VARIABLE GEOMETRY --
FVOP = -1.70040
CVOP = 4.00000
THROAT AREA = 430.000

FSHIFT =0.398606E-06
CSHIFT =0.211876E-07

CONVERGED STEADY STATE POINT

TIME = 0.0000 SECONDS

	STA 2	STA 13	STA 2.2	STA 3	STA 4	STA 4.1	STA 6	STA 7
PRESSURE	14.6960	34.4997	35.9997	266.999	255.999	69.9996	31.7996	30.5996
TEMPERATURE	518.670	695.999	698.000	1325.00	2520.01	1780.00	1160.00	1160.00
DERIVATIVE		-.624854E-03		-.708905	1.53016	0.553536E-01	0.199381E-01	-.364641E-02
MASS FLOW	193.500	86.5008	106.999	88.0983	89.7994	106.999	194.940	194.940
DERIVATIVE		0.117188E-01					-.251465E-01	
STORED MASS		6.73719		0.912942	0.460242	2.45746	2.22700	1.77206
DERIVATIVE		-.152588E-04		0.106812E-02	-.108051E-02	0.106812E-03	-.915527E-04	-.152588E-04
ENERGY DER.		-.420976E-02		-.647189	0.704246	0.136030	0.444021E-01	-.646167E-02
DELTA H					167.001	75.5002		

LOW SPEED SPOOL = 9200.05 RPM
DERIVATIVE = -.361477E-01 RPM/SEC

HIGH SPEED SPOOL = 11900.0 RPM
DERIVATIVE = 0.489058E-01RPM/SEC

MAIN COMBUSTOR FUEL FLOW = 1.70000

AFTERBURNER FUEL FLOW =0.000000

BLEED MASS FLOWS--
LOW PRESSURE = 1.43998
HIGH PRESSURE = 17.1999
OVERBOARD =0.260008

VARIABLE GEOMETRY --
FVOP = -1.70040
CVOP = 4.00000
THROAT AREA = 430.000

FSHIFT =-.447921E-06
CSHIFT =0.000000

(a) Operating point 1 (dry design point).

Figure 14. - Steady-state operating points.

ORIGINAL PAGE IS
OF POOR QUALITY

INPUT DATA

OPERATING POINT NUMBER 2

TIME = 0.0000 SECONDS

	STA 2	13	STA 2.2	STA 3	STA 4	STA 4.1	STA 6	STA 7
PRESSURE	14.6960	24.2000	26.1800	158.700	151.500	41.2399	21.7000	21.2100
TEMPERATURE	518.670	614.000	620.941	1106.00	1918.00	1343.00	891.000	891.000
DERIVATIVE		-12 8815		8.30725	18.0497	30.6131	10.6789	126.017
MASS FLOW	147.379	75.0000	72.4762	60.1456	60.9108	72.1240	148.000	147.412
DERIVATIVE		0.625000E-01					-.603027E-01	
STORED MASS		5.35696		0.650088	0.357861	1.91891	1.97851	1.59913
DERIVATIVE		-.970764E-01		0.289764E-01	-.271825E-01	-.181122E-01	0.612488E-01	0.588333
ENERGY DER.		-69.0056		5.40044	6.45929	58.7438	21.1283	201.517
DELTA H					127.591	46.7860		

LOW SPEED SPOOL = 7706.00 RPM
DERIVATIVE = -19.9786 RPM/SEC

HIGH SPEED SPOOL = 10434.0 RPM
DERIVATIVE = 6.62954 RPM/SEC

MAIN COMBUSTOR FUEL FLOW =0.738000

AFTERBURNER FUEL FLOW =0.000000

BLEED MASS FLOWS--
LOW PRESSURE =0.937253
HIGH PRESSURE = 11.1951
OVERBOARD =0.169234

VARIABLE GEOMETRY --
FVGP = -24.9900
CVGP = -4.80000
THROAT AREA = 430.000

FSHIFT =0.470579E-04
CSHIFT =-.141049E-03

CONVERGED STEADY STATE POINT

TIME = 0.0000 SECONDS

	STA 2	STA 13	STA 2.2	STA 3	STA 4	STA 4.1	STA 6	STA 7
PRESSURE	14.6960	24.1867	26.1554	158.752	151.542	41.2461	21.7204	21.2331
TEMPERATURE	518.670	613.502	620.708	1106.18	1917.88	1343.57	892.054	892.054
DERIVATIVE		0.418344E-02		0.175164	0.248939E-01	-.321751E-01	-.403699E-01	0.000000
MASS FLOW	146.998	74.5027	72.4956	60.1913	60.9291	72.1270	147.567	147.567
DERIVATIVE		0.351563E-01					-.388184E-01	
STORED MASS		5.35836		0.650195	0.357983	1.91839	1.97802	1.59898
DERIVATIVE		0.915527E-04		-.274658E-03	0.222266E-03	-.457764E-04	0.305176E-04	0.000000
ENERGY DER.		0.224164E-01		0.113891	0.891161E-02	-.617243E-01	-.798526E-01	0.000000
DELTA H					127.600	46.7440		

LOW SPEED SPOOL = 7694.50 RPM
DERIVATIVE = 0.229609E-01 RPM/SEC

HIGH SPEED SPOOL = 10437.4 RPM
DERIVATIVE = 0.796561E-02RPM/SEC

MAIN COMBUSTOR FUEL FLOW =0.738000

AFTERBURNER FUEL FLOW =0.000000

BLEED MASS FLOWS--
LOW PRESSURE =0.937482
HIGH PRESSURE = 11.1978
OVERBOARD =0.169275

VARIABLE GEOMETRY --
FVGP = -24.9900
CVGP = -4.80000
THROAT AREA = 430.000

FSHIFT =0.469834E-04
CSHIFT =-.296514E-03

(b) Operating point 2.

Figure 14. - Continued.

ORIGINAL PAGE IS
OF POOR QUALITY

INPUT DATA

OPERATING POINT NUMBER 3

TIME = 0.0000 SECONDS

	STA 2	STA 13	STA 2.2	STA 3	STA 4	STA 4.1	STA 6	STA 7
PRESSURE	14.6960	19.1000	20.6036	99.3999	94.5999	27.0999	17.5000	17.3000
TEMPERATURE	518.670	571.000	578.205	966.000	1580.00	1117.00	785.000	785.000
DERIVATIVE		1.52573		53.3228	-23.8950	-.416268	10.5138	-93.3126
MASS FLOW	103.567	54.0000	49.7557	41.5867	41.8824	49.3406	104.000	104.451
DERIVATIVE		0.244141E-03					0.268555E-02	
STORED MASS		4.54641		0.466186	0.271259	1.51610	1.81102	1.48046
DERIVATIVE		-.188446		-.771942E-01	0.742999E-01	0.462494E-01	-.311279E-01	-.450562
ENERGY DER.		6.93660		24.8583	-6.48174	-.631104	19.0407	-138.146
DELTA H					101.309	27.1968		

LOW SPEED SPOOL = 6175.00 RPM
DERIVATIVE = -25.4913 RPM/SEC

HIGH SPEED SPOOL = 9439.00 RPM
DERIVATIVE = 16.1629 RPM/SEC

MAIN COMBUSTOR FUEL FLOW =0.370000

AFTERBURNER FUEL FLOW =0.000000

BLEED MASS FLOWS--
LOW PRESSURE =0.628276
HIGH PRESSURE = 7.50448
OVERBOARD =0.113444

VARIABLE GEOMETRY --
FVGP = -24.9900
CVGP = -20.0000
THROAT AREA = 430.000

FSHIFT =0.216844E-04
CSHIFT =-.339364E-02

CONVERGED STEADY STATE POINT

TIME = 0.0000 SECONDS

	STA 2	STA 13	STA 2.2	STA 3	STA 4	STA 4.1	STA 6	STA 7
PRESSURE	14.6960	19.0887	20.6006	99.6367	94.8361	27.1478	17.4849	17.2840
TEMPERATURE	518.670	571.375	578.098	966.401	1578.93	1115.84	784.934	784.934
DERIVATIVE		-.461090E-02		-.133642	0.244831	-.870769E-01	-.525365E-01	0.221378E-01
MASS FLOW	103.927	54.0319	49.8948	41.6306	42.0007	49.5215	104.183	104.183
DERIVATIVE		-.166016E-01					-.131836E-01	
STORED MASS		4.54076		0.467103	0.272121	1.52035	1.80961	1.47922
DERIVATIVE		-.915527E-04		0.305176E-04	-.562072E-04	-.152588E-04	-.152588E-04	0.106812E-03
ENERGY DER.		-.209370E-01		-.624246E-01	0.666237E-01	-.132387	-.950707E-01	0.327466E-01
DELTA H					101.306	27.3107		

LOW SPEED SPOOL = 6181.22 RPM
DERIVATIVE = 0.151318E-01 RPM/SEC

HIGH SPEED SPOOL = 9444.84 RPM
DERIVATIVE = 0.264081E-01RPM/SEC

MAIN COMBUSTOR FUEL FLOW =0.370000

AFTERBURNER FUEL FLOW =0.000000

BLEED MASS FLOWS--
LOW PRESSURE =0.629642
HIGH PRESSURE = 7.52079
OVERBOARD =0.113691

VARIABLE GEOMETRY --
FVGP = -24.9900
CVGP = -20.0000
THROAT AREA = 430.000

FSHIFT =0.218332E-04
CSHIFT =-.415303E-02

(c) Operating point 3.

Figure 14. - Continued.

ORIGINAL PAGE IS
OF POOR QUALITY

INPUT DATA

OPERATING POINT NUMBER 4

TIME = 0.0080 SECONDS

	STA 2	STA 13	STA 2.2	STA 3	STA 4	STA 4.1	STA 6	STA 7
PRESSURE	14.6969	34.5000	36.0000	267.000	256.000	70.0000	31.8000	30.6000
TEMPERATURE	518.670	696.000	698.000	1325.00	2520.00	1780.00	1160.00	2682.90
DERIVATIVE		-.160517E-01		-.333886	0.580432	0.157796E-01	-.144589	-.873595E-01
MASS FLOW	193.500	86.5000	107.000	88.0995	89.7998	107.000	194.940	198.009
DERIVATIVE		0.390625E-01					-.312500E-01	
STORED MASS		6.73723		0.912947	0.460246	2.45748	2.22702	0.766192
DERIVATIVE		-.198364E-03		0.350952E-03	-.302315E-03	-.610352E-04	-.122070E-03	1.93141
ENERGY DER.		-.108144		-.304821	0.267142	0.387785E-01	-.322003	-.439453E-01
DELTA H					167.000	75.5001		

LOW SPEED SPOOL = 9200.00 RPM
DERIVATIVE = 0.361479E-01 RPM/SEC

MAIN COMBUSTOR FUEL FLOW = 1.70000

BLEED MASS FLOWS--
LOW PRESSURE = 1.43999
HIGH PRESSURE = 17.2000
OVERBOARD =0.260009

HIGH SPEED SPOOL = 11900.0 RPM
DERIVATIVE = 0.698657E-02RPM/SEC

AFTERBURNER FUEL FLOW = 5.00000

VARIABLE GEOMETRY --
FVGP = -2.50040
CVGP = 4.00000
THROAT AREA = 660.000

FSHIFT =-.238222E-02
CSHIFT =0.211876E-07

CONVERGED STEADY STATE POINT

TIME = 0.0000 SECONDS

	STA 2	STA 13	STA 2.2	STA 3	STA 4	STA 4.1	STA 6	STA 7
PRESSURE	14.6960	34.6747	36.1188	267.469	256.443	70.1325	32.0260	30.8377
TEMPERATURE	518.670	696.497	697.491	1323.39	2515.76	1777.01	1161.12	2680.78
DERIVATIVE		-.459710E-02		-.953746E-01	0.705264	-.630177E-01	0.649424E-01	-.569567
MASS FLOW	193.139	85.8615	107.278	88.3327	90.0329	107.274	194.579	199.578
DERIVATIVE		-.390625E-02					0.000000	
STORED MASS		6.76653		0.915664	0.461821	2.46628	2.24068	0.772756
DERIVATIVE		0.106812E-03		0.123105E-03	-.180244E-03	-.762939E-04	0.000000	0.106812E-03
ENERGY DER.		-.311064E-01		-.873311E-01	0.325705	-.155419	0.145515	-.440136
DELTA H					166.690	75.1431		

LOW SPEED SPOOL = 9175.59 RPM
DERIVATIVE = 0.422847E-01 RPM/SEC

MAIN COMBUSTOR FUEL FLOW = 1.70000

BLEED MASS FLOWS--
LOW PRESSURE = 1.44340
HIGH PRESSURE = 17.2407
OVERBOARD =0.260625

HIGH SPEED SPOOL = 11888.4 RPM
DERIVATIVE = 0.000000 RPM/SEC

AFTERBURNER FUEL FLOW = 5.00000

VARIABLE GEOMETRY --
FVGP = -2.50040
CVGP = 4.00000
THROAT AREA = 660.000

FSHIFT =-.731486E-03
CSHIFT =0.509492E-04

(d) Operating point 4 (wet design point).

Figure 14. - Continued.

ORIGINAL PAGE IS
OF POOR QUALITY

INPUT DATA

OPERATING POINT NUMBER 5

TIME = 0.0000 SECONDS

	STA 2	STA 13	STA 2.2	STA 3	STA 4	STA 4.1	STA 6	STA 7
PRESSURE	14.6960	34.5000	36.0000	267.000	256.000	70.0000	31.8000	30.6000
TEMPERATURE	518.670	696.000	698.000	1329.00	2520.00	1780.00	1160.00	1971.40
DERIVATIVE		-.667891E-02		-.333886	0.580432	0.157798E-01	-.144589	-.567318
MASS FLOW	193.500	86.5000	107.000	88.0995	89.7998	107.000	194.940	195.994
DERIVATIVE		0.390625E-01					-.312500E-01	
STORED MASS		6.73723		0.912947	0.460246	2.45748	2.22702	1.04272
DERIVATIVE		0.305176E-04		0.350952E-03	-.302315E-03	-.610352E-04	-.122070E-03	1.74974
ENERGY DER.		-.449973E-01		-.304821	0.267142	0.387789E-01	-.322003	-.591593
DELTA H					167.000	75.5001		

LOW SPEED SPOOL = 9200.00 RPM
DERIVATIVE = 0.180739E-01 RPM/SEC

HIGH SPEED SPOOL = 11900.0 RPM
DERIVATIVE = 0.698657E-02RPM/SEC

MAIN COMBUSTOR FUEL FLOW = 1.70000

AFTERBURNER FUEL FLOW = 2.80000

BLEED MASS FLOWS--
LOW PRESSURE = 1.43999
HIGH PRESSURE = 17.2000
OVERBOARD =0.260009

VARIABLE GEOMETRY --
FVGP = -2.50000
CVGP = 4.00000
THROAT AREA = 560.500

FSHIFT =-.238105E-02
CSHIFT =0.211876E-07

CONVERGED STEADY STATE POINT

TIME = 0.0000 SECONDS

	STA 2	STA 13	STA 2.2	STA 3	STA 4	STA 4.1	STA 6	STA 7
PRESSURE	14.6960	34.6585	36.1078	267.425	256.402	70.1201	32.0049	30.8156
TEMPERATURE	518.670	696.450	697.538	1323.54	2516.15	1777.29	1161.02	1969.81
DERIVATIVE		0.323497E-02		-.141692	0.165711E-01	-.691308E-01	0.893214E-01	0.246335E-01
MASS FLOW	193.173	85.9211	107.252	88.3117	90.0111	107.248	194.612	197.412
DERIVATIVE		0.976563E-01					0.224609E-01	
STORED MASS		6.76381		0.915411	0.461673	2.46546	2.23941	1.05091
DERIVATIVE		-.167847E-03		-.305176E-03	0.643730E-03	-.198364E-03	0.305176E-04	0.419617E-04
ENERGY DER.		0.218807E-01		-.129706	0.765043E-02	-.170439	0.200027	0.258877E-01
DELTA H					166.718	75.1762		

LOW SPEED SPOOL = 9177.87 RPM
DERIVATIVE = 0.181175E-01 RPM/SEC

HIGH SPEED SPOOL = 11889.5 RPM
DERIVATIVE = -.699273E-01RPM/SEC

MAIN COMBUSTOR FUEL FLOW = 1.70000

AFTERBURNER FUEL FLOW = 2.80000

BLEED MASS FLOWS--
LOW PRESSURE = 1.44308
HIGH PRESSURE = 17.2369
OVERBOARD =0.260568

VARIABLE GEOMETRY --
FVGP = -2.50000
CVGP = 4.00000
THROAT AREA = 560.000

FSHIFT =-.887099E-03
CSHIFT =0.461726E-04

(e) Operating point 5.

Figure 14. - Concluded.

Correction coefficient	Value
1	1.0000000
2	1.0000000
3	1.0000000
4	1.0000000
5	0.99615240
6	1.0000000
7	1.0028696
8	1.0000000
9	1.0099678
10	1.0024300
11	1.0010843
12	1.0267143
13	1.0045977
14	0.99256819
15	1.0016937
16	1.0226727
17	0.99627388
18	1.0000000
19	1.0089293

Figure 15. - Correction coefficients for dry design point.

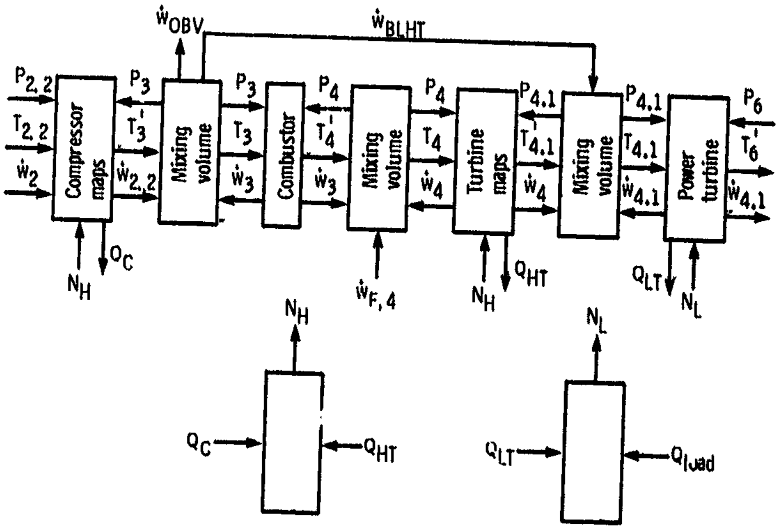

Figure 16. - Computational flow diagram of turboshaft engine.

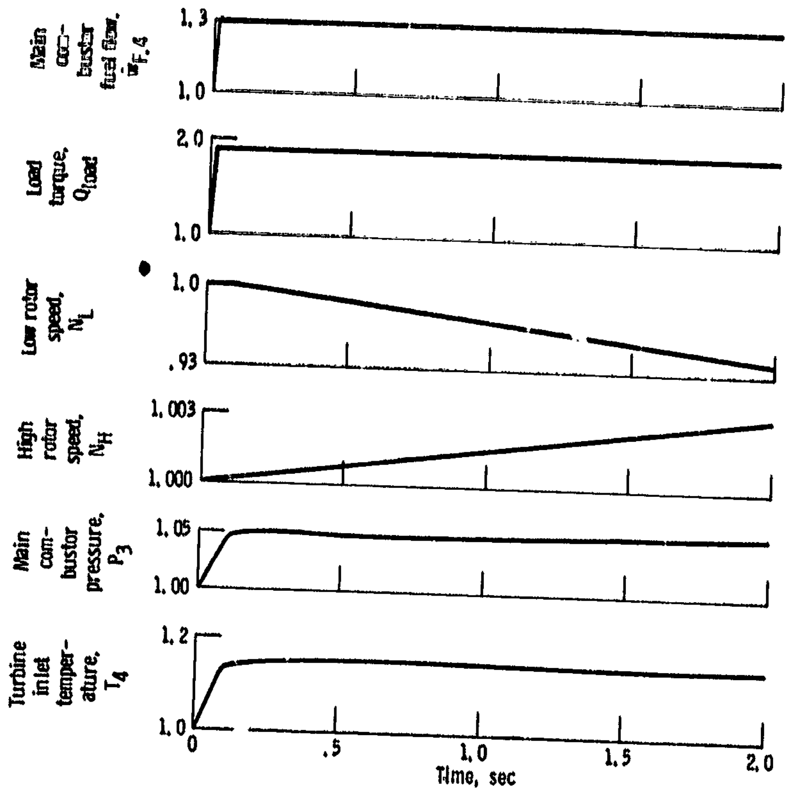

Figure 17. - Transient response of a small turboshaft engine to simultaneous steps in fuel flow and load. (Values are normalized to design point.)